Advanced BRT Volume I: Innovative Technologies for Dedicated Roadways

Final Report

Prepared by:

Lee Alexander
Pi-Ming Cheng
Alec Gorjestani
Arvind Menon
Bryan Newstrom
Craig Shankwitz

Intelligent Transportation Systems Institute
Center for Transportation Studies
University of Minnesota

CTS 08-06

Technical Report Documentation Page

1. Report No. CTS 08-06	2.	3. Recipients Accession No.	
4. Title and Subtitle Advanced BRT Volume I: Innovative Technologies for Dedicated Roadways		5. Report Date March 2008 6.	
7. Author(s) Lee Alexander, Pi-Ming Cheng, Alec Gorjestani, Arvind Menon, Bryan Newstrom, Craig Shankwitz		8. Performing Organization Report No.	
9. Performing Organization Name and Address Intelligent Transportation Systems Institute Center for Transportation Studies University of Minnesota 200 Transportation and Safety Building 511 Washington Ave. SE Minneapolis, MN 55455		10. Project/Task/Work Unit No. CTS project # 2002041 11. Contract (C) or Grant (G) No.	
12. Sponsoring Organization Name and Address Intelligent Transportation Systems Institute University of Minnesota 200 Transportation and Safety Building 511 Washington Ave. SE Minneapolis, MN 55455		13. Type of Report and Period Covered Final Report 14. Sponsoring Agency Code	
15. Supplementary Notes http://www.cts.umn.edu/pdf/CTS-08-06.pdf			

16. Abstract (Limit: 250 words)

Presented herein is a novel approach to vehicle positioning using RFID technology (Vehicle Positioning System, or VPS). By installing in the road RFID tags encoded with road name or other designation, the specific lane, the direction of travel, and the longitudinal distance from a known reference, a vehicle outfitted with an RFID tag reader can determine its position each time it passes over and reads a tag, thus, providing precisely the information needed for many ITS applications – the longitudinal position of a vehicle in a particular lane on a particular road of the transportation network.

Knowledge of lane of travel and distance from a known reference provided by VPS enables many transit applications, including headway control of bus platoons, merge/lane change assistance, rear-end collision avoidance, and bay mark-up applications. For lane assist systems, VPS and a lateral positioning system can augment DGSP in urban areas, providing seamless operation where DGPS accuracy is insufficient for lane keeping.

This research focused on designing and building a prototype VPS using existing third party RFID hardware. The hardware was evaluated and characterized to determine if it could be used to create a viable, robust VPS. After the development and characterization of the positioning system, an implementation of a rear-end collision avoidance system was built to demonstrate the use of VPS. Finally, a more sophisticated rear-end collision avoidance system was designed and simulated, after which its implications to the accuracy specifications for VPS were analyzed.

17. Document Analysis/Descriptors Vehicle positioning, radio frequency identification (RFID), rear-end collision avoidance		18. Availability Statement No restrictions. Document available from: National Technical Information Services, Springfield, Virginia 22161	
19. Security Class (this report) Unclassified	20. Security Class (this page) Unclassified	21. No. of Pages 124	22. Price

Advanced BRT Volume I:
Innovative Technologies for Dedicated Roadways

Final Report

Prepared by:

Lee Alexander
Pi-Ming Cheng
Alec Gorjestani
Arvind Menon
Bryan Newstrom
Craig Shankwitz

Intelligent Transportation Systems Institute
Center for Transportation Studies
University of Minnesota
200 Transportation and Safety Building
511 Washington Ave SE
Minneapolis, MN 55455

March 2008

Published by:

Minnesota Department of Transportation
Research Services Section
395 John Ireland Boulevard, MS 330
St. Paul, Minnesota 55155-1899

Acknowledgements

This work was sponsored by the ITS Institute. The support of the ITS Institute is greatly appreciated.

Jack Herndon and the Mn/ROAD staff also deserve special thanks. Without use of the Mn/ROAD facility, none of the experimental work would have been possible. They were extremely flexible with scheduling, and were always willing to offer any assistance they could.

Finally, Nissan North America is to be thanked for providing the research vehicle used in all of the experimental work.

Table of Contents

List of Tables

List of Figures

Executive Summary

Presented herein is a novel approach to vehicle positioning using RFID technology (Vehicle Positioning System, or VPS). By installing in the road RFID tags encoded with road name or other designation, the specific lane, the direction of travel, and the longitudinal distance from a known reference, a vehicle outfitted with an RFID tag reader can determine its position each time it passes over and reads a tag, thus, providing precisely the information needed for many ITS applications – the longitudinal position of a vehicle in a particular lane on a particular road of the transportation network.

Knowledge of lane of travel and distance from a known reference provided by VPS enables many transit applications, including headway control of bus platoons, merge/lane change assistance, rear-end collision avoidance, and bay mark-up applications. For lane assist systems, VPS and a lateral positioning system can augment DGSP in urban areas, providing seamless operation where DGPS accuracy is insufficient for lane keeping.

This research focused on designing and building a prototype VPS using existing third party RFID hardware. The hardware was evaluated and characterized to determine if it could be used to create a viable, robust VPS. After the development and characterization of the positioning system, an implementation of a rear-end collision avoidance system was built to demonstrate the use of VPS. Finally, a more sophisticated rear-end collision avoidance system was designed and simulated, after which its implications to the accuracy specifications for VPS were analyzed.

1 Introduction

1.1 Motivation

Many intelligent transportation systems (ITS) require accurate knowledge of the vehicle's position. Presently, GPS is used to provide this vehicle position information. However, GPS suffers from four primary problems if it is to be used to identify within which lane the vehicle is traveling. These are:

1. Variable accuracy (accuracy affected by atmospheric, geometric, and multi-path conditions)
2. Satellite and correction availability (passing under a bridge or through a tunnel blocks satellite and correction signals; driving through naturally occurring canyons or adjacent buildings cause restricted sight lines to the satellite constellation and reduce solution accuracy)
3. High accuracy digital maps, with which to correlate one's position, are not yet widely available.
4. GPS receivers are not universally deployed on all vehicles.

These four problems prevent GPS from becoming a ubiquitous vehicle positioning technology [1]. Of even greater concern is the fact that the first two problems are much more pronounced in urban areas; the environment where many ITS applications requiring vehicle position are particularly useful since these areas present the most severe traffic congestion. These problems have been recognized, and many systems have been developed to attempt to overcome them.

The magnetic sensing approach, used by the California PATH project and FROG Navigation Systems, also poses difficulties which prevent its use from becoming widespread. Most notably, the magnetic plugs, which are embedded in the roadway, must be placed very accurately (PATH)

or their position must be measured accurately after installation (FROG). This makes the installation of magnetic based systems quite expensive. The system described here involves the use of devices embedded in or on the roadway; however, a high degree of accuracy is not required when installing the devices.

Proposed herein is an inexpensive Vehicle Positioning System using RFID technology (VPS) designed to augment GPS in problematic areas and for applications where GPS provides insufficient performance, or is unavailable. This proposed system uses passive RFID tags placed periodically in or over the pavement and an on-vehicle RFID reader. The RFID tag contains the road name/designation, longitudinal position information in the form of a distance from a known reference, and the lane in which the tag is placed. As a vehicle passes over the RFID tag, the RFID tag reader collects this information, allowing the vehicle to "know" unambiguously its position on the road network. Integration of RFID data with vehicle odometry yields greater longitudinal distance accuracy. Lane position, as used herein, includes an identifier of the road of travel, the specific lane, the direction of travel, and the longitudinal distance from a known reference. It is important to note that by using the described lane position, no separate map database is needed on-vehicle, as would be the case for a method based on storing GPS coordinates in the RFID tags[1].

This system does provide global positioning, but with a reference system different than the WGS 84 or NAD 83 used by most GPS systems. Although the VPS provided position information does not allow one to place oneself at a specific location on Earth, it provides precisely the information needed for many ITS applications – the longitudinal position of a vehicle in a particular lane on a particular road of the transportation network. In addition to providing the core set of information required to position vehicles on the transportation network, the RFID tags could also be programmed with additional information to tailor the system for specific ITS applications, such as intelligent speed adaptation, or in-vehicle signing.

One such ITS application, which we believe requires the greatest degree of positioning accuracy, is rear-end collision avoidance. Rear-end collision avoidance has also been identified by the Crash Avoidance Metrics Partnership (CAMP) as being a high priority application which requires the use of inter-vehicle communication. In order to better understand the performance requirements of VPS for rear-end collision avoidance, its implications on the needed specifications for VPS were further investigated.

In 2003 the National Highway Traffic Safety Administration (NHTSA) estimated that there were over 1.8 million rear-end crashes in the United States, which accounted for 29.6% of all crashes. Of those 1.8 million crashes, 1% resulted in fatalities, 30% resulted in injuries and 69% resulted in property damage only [2]. Similarly, in 2004 the Minnesota Department of Transportation (Mn/DOT) estimated that there were over 25,000 rear-end crashes, which accounted for 28% of all crashes. Of these 25,000 crashes, 0.07% resulted in fatalities, 31.14% resulted in injuries, and 68.79% resulted in property damage only [32]. While these statistics show that the severity of rear-end crashes is usually relatively low, the large number of occurrences make them quite costly in both property damage, and lost time due to the traffic congestion which they generate. Reducing the likelihood of rear-end crashes has been an active area of research for several years;

[1] The RFID tags, however, could store/provide latitude and longitude in the WGS 84 coordinate frame.

however, GPS has never been chosen as the enabling position sensing technology, because it lacks robustness in urban environments.

Also important to note is that the areas in which the greatest benefit would be seen from the deployment of driver support systems, are the urban areas in which GPS lacks robustness. In 2004, there were nearly 11,000 crashes on the Twin Cities metro area freeways[2] and "these types of crashes are typically side-swipe or rear-end type collisions" [33]. Figure 1.1 shows a map of the Twin Cities freeways, which indicates the locations of these crashes. Given the rear-end/side-swipe nature of these crashes, it is likely that the number of crashes on the Twin Cities freeways could be significantly reduced by deploying new driver support systems which assist the driver with lane change maneuvers, and which help to reduce the risk of rear-end collisions. As we see it, the longitudinal position and lane-position capabilities required to enable the development of such driver support systems can be provided by VPS, but cannot be provided by existing positioning technologies such as GPS, radar, or computer vision due to their lack of robustness.

[2] Data and corresponding Figure 1.1 provided by Brian Kary at the Minnesota Department of Transportation. Data will appear in "Freeway Volume-Crash Summary, 2004 Data".

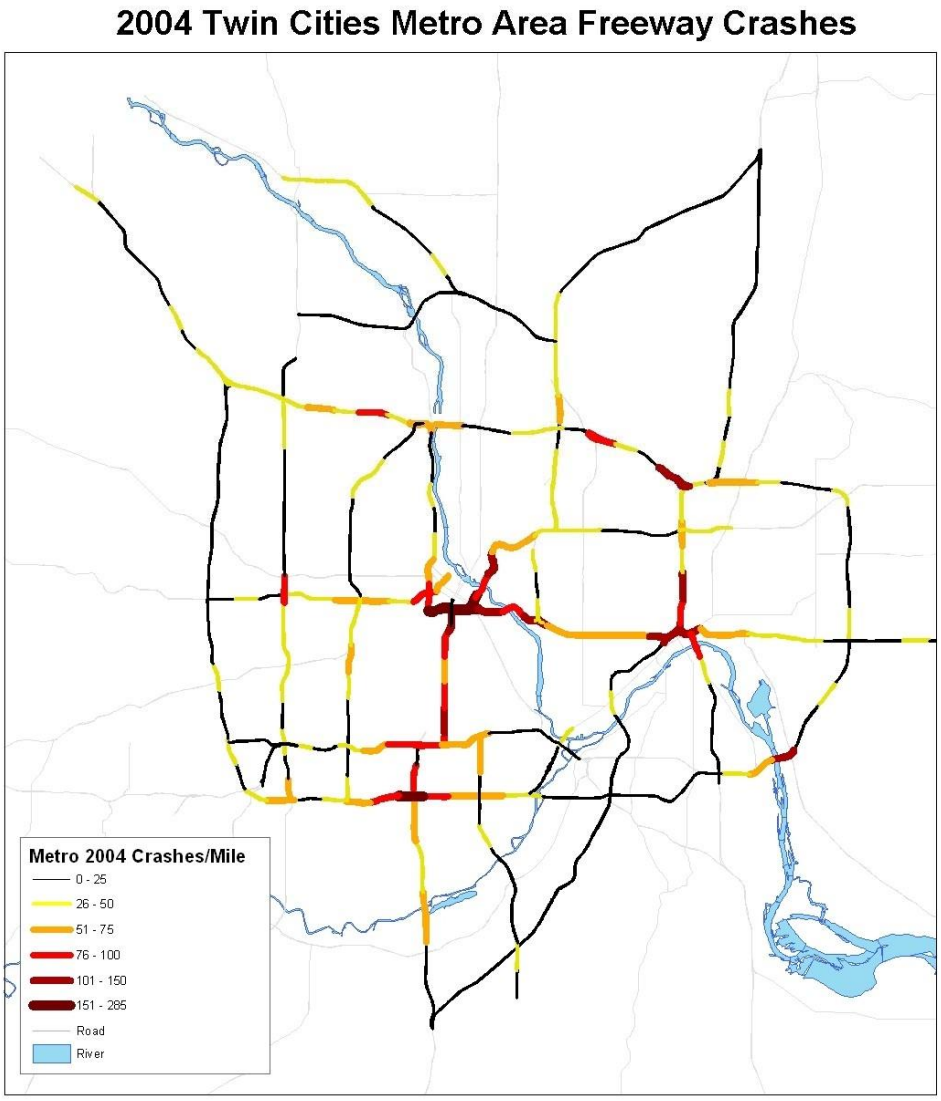

Figure 1.1: Location of crashes on Twin Cities metro area freeways in 2004.

Despite these limitations, there have been several attempts at designing systems to help drivers avoid rear-end crashes using radar; the systems range from adaptive cruise control (ACC) to rear-end collision warning systems. Previous designs for rear-end collision warning systems [3, 4, 26 – 31] used radar to acquire range, range rate and deceleration data. A more novel approach proposed the use of radar to detect the range and range rate for a platoon of three vehicles, which included the host, and the two vehicles immediately downstream[3] of the host [5]. It is likely that these systems could be improved upon if the host was able to acquire range, range rate, deceleration, vehicle length and brake light status data for a lead platoon. With the emergence of dedicated short range communication (DSRC) as a means to support the necessary vehicle-vehicle and vehicle-infrastructure communication [6, 24], the ability to gain access to this data becomes increasingly more viable.

[3] Downstream vehicles are those located in front of the host, whereas upstream vehicles are located behind the host.

Assuming that DSRC coupled with VPS will enable the host vehicle to have access to the position, velocity, acceleration, vehicle length and brake light status data for each vehicle in its immediate surrounding, one has the ability to assess the stability of a platoon of vehicles located immediately in front of the host vehicle, and to provide feedback to the driver informing him or her of their current level of risk. Such a risk metric can be used by the driver to stop as needed. This is especially important when the driver of the host vehicle cannot see vehicles in front of the vehicle immediately downstream, either because that vehicle is too large, or sight lines on the road are inadequate. Given this concept, three significant questions arise:

1. How does one assess the stability of the vehicles located immediately in front of the host (lead platoon) and compute a level of risk associated with this platoon?
2. How accurately must the positions of the vehicles in the platoon be known, in order to compute the risk metric within some acceptable tolerance?
3. Using VPS as the positioning medium, what are its minimum specifications such that the vehicles in the platoon are positioned accurately enough to compute the level of risk within the acceptable tolerance?

This document will focus on describing an attempt at building VPS using existing third party RFID technology. Also, in order to give some indication of how accurately VPS must be able to position vehicles, it will focus on answering the above three questions.

1.2 RFID Overview

Commonly available RFID systems contain two major components:

1. RFID tags encoded with relevant information
2. An RFID reader

RFID tags store a small amount of information, which is transferred to the reader when it comes in close proximity to the tag. RFID technology is particularly useful because the RFID tags are passive (require no power), and have very low cost. A typical RFID system involves many tags, and one reader, where the reader would be used to gather information from each of the tags. Figure 1.2 shows a simple demonstration of how an RFID system works [25].

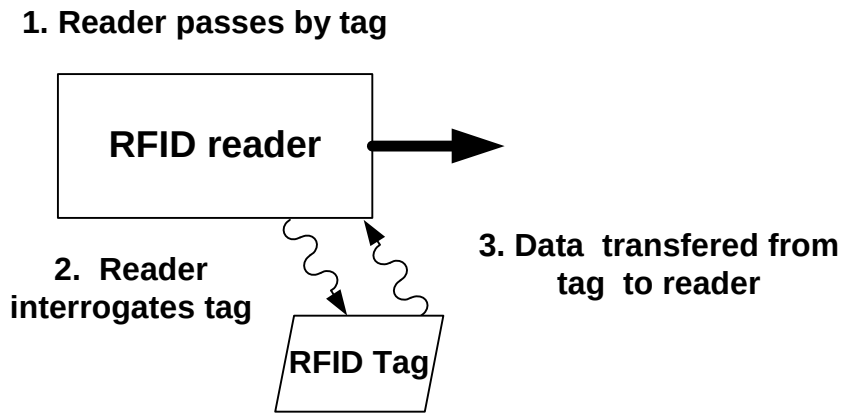

Figure 1.2: Demonstration of RFID. Right pointing arrow indicates direction of travel.

1.3 Prior Art

Given the unique nature of VPS, a complete search for relevant prior art was performed. The search encompassed all academic literature, as well as the United States Patent and Trademark Office [7] and the European Patent Office [8]. At the end of the search, four patents and one conference paper were found [9, 10, 11, 12, 13] to be relevant. Upon further inspection, it was determined that the proposed system, VPS, was clearly unique and different than the systems proposed in these patents and conference paper. The abstracts from each of the patents, as well as a summary of the conference paper can be found in Appendix A.

1.4 Document Overview

The following chapters describe the concept and a working VPS prototype using existing RFID hardware. Chapter 2 outlines the system's main components, as well as its functionality. It also discusses some of the technical considerations that must be taken into account when designing VPS, as well as some system enhancements that could be used to enable various other applications. Chapter 3 presents the results from experiments in which an existing RFID sensor was characterized to determine if it could provide the performance required to implement a fully functional VPS. Chapter 4 describes the implementation of an electronic brake light application which used VPS as the vehicle positioning medium. It also discusses a demonstration of the application's functionality on a test track. Chapter 5 discusses a novel approach to the problem of rear-end collision avoidance. In this chapter, a rear-end crash risk metric was derived using data from several lead vehicles rather than from only the lead vehicle. Finally, conclusions from this work are drawn, and recommendations for future are research are made.

2 The VPS System

2.1 System Concept

By installing RFID readers on vehicles, and by placing inexpensive RFID tags along a road, passing vehicles are able to acquire the data encoded in the tags' memory. This simple concept leads to a multitude of potential applications ranging from vehicle positioning, to current loop detector replacement, to traffic signal priority. Here, we focus our attention on the positioning of vehicles using RFID tags, which is at the core of many ITS applications. Current technology has proven itself to be insufficient for positioning vehicles accurately enough to unambiguously determine the lane in which the vehicle is driving. The VPS system is specifically designed for this task, and as such enables a number of ITS applications where a global position reference, in the sense of GPS coordinates, are not required, but where accurate, lane level positioning is required. A more complete list of potential applications which could be enabled by VPS have been identified and are listed below.

- High occupancy tolling lanes (HOT lanes)
- Truck-only tolling (TOT)
- Rear-end collision warning
- Electronic brake light
- Current loop detector replacement
- Traffic signal priority for emergency and transit vehicles
- Sharp curve ahead or curve speed warning
- In-vehicle signing, including prevailing speed limit, stop sign ahead, etc.
- Traffic signal violation warning
- Pre-crash sensing for cooperative collision mitigation
- Detection of approaching vehicles; left turn assistant

- Lane change warning
- Stop sign movement assistant
- Route guidance in the absence of GPS
- Platooning
- Adaptive cruise control
- Open parking space sensing
- Engine and transmission control for improving fuel efficiency and emissions
- Indoor bus location system

Based on these potential applications, a proposed VPS system is outlined in the remainder of this chapter.

2.2 Lane Positioning Using RFID Technology

In order to perform lane positioning using RFID technology, RFID tags encoded with lane position (lane ID tags) are placed down the center of a lane, and an RFID reader (lane ID tag reader) is attached to each vehicle. As each vehicle passes over a lane ID tag, the lane ID tag reader acquires the lane position encoded in the tags.

Lane position, as previously described, includes a road identifier, lane identifier, direction of travel identifier[4], and longitudinal position. Table 2.1 shows a more detailed description of the data fields to be stored within the lane ID tags. It is worth noting that the information stored in each lane ID tag must include, but is not limited to these fields. Additional fields for different ITS applications will be discussed in section 2.5.3.

Table 2.1: Definition of lane ID tag memory fields.

Data	Description
Road identifier	Used to identify the name of the road being traveled. It stores either the name of the road, if memory permits, or an identifying code.
Lane identifier	Identifies the specific lane of travel based on a standard referencing scheme. .
Direction of travel identifier	N,S,E,W,NE,NW,SE,SW
Longitudinal position	Used to identify the distance from a reference point on the road being traveled. On an interstate highway, for example, the most recently passed mile marker can serve as the reference. Longitudinal distance could, for example, be the mile marker number plus the distance along the center of the lane from the tag to the mile marker.

[4] The direction of travel indicator may indicate the actual direction of travel of the road, or the direction designation given to the road. Consider that the actual direction of travel of a road, and its direction designation are not always the same.

2.3 System Technical Description

2.3.1 Lane ID Tag Placement

Lane ID tags are installed at periodic intervals along the center of each lane of a roadway for which vehicles require position information and/or other data needed for the various applications mentioned earlier. The spacing of the tags, as well as which lanes are outfitted with the tags, is governed by the application for which they are being used. For example, for HOT lanes, where accurate positioning is not required, one would likely space the tags farther apart than for the electronic brake light application, for which accurate positioning is required.

2.3.2 Lane ID Tag Reader Placement: E-plate

Vehicles can be outfitted with the RFID reader through the use of an electronic license plate (e-plate) which enables simple, rapid deployment. The e-plate is installed at the front of the vehicle to provide the lane ID tag reader's antennas with a less obstructed "view" of the lane ID tags. In addition to the lane ID tag reader, the e-plate includes a single board computer, which is used to control the lane ID tag reader and to store and process acquired lane positions. The e-plate may also contain an additional means of communication which allows it to interface with an infrastructure based system (ie. a road side unit), or with an in-vehicle computer. The additional means of communication may include any combination of the following:

1. Hard wire connection to/from an in-vehicle computer or short-range wireless communication (e.g. Bluetooth or Zigbee[5]) to/from an in-vehicle computer or the vehicle data bus (TX/RX)
2. Longer range wireless communication (e.g. DSRC[6]) to/from infrastructure (TX/RX) or to/from other vehicles

Figure 2.1 shows the connectivity between the various components of VPS.

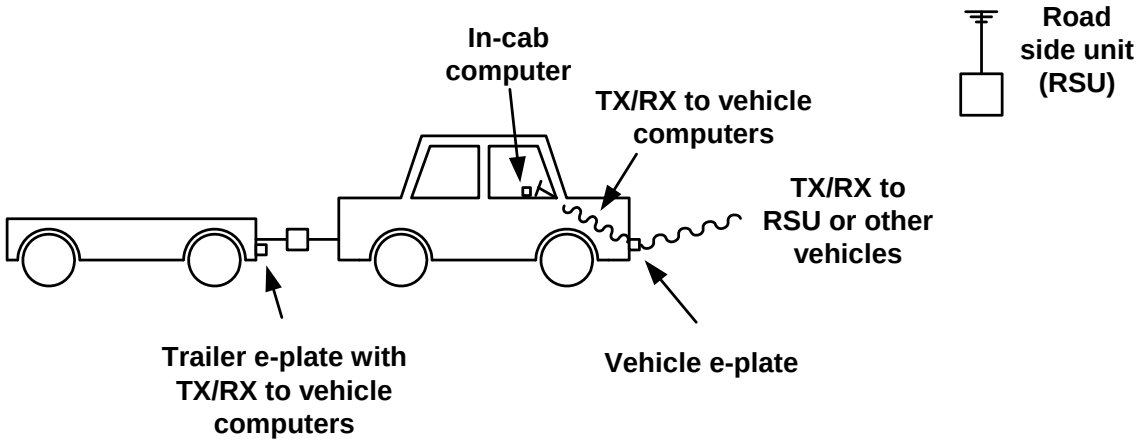

Figure 2.1: Connectivity between VPS system components.

[5] If wireless communication between the e-plate and in-vehicle computer is used, one must ensure that the messages are encrypted to avoid other vehicles from intercepting the messages.

[6] While DSRC is a likely candidate for longer range communication, VPS is not constrained to its use.

Installing both 1 and 2 on the e-plate will enable the development of a number of ITS applications which require vehicle-to-infrastructure or vehicle-to-vehicle communication. The e-plate's block diagram is shown in Figure 2.2. Notice the two optional blocks: short range TX/RX, and longer range wireless TX/RX. Only when at least one of these optional blocks is installed in the e-plate, does the system become useful.

The in-vehicle computer, which is mentioned above in communication option 1, provides vehicle data to the e-plate, or receives vehicle position or other data from the e-plate enabling the in-vehicle computer to perform functions associated with the described application. The in-vehicle computer may be one installed by the vehicle manufacturer, or one added to provide the needed functionality.

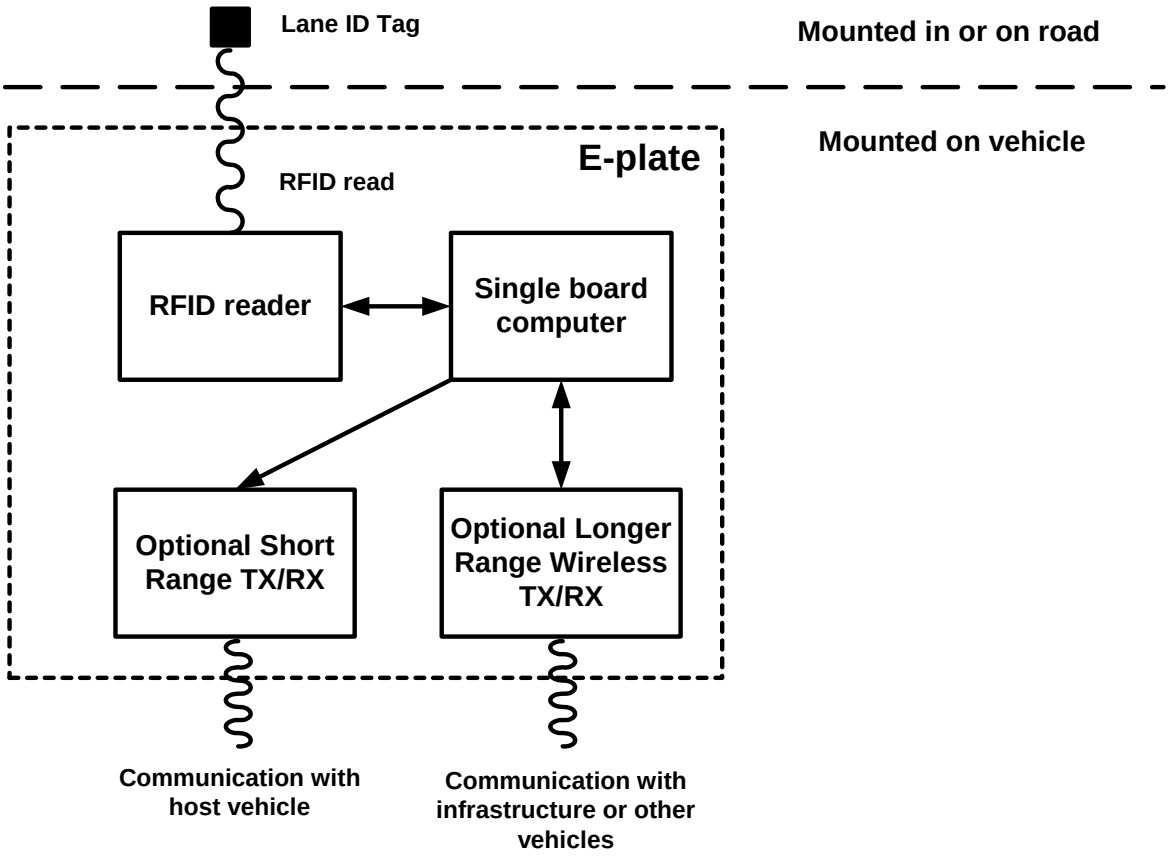

Figure 2.2: E-plate system block diagram

If neither 1 nor 2 is included in the e-plate, some other means of communicating information to the infrastructure is needed to make the system useful. One such implementation would involve placing a programmable RFID tag inside the e-plate. The lane ID tag reader/writer could then program pertinent information into the e-plate tag's memory, and a roadside RFID reader could be used to interrogate the e-plate's tag to extract the information. Figure 2.3 shows the block diagram for such an e-plate.

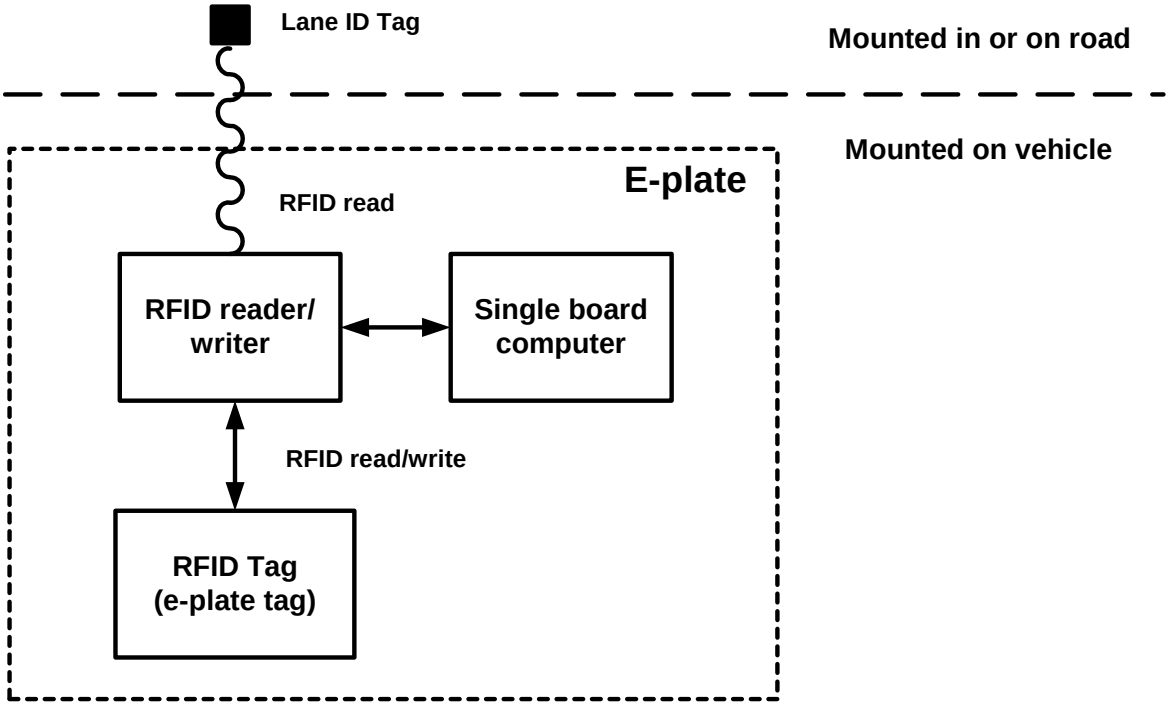

Figure 2.3: E-plate system block diagram

In addition to these functional blocks which are used to communicate information from the e-plate to the host vehicle, other vehicles, or the infrastructure, the e-plate can also be configured to store the vehicle's length[7], which is important for many safety applications. This vehicle length would be communicated along with the vehicle position. Consider that if the positions of all vehicles are known, and if the lengths of all vehicles are known, then the locations and sizes of all of the gaps can be computed. This knowledge of the gaps would enable lane change warning systems, rear-end collision avoidance systems, and various headway control applications such as platooning, and adaptive cruise control.

Figure 2.4 illustrates the computation of the gaps using the vehicle length and position information. The cross-hatched areas are known to be occupied by vehicles, and thus, the gaps can be computed. This information can be used to support a lane change warning application. For example, assume that vehicle 2 attempts to move to the middle lane. Via the computed gap information, the driver would be warned that there is not a suitable gap in the middle lane due to the presence of vehicle 4 which may not be visible to the driver of vehicle 2 because of that driver's blind zone. If vehicle 5 attempted a lane change into the right lane, however, the driver would not be warned, since there is a suitable gap.

[7] The vehicle length stored in the e-plate could be automatically adjusted when a vehicle pulls a trailer (e.g. a tractor pulling a double or triple). The vehicle length could either be programmed into the e-plate by the issuing agency when the e-plate is first initialized, or could be transmitted to the e-plate from the vehicle data bus.

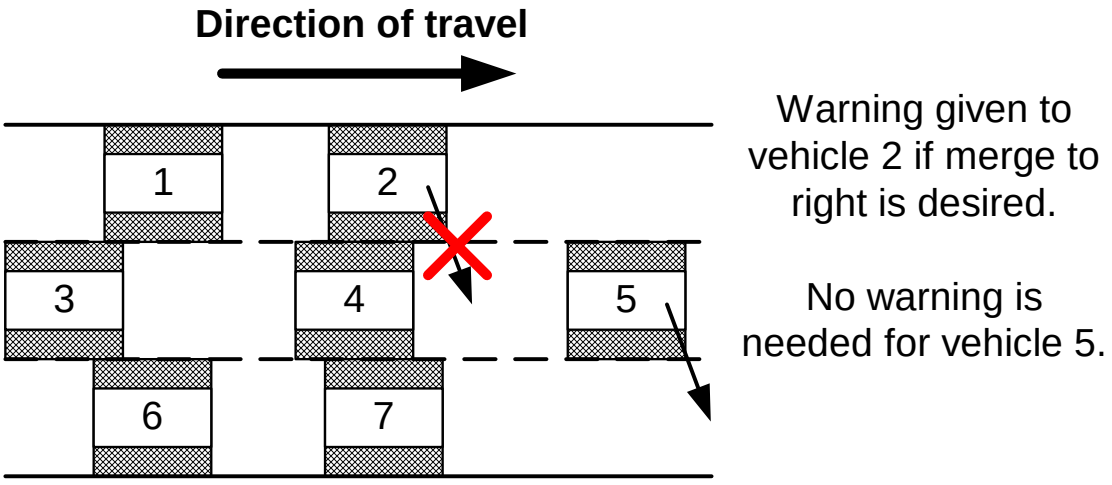

Figure 2.4: Illustration of gap computation.

2.3.3 Other Hardware

For some applications, data from the vehicle's bus is required. The e-plate should be able to acquire data from the bus using an OBDII connector (or its equivalent on a truck) and one of the communication schemes described in option 1 of Section 2.3.2.

2.3.4 Example of Preferred Operation

Figure 2.5 shows a demonstration of how the preferred system operates. Each time the vehicle passes over a lane ID tag, the vehicle's e-plate acquires the vehicle's lane position. In this particular example, the vehicle acquires the following data:

Road: I94
Direction of travel: West
Lane: 2
Longitudinal Position: 302 + x

This information can then be communicated to the infrastructure, or to other vehicles, or to the driver in the cab, depending on the application and configuration of the e-plate.

It is important to remember that the above data set works well for the simple example illustrated in Figure 2.5. However, in reality, additional consideration must be given to the exact nature of the data set so that problems associated with special cases are overcome. One such special case would involve handling the mile marker roll-over associated with the crossing of state lines.

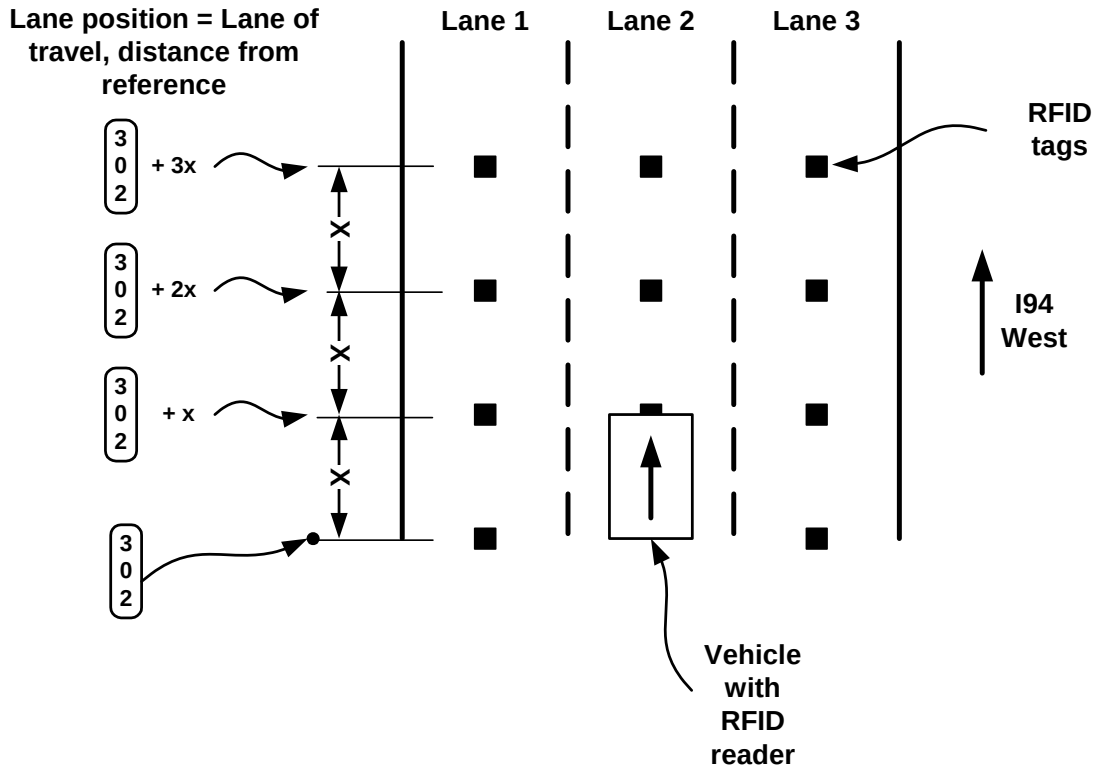

Figure 2.5: Demonstration of preferred system operation.

2.4 Technical Considerations

2.4.1 Creating the Desired RFID Reader Read Field via Antenna Design

The design of the antennas for the lane ID tag reader located in the proposed e-plate has a significant effect on the performance and accuracy of the VPS system. Ideally, the VPS system will provide high accuracy as well as highly reliable reads of the lane ID tags. However, as with all things, tradeoffs exist between accuracy and reliability.

Figure 2.6 shows some of the possible read fields for VPS's lane ID tag reader, which could be created by designing the antennas to obtain specific beam sensitivity regions[8] (typically but not necessarily elliptical shapes). Notice that the only differences between each of the configurations are the lengths of the read field's longitudinal and lateral axes. This is because the lengths of these axes are responsible for the most significant tradeoffs associated with VPS.

[8] Read field, or range of lane ID tag reader's antenna sensitivity.

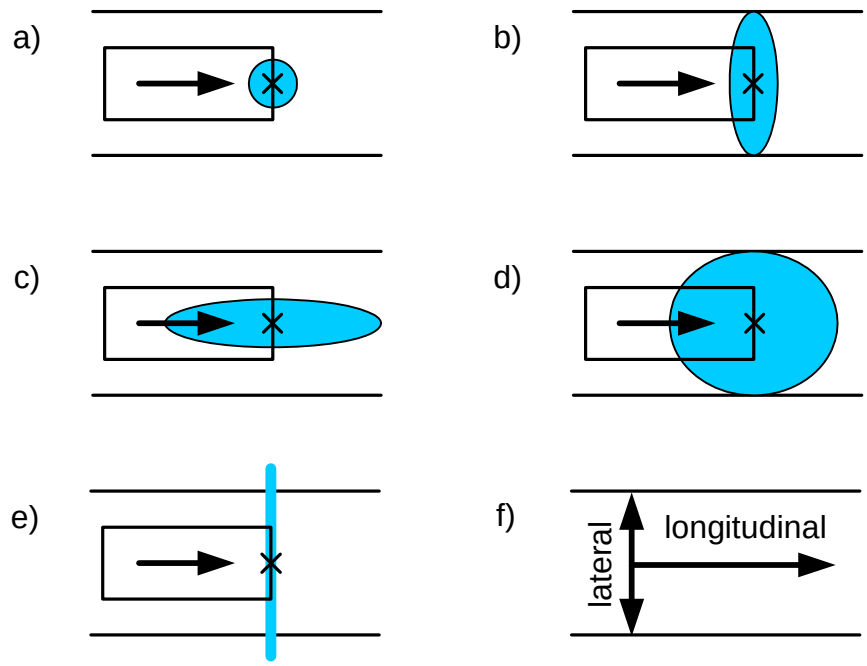

Figure 2.6: Possible read field configurations.

First consider the effects of changes to length of the longitudinal axis. By increasing the length of the longitudinal axis, one increases the length of time over which the lane ID tags will be inside the read field. This increases the likelihood of reading the lane ID tag, since the lane ID tag reader can attempt to read the lane ID tag a greater number of times. It also increases the amount of data that can be transferred from the lane ID tag to the lane ID reader, since the amount of time for the data to be transferred has increased. Also consider that the lane ID tag can be read any time during its presence inside the read field. Thus, as the length of the longitudinal axis increases, so too does the variability in the time at which the tag is read, which would lead to vehicle positioning errors since the estimate of the vehicle's position is updated only when a new lane ID tag is read. Thus, the shorter the longitudinal axis, the more accurate the longitudinal position reading and the thus, the more accurate the longitudinal position as determined by dead reckoning.

Now consider the effects of changes to the length of the lateral axis. The length of the lateral axis affects the distance by which the antenna can be separated from the lane ID tag and still produce a valid read. A large lateral axis is desirable as it increases the likelihood that a lane ID tag will be read, regardless of the lateral position of the vehicle in the lane. However, too great a lateral axis will result in reading lane ID tags in adjacent lanes, which would position the vehicle in the incorrect lane.

Figure 2.6e) represents the optimum theoretical read field. It would have a lateral axis which extended some distance over each lane boundary, a longitudinal axis of zero, and it would read

each lane ID tag passed. The longitudinal axis of zero would ensure that no positioning error would be introduced due to the variability in the time at which the lane ID tag was read. The lateral axis would extend just beyond both lane boundaries to ensure that regardless of the vehicle width and the lateral position of the vehicle within the lane, each lane ID tag would pass through the read field.

While the extension of the read field beyond the lane boundaries may seem counter intuitive, since it increases the risk of reading lane ID tags in the adjacent lane, it is in fact desirable. In order to properly position vehicles during lane change maneuvers, the lane ID tags in both lanes should be read, so that the vehicle is thought to be present in both lanes. Figure 2.7 illustrates this concept. In step 1 the vehicle is located in the right lane. Notice that since the vehicle is close to the center of the lane, the lane ID tags of the adjacent lane will not pass through the read field, and thus, will not be read. Step 2 shows the vehicle halfway through a lane change. Since the vehicle is present in both lanes of travel, it is important that the vehicle read the lane ID tags in both lanes[9]. In step 3, the vehicle has completed the lane change, and begins to read only those tags located in the left lane. Figure 2.7 also illustrates that for applications in which lane change detection is required, the lane ID tags should be installed longitudinally along the lane with a spacing of half the minimum distance required to make a lane change. A typical lane change requires a minimum of approximately 50 m of longitudinal travel (at 60 mph). Thus, the longitudinal spacing should be approximately 25 m to ensure that the transition state (step 2) is detected.

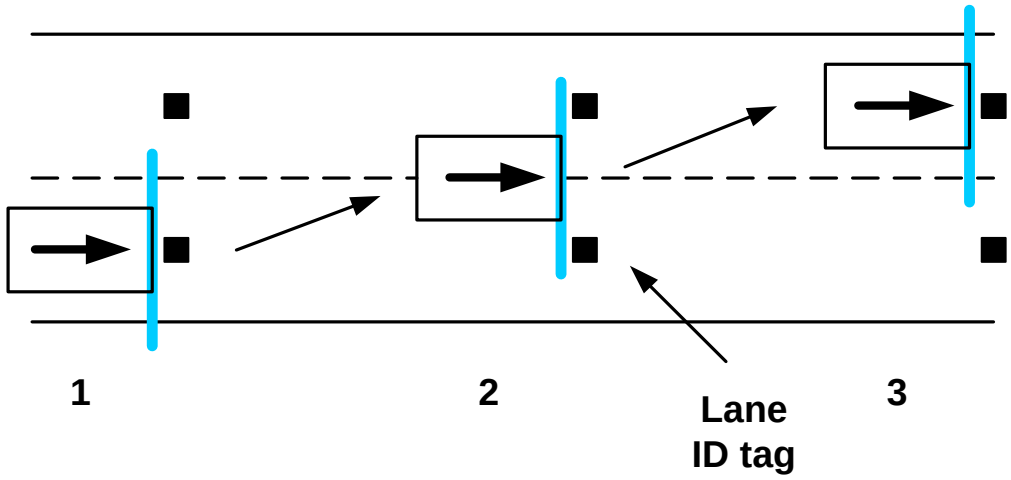

Figure 2.7: Illustration of VPS's handling of lane change maneuvers.

It is unlikely that the theoretical optimum read field can be perfectly realized[10], however, the general design of the antennas should ensure that all lane ID tags passed are read, that the read

[9] Detection of vehicles in both lanes of travel when executing a lane change is very important for applications such as rear-end collision avoidance, since a vehicle in this state is a potential threat to both lanes of travel.
[10] The theoretically desirable read field may be possible with a phased array of antennas, but this may be prohibitively expensive.

field's longitudinal axis is a minimum, and that the read field's lateral axis extends far enough beyond the lane boundaries so that lane changes can be detected, as described above.

2.4.2 Data Storage

Here we will begin by assuming an omni-directional antenna which provides a circular read field with a diameter of one lane width, 3.66 m (12 ft), as shown in Figure 2.6d). This spatial limitation, combined with the maximum speed of vehicles for which the system must operate properly, and the maximum data transfer rate of the RFID system, defines the amount of data that can be stored in the lane ID tag.

To determine the amount of data that can be read in this 3.66 m segment, consider the following definitions:

- **Response time** t_R: time (seconds) between the lane ID tag entering the read field of the lane ID tag reader, and when the data transfer begins
- **Transfer rate** TR: rate (bit/s) at which data is transferred from the lane ID tag to the lane ID tag reader
- **Distance of travel** DT: distance for which the lane ID tag reader is within the range of the tag (3.66 m)
- **Maximum speed** of passing vehicles: v_{MAX} (m/s)
- **Maximum amount of data which can be transferred**: $d_{\max}$ (bits)

With these definitions, it follows that

$$d_{\max} = \left(\frac{DT}{v_{mzx}} - t_r \right) * TR$$

Assuming a maximum speed of 128.7 km/h (80 mph), a response time of 0.075 seconds, a distance of travel of 3.66 m, and a data transfer rate of 70,000 bits/s, the theoretical maximum amount of data which can be transferred from the lane ID tag to the lane ID tag reader is ~ 1900 bits.

This compares favorably to the data load for the positioning system. Assuming lane distance, lane of travel, heading, and lane number are stored in the lane ID tag, the data payload can be described as:

a. distance from reference (probably mile post + feet from milepost)[11] = two 16 bit integers = 32 bits

[11] Here we refer to typical United States longitudinal references, and thus, we do not use metric units.

b. lane of travel = 8 bits
c. heading = 4 bits
d. road name or identifier = 32 bits

Thus, 80 bits are needed to store the positioning information. Including header and footer (checksum) overhead, the expected total amount of data to be transferred is a maximum of 120 bits, which is considerably less than the proposed allowable maximum of 1900 bits.

It is worth restating that the above analysis assumes the use of an omni-directional antenna. Other antenna designs, as discussed in section 2.4.1, could be used to achieve elliptical read fields, which would improve the maximum data transfer capability of the system.

2.4.3 Vehicle Position Estimation

Using VPS, vehicles have an accurate estimate of their lane position only at the instant they pass over each lane ID tag. In order to develop a better estimate of the vehicle's longitudinal position when the vehicle is between lane ID tags, vehicle odometry can be used. This would involve simply integrating the speed (as obtained from the vehicle data bus as described in section 2.3.3) over time to determine the distance the vehicle has traveled since reading the last lane ID tag.

2.5 System Enhancements

The calculation shown in section 2.4.2 showed that there exists considerable excess capacity in the lane ID tags. Small enhancements to the data stored in each lane ID tag will facilitate a much broader range of applications.

2.5.1 Alternative Installation – Two Lane ID Tag Readers

The installation discussed in this chapter involved lane ID tags placed down the center of each lane, with the lane ID tag reader centered at the front of vehicles. This particular installation method is preferred because it allows for rapid deployment through the use of an e-plate with a single lane ID tag reader. Another installation method involves two lane ID tag readers (one on each side of the vehicle[12]) with the lane ID tags installed along the lane boundaries. This method simplifies the procedure for installing the lane ID tags in the road, since a lane marking tape with lane ID tags embedded could be used. Figure 2.8 shows this alternative installation.

[12] The lane ID tag readers need not be installed on the sides of the vehicles. One configuration would have them installed 1 m offset in both directions from the vehicle center line.

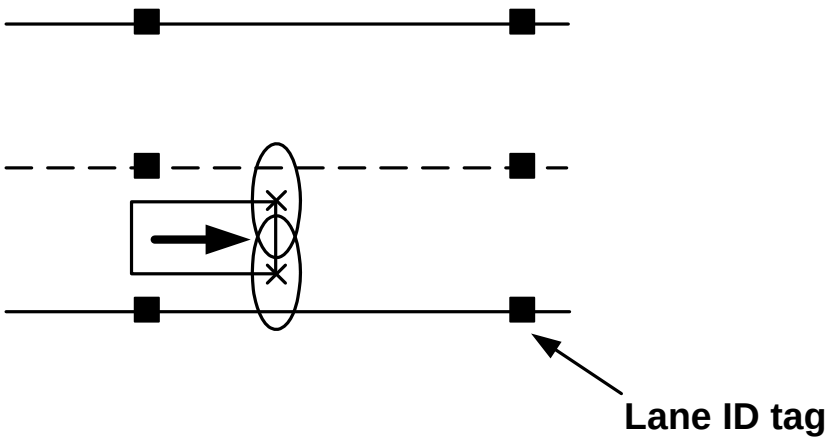

Figure 2.8: Alternative installation for lane ID tags and lane ID tag reader.

For this alternative, each lane ID tag would be encoded with the lane boundary, rather than the lane. This would allow the vehicle to determine which lane boundaries it was in-between, and thus, the lane of travel.

For the same reasons as in the previously discussed installation, the theoretical optimum read field has a longitudinal axis of zero. The lateral axis, in order to guarantee correct operation for narrow vehicles, must be slightly less than a lane width. This will ensure that the left lane ID tag reader cannot read the right lane ID tag, and vice versa, even for narrow vehicles. Also, it would allow for the lane ID tag readers to be installed any distance from the center of the vehicle. Figure 2.9 shows this theoretical optimum, where each lane ID tag reader has a lateral axis of slightly less than a lane width. The locations of the two lane ID tag readers, their individual read fields, as well as the combined read field are shown in the diagram.

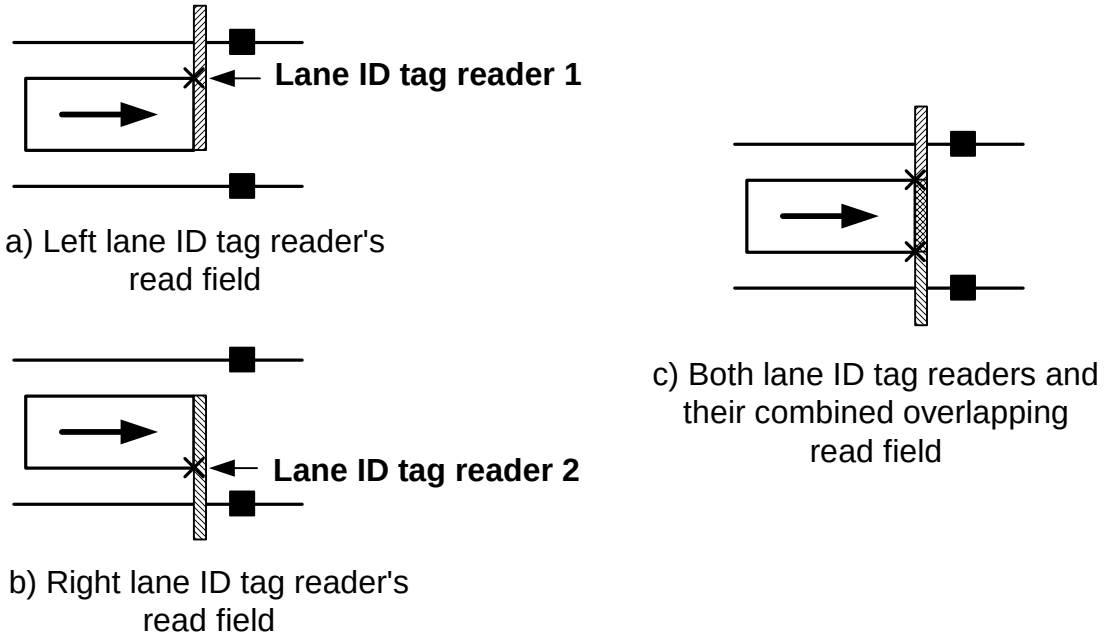

Figure 2.9: Optimum theoretical read field.

Figure 2.10 shows a lane change maneuver, and illustrates how the alternative installation handles lane change detection. In step 1, the vehicle's left lane ID tag reader reads the lane ID tags in the left lane boundary, and the right lane ID tag reader reads the lane ID tags in the right lane boundary. When the vehicle straddles the middle lane boundary, as depicted in step 2, both the left and right lane ID tag readers read the lane ID tags of the middle lane boundary, which indicates that the vehicle is straddling the middle lane boundary. Finally, in step 3, the vehicle has completed the lane change, and is back to reading lane ID tags as in step 1.

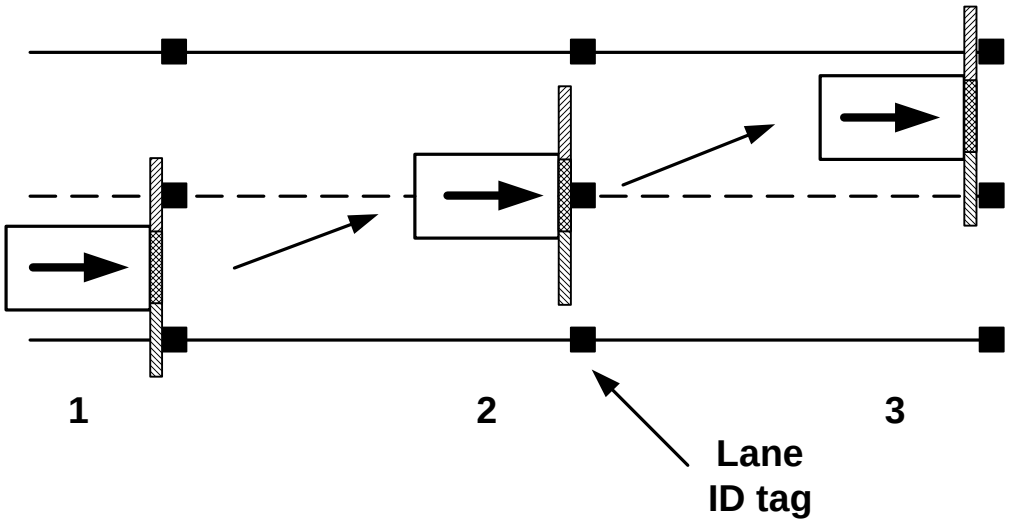

Figure 2.10: Illustration of VPS's handling of lane change maneuvers for the alternative installation.

As with the single reader installation, it is unlikely that the theoretical optimum read field can be realized. Most probably, the read field for each reader would be narrower than a lane width. This would present difficulties for installations which required the two lane ID tag readers to be separated by a distance greater than half of one lane width, since there may be insufficient overlap of the two read fields at the center, which would prevent lane change detection. Also, regardless of the width of the read field, narrow vehicles present installation difficulties. Remember that the lane ID tag readers need to be separated by some distance so that the left lane ID tag reader does not read the right lane ID tag, and vice versa. Achieving the necessary lane ID tag reader spacing for narrow vehicles, such as motorcycles, may be problematic.

2.5.2 Alternative Installation – Multiple Lane ID Tag Readers

As an extension to the installation method discussed in the previous section, consider installing multiple lane ID tag readers at the front of the vehicle. In the two reader case, there are three distinct read zones, as shown in Figure 2.11. Read zone 2, located between the two readers, is an area in which the read fields of the two readers overlap. Thus, if a tag was present in this zone, it would be detected by both readers. As discussed previously, this zone would be used to detect that the vehicle is straddling a lane boundary.

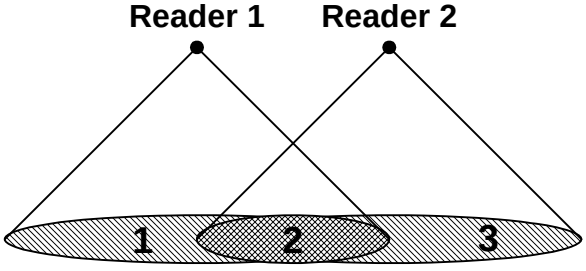

Figure 2.11: 3 distinct read field zones with 2 readers installed.

Now consider the case when additional readers are added; more read zones would now be present. Figure 2.12 shows a system which includes four readers, yielding 7 distinct read zones. By adding even more readers, a greater number of read zones would be present. These read zones could be used to detect the lateral position of the vehicle within a lane, which would be useful for applications such as lane change assist, merge assist, lane departure warning, etc.

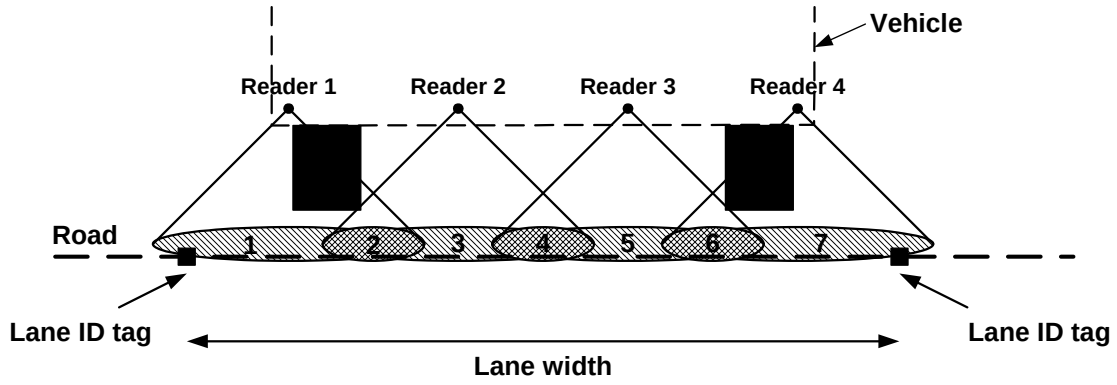

Figure 2.12: 7 distinct read field zones with 4 readers installed.

2.5.3 Additional Memory in RFID Tags

If additional information is stored in each lane ID tag, additional applications are possible. The types of additional information that could be stored in the lane ID tags include, but are not limited to:

1. Information needed for safety purposes
   - Distance to traffic signal ahead
   - Distance to stop bar of an upcoming intersection
   - Sharp curve ahead
   - Information about the geometry of upcoming intersections to help prevent crashes or to help with merging
   - Local speed limits (and other information for in-vehicle signing or display)

2. Information needed for navigation purposes
   - Upcoming ramp on right or left
   - Identify protected left and right turn lanes
   - Distance to protected right and left turn lanes

3. Other information that is dependent upon the application

2.5.4 Using Read/Write RFID Tags

By using read-write lane ID tags rather than read-only tags, even a wider range of applications can be enabled by VPS. For example, the lane ID tags could be programmed to relay up-to-date

road information to passing vehicles, such as construction zones, lane closures, road conditions, etc. in the event that other means of communicating to the vehicle are unavailable.

The use of such read/write lane ID tags would, however, require the use of a data encryption scheme to ensure the security of the lane ID tags' data. Also, some type of write protection would need to be employed to avoid the lane ID tags from being written to by unauthorized parties.

2.5.5 Other Internal or Administrative Functionality

Clearly other functionalities would have to be designed into the system such as e-plate initialization, automated self-diagnostics that would flag the driver, the vehicle and the road side unit that the e-plate is not functional and requires maintenance. A watchdog processor might be included to always monitor the system. And last but not least, a cost-efficient system would need to be designed for installing and programming the lane ID tags.

3 Characterizing an RFID Sensing System

3.1 Test Motivation

In order to determine if existing RFID technology could meet the needs of VPS, RFID equipment was purchased, and a development system was built so that it could be characterized. The Matrics AR400 reader/writer as well as Matrics Class 0 (passive, read only) and 0+ (passive, read/write) tags were purchased. The reader, which operated in the unlicensed 902 – 928 MHz band, was widely regarded as one of the highest performance readers in the passive RFID market. The passive tags, which offered 12 bytes of user memory, were also considered to be some of the highest performance tags available. For these reasons, the Matrics equipment was purchased, and integrated into the development system. At the completion of the sensor characterization experiments, the likelihood of using existing RFID technology to enable VPS will be known. If existing RFID technology does not provide the desired performance, a better understanding of what characteristics must be improved to make the development of VPS feasible.

To ensure that VPS will function as desired, the RFID equipment would have to provide a minimum level of performance. The most stringent requirements were placed on the RFID equipment's read range, read percentage, new tag reliability and latency. Ideally, the read range would be optimized, as discussed in the section 2.4.1, read percentage would be 100%, new tag reliability would be 100%, and the variability in latency would be extremely small. Table 3.1 summarizes some of the adverse effects that would be introduced by deviation from these idealities.

Table 3.1: Implications of non-ideal RFID system performance on VPS operation.

Read range	If the read range was too large, it would extend beyond the lane boundaries, and vehicles may read lane ID tags from the adjacent lane. If the read range was too small, vehicles may not read lane ID tags in their own lane of travel.
Read percentage	If the read percentage was too low, vehicles would not read each lane ID tag passed over, which would lead to longitudinal positioning errors.
New tag reliability	If each new tag was not guaranteed to be functional, the installation process would be complicated, since each tag would have to be tested prior to installation.
Latency	Mean latency can be corrected for, but the variability in latency cannot. Thus, the variability in latency must be small enough so that the position estimate falls within some allowable tolerance. ($2\sigma = 0.01$ s would yield sub-meter longitudinal positioning accuracy at speeds up to 100 mph).

Also crucial to the operation of VPS was that the RFID equipment provide acceptable performance for the above four characteristics over the range of typical driving speeds (30 – 70 mph).

The characterization experiments would also be used to determine which RFID antenna orientation (height above pavement, pitch angle, yaw angle) yielded the best performance for the above four characteristics over the range of typical driving speeds[13].

3.2 Physical Test Setup

3.2.1 Vehicle Installation

In order to characterize the RFID sensor (Matrics AR400), the test vehicle (Infiniti M45) was outfitted with a system that would ideally be miniaturized, and deployed through the use of an electronic license plate (e-plate). The e-plate would contain an RFID reader, RFID antennas, and a control computer. A block diagram of the development system is shown below in Figure 3.1.

[13] Another variable, known as "tries", was tested, as well. "Tries" is a configurable RFID reader parameter. It is an indicator of how "hard" the reader tries to read each tag that passes through the read field. The higher the number of tries, the harder the reader tries to read each tag in its read field, and thus, the greater the latency.

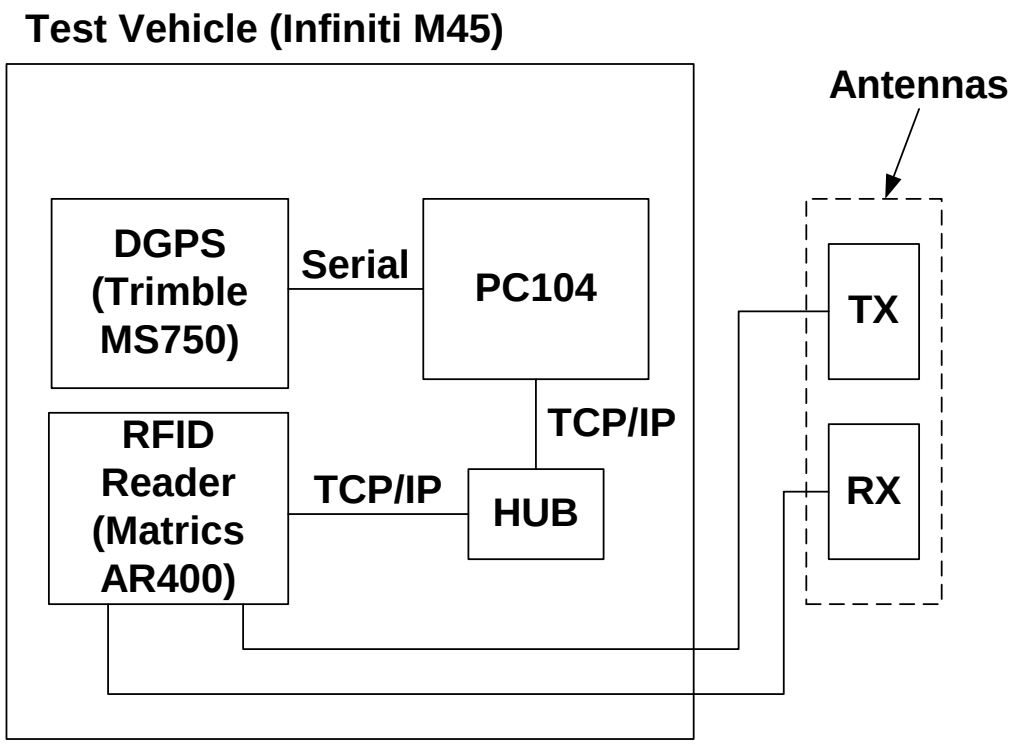

Figure 3.1: Development system block diagram.

Notice the DGPS block, and the TCP/IP connection between the control computer and the RFID reader. In an actual implementation of the e-plate, both of these blocks would be removed. The DGPS block was included strictly for the purpose of post-experiment data analysis, and the TCP/IP interface was necessary for communication with the third party RFID reader. Ideally, the RFID reader would be tied directly to the processor in the control computer, eliminating the TCP/IP interface.

Also shown in Figure 3.1 are the RFID reader's antennas, which were installed at the front of the test vehicle as shown in Figure 3.2. Notice that both RFID antennas were positioned at same height above the pavement, h, had the same pitch angle, θ, and had the same yaw angle, ψ. Also note that the nominal installation for the RFID antennas, $\theta = 0^o$, $\psi = 0^o$, was chosen such that the RFID antennas were parallel to the pavement, and the long edge (8.8 inch side) of the RFID antennas were facing forward, as shown in Figure 3.2. Figure 3.3 shows a picture of the antennas installed on the test vehicle.

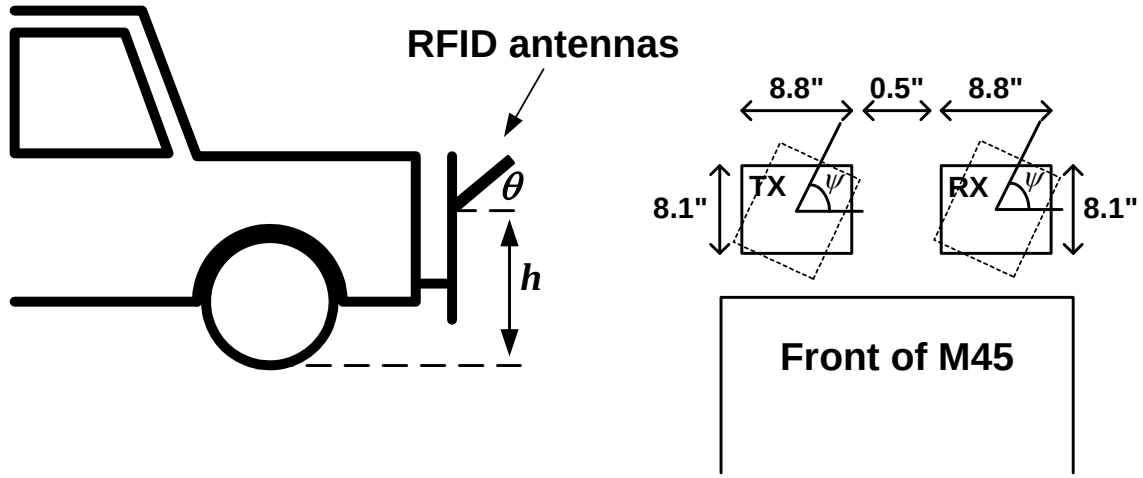

Figure 3.2: Installation of RFID antennas at front of test vehicle.

Figure 3.3: Test vehicle RFID reader antenna installation.

3.2.2 Test Track Installation

3.2.2.1 Test Track

The Minnesota Road Research Project (Mn/ROAD) was selected as the test track to be used for the characterization experiments. Mn/ROAD, which is a 4 km track with two 1.6 km straightaways, is located near Albertville, MN. Figure 3.4 shows the general shape of the track.

3.2.2.2 RFID Tag Placement

A total of 50 RFID tags (Matrics Class 0+) were placed every 76.2 m along the test track. Each tag was programmed with its corresponding tag number, which ranged from 1 – 50. The tag installation procedure involved placing a tag directly underneath the phase center of the RFID reader's transmit antenna[14], and recording the vehicle's DGPS position into a database, which would be used for post-experiment data processing. Note that the vehicle's position rather than the tag's position was recorded in the database, so that converting between the vehicle's coordinate frame and the tag's coordinate frame during data analysis could be avoided. The installation procedure for the RFID tags was as follows:

1. Place tag directly underneath RFID transmit antenna's phase center.
2. Record vehicle's DGPS position in database.
3. Drive forward 76.2 m feet.
4. Go to step 1.

Figure 3.4 shows the location of each RFID tag placed on the test track. Also, Table 3.2 gives a physical description of the location of each tag.

[14] Through lab experimentation, it was determined that the reading of RFID tags was sensitive only to the location of the transmit antenna. As long as the receive antenna was sufficiently close to the RFID tag, so that it could receive the tag's transmitted data packet, the read performance remained the same. Thus, the tag was placed directly beneath the phase center of the transmit antenna.

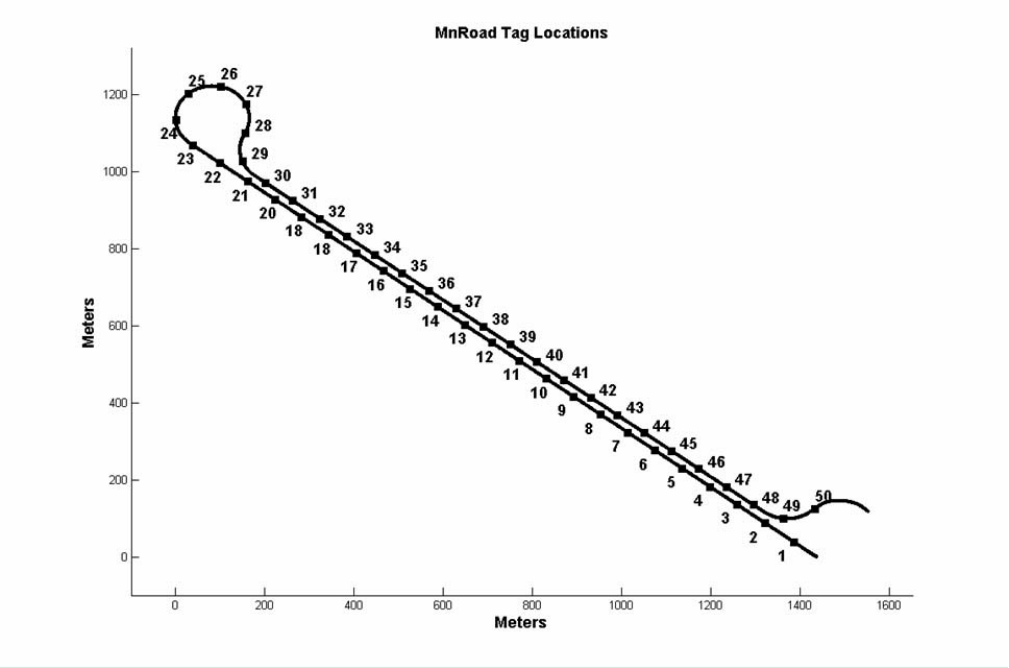

Figure 3.4: RFID tag locations at Mn/ROAD.

Table 3.2: Physical description of tag locations.

	Asphalt	Concrete
Straight	5-22, 31-37	1-4, 38-48
Curve	none	23-29, 49, 50

3.3 Data Acquisition

3.3.1 Data to be Acquired

In order to characterize the RFID sensor, the following data was collected:

1. DGPS position, timestamp, and quality (fix, float, autonomous) recorded for all laps.
2. Tag reads recorded for all laps.
3. A high accuracy timer (µs resolution) was also used. The timer's value was recorded for each DGPS sample, and for each tag read.

Figure 3.5 shows a signal flow graph for the data which was acquired during the experimentation.

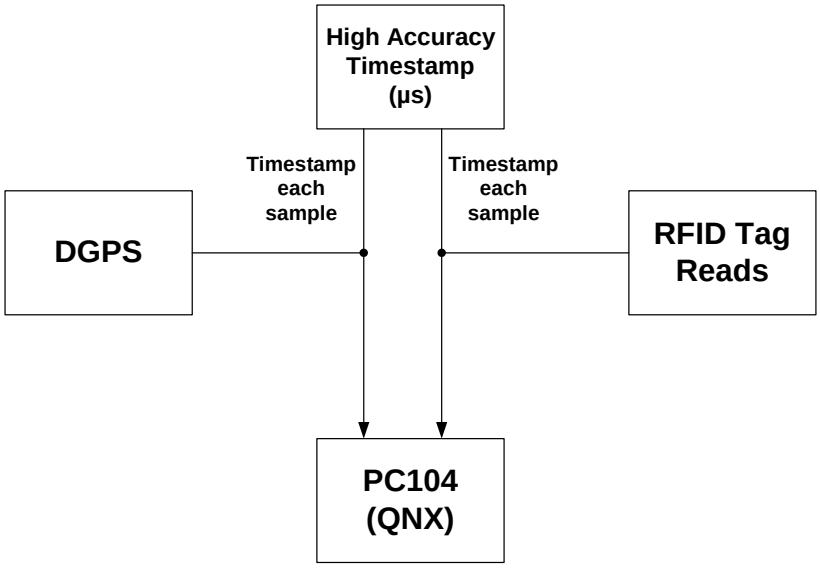

Figure 3.5: Data acquisition signal flow chart.

3.3.2 Role of DGPS in the Data Analysis

DGPS data was collected by the data acquisition software at all times during the experimentation at the test track. The accuracy of the DGPS samples is shown in Table 3.3. Notice that the short baseline errors are provided, since a local base station was installed at Mn/ROAD to provide the correction signal.

Table 3.3: DGPS Accuracy

	Mean Lateral Error (cm)	SD [σ] Lateral Error (cm)	Mean Longitudinal Error (cm)	SD [σ] Longitudinal Error (cm)
Short baseline RTK	0.6	11.9	-3.3	4.4

Using the acquired DGPS data, the value of the high accuracy timer, and the positions of the RFID tags which were stored in a database, it was possible to determine the lateral deviation between the phase center of the transmit antenna and the RFID tag at the instant each tag was passed over. This information was used to create histograms for each experiment which characterized the read range. It was also used to determine the tag read latency information.

3.4 Experimental Design

Characterizing the RFID sensor involved determining the read range, read percentage, new tag reliability, and latency as a function of the RFID antenna orientation, vehicle speed, and "tries". Experiments were designed so that the dependent variables (RFID antenna orientation, vehicle speed, and "tries") could be quantified.

Determining these dependent variables allowed us to find the RFID antenna orientation which provided a read range closest to the desired read range, as described in section 2.4.1. They also allowed us to determine how reliably the reader could read the tags at typical driving speeds (30

– 70 mph), as well as the variability in tag read latency, which is crucial to being able to accurately position vehicles using RFID technology. Finally, they allowed us to determine the variability in the performance of new tags.
Tables 5, 6, and 7 show the experiments that were conducted. They outline the exact RFID antenna orientation, "tries", and speed conditions that were used for each lap.

Table 3.4: Experimental settings and laps to compute read percentage and new tag reliability as a function of RFID antenna orientation and speed.

Height (h)	Pitch (θ)	Yaw (ψ)	Tries	Speed (mph)	Laps	Tag Read Attempts
Low (10")	0^o	0^o	3	30	4	200
				40	4	200
				50	4	200
				60	4	200
				70	4	200
Low (10")	45^o	0^o	3	30	4	200
				40	4	200
				50	4	200
				60	4	200
				70	4	200
Low (12")	90^o	0^o	3	30	4	200
				40	4	200
				50	4	200
				60	4	200
				70	4	200
Medium (21")	0^o	0^o	3	30	4	200
				40	4	200
				50	4	200
				60	4	200
				70	4	200
Medium (21")	45^o	0^o	3	30	4	200
				40	4	200
				50	4	200
				60	4	200
				70	4	200
Medium (21")	0^o	90^o	3	30	4	200
				40	4	200
				50	4	200
				60	4	200
				70	4	200
Medium (21")	45^o	90^o	3	30	4	200
				40	4	200
				50	4	200
				60	4	200

				70	4	200
Medium (18")	90°	0°	3	30	4	200
				40	4	200
				50	4	200
				60	4	200
				70	4	200
High (32")	0°	0°	3	30	4	200
				40	4	200
				50	4	200
				60	4	200
				70	4	200
High (32")	45°	0°	3	30	4	200
				40	4	200
				50	4	200
				60	4	200
				70	4	200

Note: height = Medium (21"), pitch = 90°, yaw = 0°, tries = 3, speed = 30 -70 mph, was attempted, but produced such poor results that the experiment was terminated prematurely. By decreasing the height to 18", results improved dramatically, so a full data set was taken for that height setting. Similarly, for the high height setting, a pitch angle of 90° produced poor results and the experiment was terminated. Also notice that yawing of the RFID antennas was only attempted on two of the data sets. After analyzing the data from these two conditions, it was determined that the yawing of the RFID antennas did not significantly affect the system's performance, and thus, no further yawing experiments were conducted. The read performance's insensitivity to yawing of the RFID antennas also confirmed that the antennas were omnidirectional.

Table 3.5: Experimental settings and laps to compute latency as a function of RFID antenna orientation and speed.

Height (h)	**Pitch (θ)**	**Yaw (ψ)**	**Tries**	**Speed (mph)**	**Laps**	**Tag Read Attempts**
Low (10")	0°	0°	3	30	2	100
				40	2	100
				50	2	100
				60	2	100
				70	2	100
Low (10")	45°	0°	3	30	2	100
				40	2	100
				50	2	100
				60	2	100
				70	2	100
Low (12")	90°	0°	3	30	2	100
				40	2	100

				50	2	100
				60	2	100
				70	2	100
Medium (21")	0^o	0^o	3	30	2	100
				40	2	100
				50	2	100
				60	2	100
				70	2	100
Medium (21")	0^o	90^o	3	30	2	100
				40	2	100
				50	2	100
				60	2	100
				70	2	100
High (32")	0^o	0^o	3	30	2	100
				40	2	100
				50	2	100
				60	2	100
				70	2	100

Note: Because of an error in the data acquisition software for the experiments conducted in Table 3.5, latency could not be computed. Thus, the experiments were repeated so that latency could be calculated, however, only those settings which yielded the best results in the previous experiments were repeated.

Table 3.6: Experimental settings and laps to compute latency and read percentage as a function of "tries" and speed.

Height (h)	**Pitch (θ)**	**Yaw (ψ)**	**Tries**	**Speed (mph)**	**Laps**	**Tag Read Attempts**
Medium (21")	0^o	0^o	1	30	4	200
				70	4	200
Medium (21")	0^o	0^o	3	30	4	200
				70	4	200
Medium (21")	0^o	0^o	5	30	4	200
				70	4	200
Medium (21")	0^o	0^o	7	30	4	200
				70	4	200
Medium (21")	0^o	0^o	9	30	4	200
				70	4	200
Medium (21")	0^o	0^o	25	30	4	200
				70	4	200

Note: Because "tries' was an internal reader configuration, it was assumed to be independent of RFID antenna orientation, and likely speed. Thus, data was only acquired for one RFID antenna orientation and for only low (30 mph) and high speeds (70 mph).

3.5 Data Analysis

3.5.1 Description of Data Analysis Parameters

3.5.1.1 Lateral Deviation

Lateral deviation is defined as the distance, to the left or right of the tag, between the RFID transmit antenna and the tag at the instant the transmit antenna passed over the tag. A positive lateral deviation occurs when the vehicle passes to the right of the tag. A negative lateral deviation occurs when the vehicle passes to the left of the tag.

Lateral deviation was computed using:

1. The DGPS sample before passing over the tag
2. The DGPS sample after passing over the tag

Figure 3.6 shows how the lateral deviation for each tag was computed using the above data.

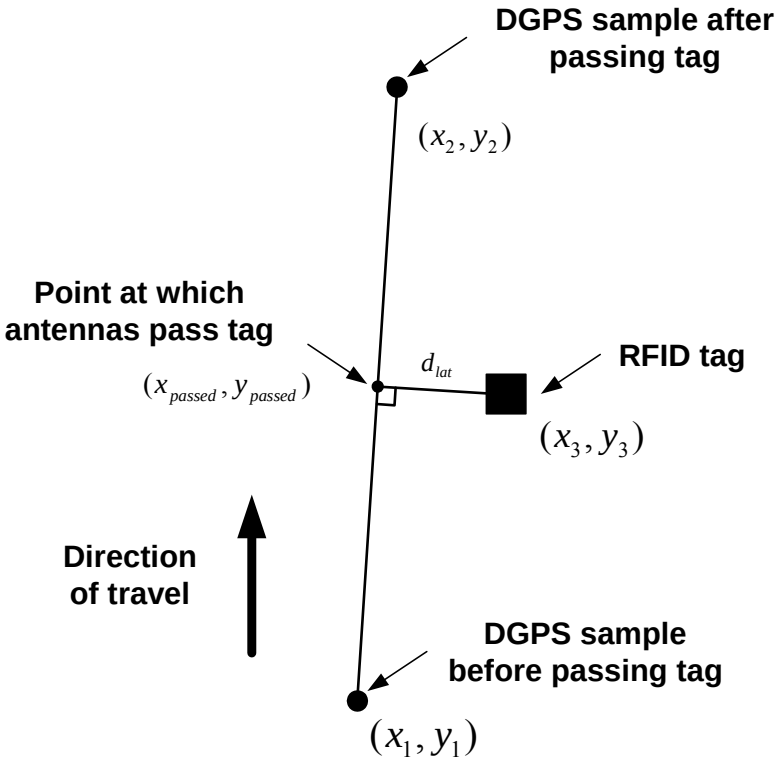

Figure 3.6: Derivation of lateral deviation.

Let the line that passes through the two DGPS samples be $y = m_1 x + b_1$.
Let the line that passes through the tag, and the point at which the phase center of the RFID transmit antenna passes the tag be $y = m_2 x + b_2$.

Solving this system of equations we get:

$$x_{passed} = \frac{b_1 - b_2}{m_2 - m_1}$$

$$y_{passed} = \frac{m_2 b_1 - m_1 b_2}{m_2 - m_1}$$

Where $m_1 = \frac{y_2 - y_1}{x_2 - x_1}$ and $m_2 = -\frac{1}{m_1}$, since the two lines are perpendicular.

Finally,

- $d_{lat} = \sqrt{\left(x_3 - x_{passed}\right)^2 + \left(y_3 - y_{passed}\right)^2}$ if the car passed to the right of the tag
- $d_{lat} = -\sqrt{\left(x_3 - x_{passed}\right)^2 + \left(y_3 - y_{passed}\right)^2}$ if the car passed to the left of the tag

3.5.1.2 Read Range

Read range is difficult to quantify. In order to properly define read range, one would need to perform a uniform distribution of read attempts, and then in some manner quantify the distribution of reads which were produced by those attempts. For example, if the uniform distribution of attempts provided a normal distribution of reads, then standard deviation would be an excellent indicator of read range. Figure 3.7 shows the ideal read attempt distribution (uniform) and a possible resulting read distribution (normal). Because of the nature of the experiment, a manually driven vehicle passing over tags, it was not possible to generate a uniform distribution of read attempts such as that depicted in Figure 3.7. Thus, rather then quantifying the read range, a read range of ±25 cm was chosen, and the read percentage within that range was computed.

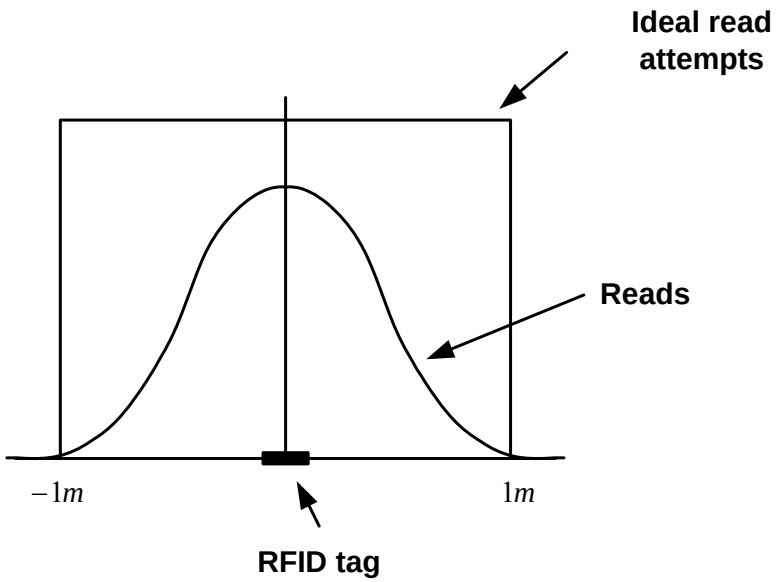

Figure 3.7: Ideal read attempt distribution (uniform) and a possible resulting read distribution (normal).

3.5.1.3 Read Percentage

Read percentage is defined as the number of tags that should have been read divided by the number of tags that were read.

$$\text{Read percentage} = \frac{reads}{attempts}$$

Based on the definition of read range, one simply must count the number of reads and read attempts within ±25 cm of the tag, and the divide the two, as shown in the above equation.

3.5.1.4 New Tag Reliability

Halfway through the experimentation the tags were replaced to determine if poor read performance for specific tags was due to:

1. The tag itself
2. Some environmental/spatial condition (interference greater at a certain location, rebar in concrete, etc…)

By comparing the read percentages of individual tags from the two tag sets, it was possible to detect which of the above two factors was responsible for the poor individual tag performance.

3.5.1.5 Latency

Latency is defined as the length of time from the moment the tag is passed over, to the moment the tag is read. Latency was computed using:

1. The DGPS sample before passing over the tag
2. The DGPS sample after passing over the tag
3. The value of the high accuracy timer for positions 1 and 2, and at the time which the tag was read

Figure 3.8 shows how latency was calculated using the above data.

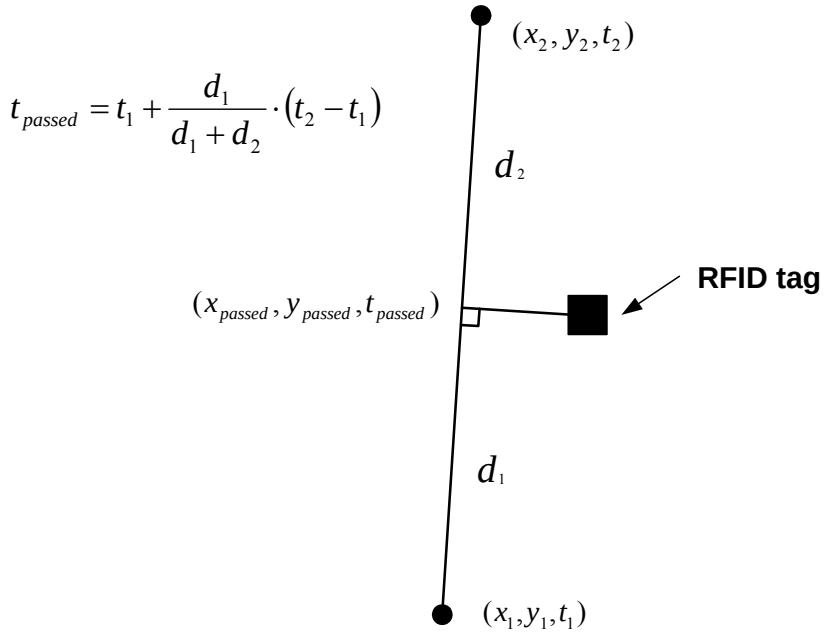

Figure 3.8: Derivation of latency.

- x_{passed}, y_{passed} were calculated as in the lateral deviation calculation shown in section 3.5.1.1
- t_{passed}, as calculated above, is the time at which the phase center of the RFID transmit antenna passed over the tag
- t_{read}, which is not shown above, is the time at which the tag was read
- Therefore, $t_{latency} = t_{read} - t_{passed}$

3.5.2 Summary of Data Analysis Results

3.5.2.1 Read Range and Read Percentage as a Function of RFID Antenna Orientation and Speed

Read range and read percentage are two important characteristics of the RFID equipment which will be used in the VPS system. In an ideal setting, the read range would be equal to one half the lane width to avoid reading tags in adjacent lanes, as illustrated in section 2.4.1. Read percentage, which is the fraction of attempted tag reads that actually resulted in a tag read, would ideally be 100%, although for certain applications such as high occupancy tolling lanes, a read percentage less than 100% suffice.

Table 3.7 summarizes the results for the first group of experiments which were conducted to determine the relationship between RFID antenna orientation, speed, read range and read percentage. The table lists each of the experimental conditions, and then provides the computed read percentages. Read ranges are best understood through inspection of the plots which follow Table 3.7.

Table 3.7: Data analysis results for read percentage as a function of RFID antenna orientation.

Height (h)	Pitch (θ)	Yaw (ψ)	Tries	Speed (mph)	Read Percentage (%)	Aggregate Read Percentage (%)
Low (10")	0°	0°	3	30	57.5	62.2
				40	77.1	
				50	62.0	
				60	77.3	
				70	70.2	
Low (10")	45°	0°	3	30	61.6	62.1
				40	69.3	
				50	59.4	
				60	79.7	
				70	66.4	
Low (12")	90°	0°	3	30	65.5	64.0
				40	69.8	
				50	59.2	
				60	69.9	
				70	66.2	
Medium (21")	0°	0°	3	30	66.3	60.7
				40	70.0	
				50	56.8	
				60	65.6	
				70	64.3	
Medium (21")	45°	0°	3	30	52.0	54.5
				40	65.0	
				50	51.6	
				60	60.1	
				70	48.6	
Medium (21")	0°	90°	3	30	59.4	59.7
				40	66.5	
				50	60.9	
				60	61.9	
				70	57.6	
Medium (21")	45°	90°	3	30	62.8	55.9
				40	65.5	
				50	53.8	
				60	58.2	
				70	50.0	
Medium (18")	90°	0°	3	30	42.3	35.2
				40	37.2	
				50	28.3	
				60	40.9	
				70	40.5	

High (32”)	0^o	0^o	3	30	71.9	68.4
				40	81.1	
				50	61.2	
				60	65.3	
				70	66.4	
High (32”)	45^o	0^o	3	30	42.6	34.2
				40	35.2	
				50	32.3	
				60	37.0	
				70	33.3	

Figures 21 – 30, which are shown below, better illustrate the data in Table 3.7, and allow one to understand read range, since quantifying it was not possible. For each experimental condition there is one set of plots, where each set contains four subplots. The subplots show histograms for the misses (top-left), reads (top-right), attempts (bottom-left), and read percentage (bottom-right). The inability to achieve a uniform distribution of attempts for each experimental condition is clearly shown in the attempts histograms for each set of plots. Because a uniform distribution of attempts was not achieved, looking at the number of reads to indicate read range would be misleading. Thus, the read percentage plots were created and are used to show the lateral range over which tags could be read. Again, because of the lack of uniformly distributed attempts, determining a single number to quantify the read range was futile, since it is fully dependent on the distribution of attempts. Thus, to gain a better understanding of the read range, one must individually investigate the read percentage plot for each experimental condition. When characterizing the overall read percentage of a particular experimental condition, the read percentage was calculated on the pre-determined range of ±25 cm as outlined in section 3.5.1.3. Notice that each subplot is overlaid with this pre-determined read range, and that the overall read percentage is printed on each read percentage subplot.

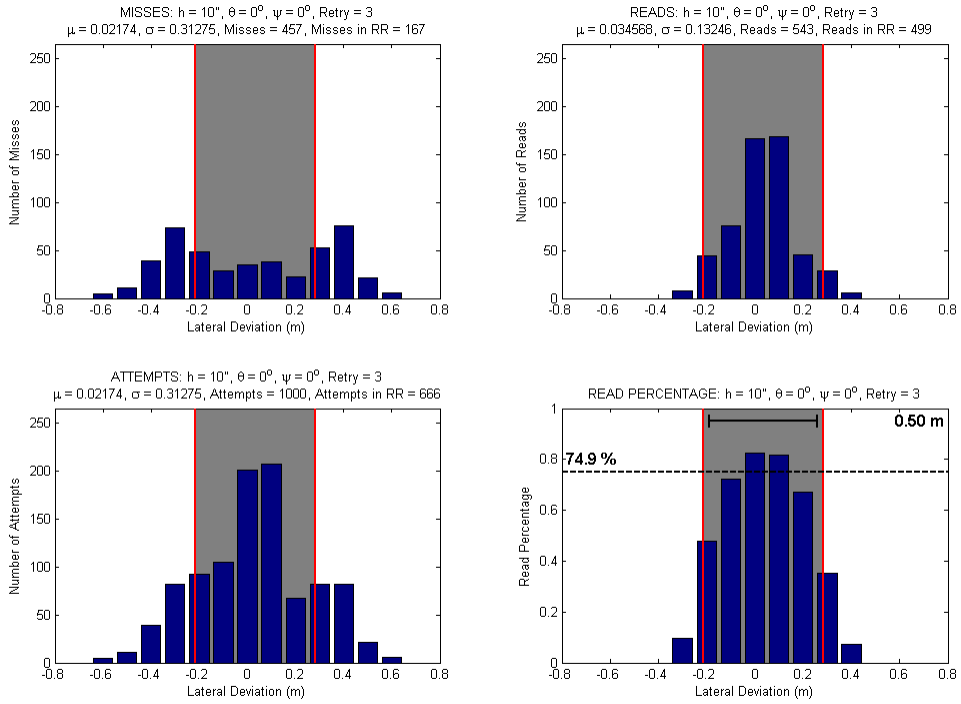

Figure 3.9: Height = Low, Pitch = 0° , Yaw = 0°

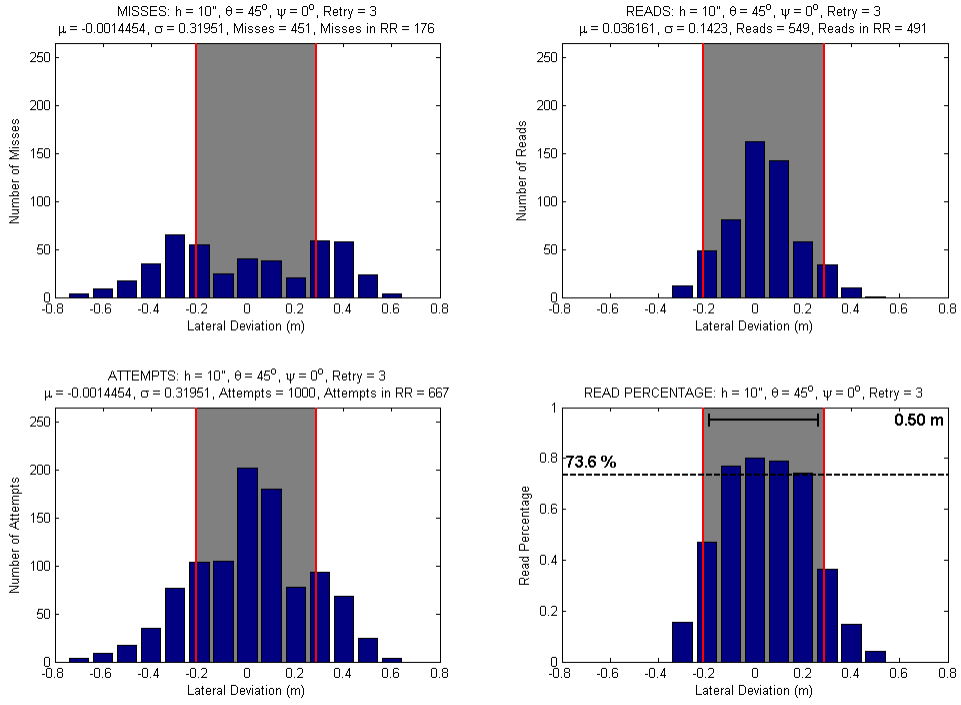

Figure 3.10: Height = Low, Pitch = 45°, Yaw = 0°

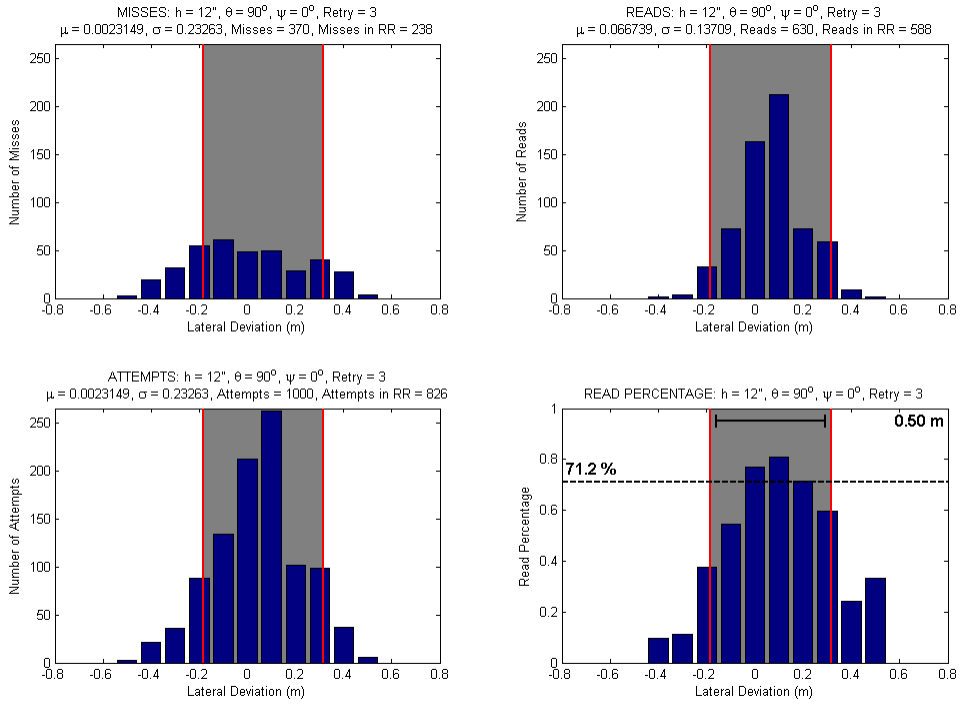

Figure 3.11: Height = Low, Pitch = 90°, Yaw = 0°

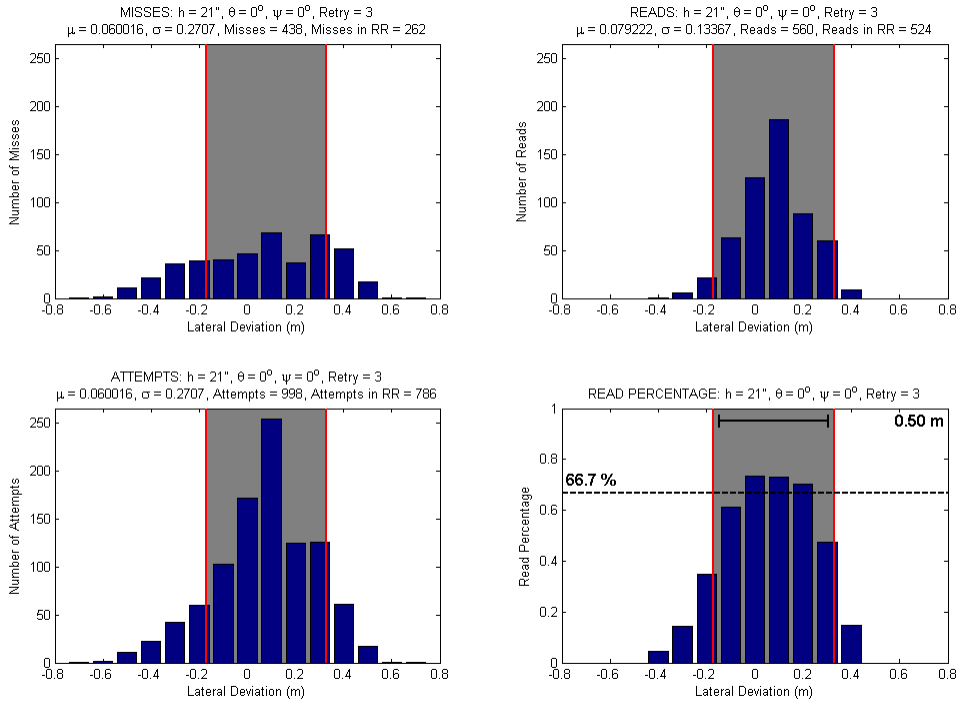

Figure 3.12: Height = Medium, Pitch = 0°, Yaw = 0°

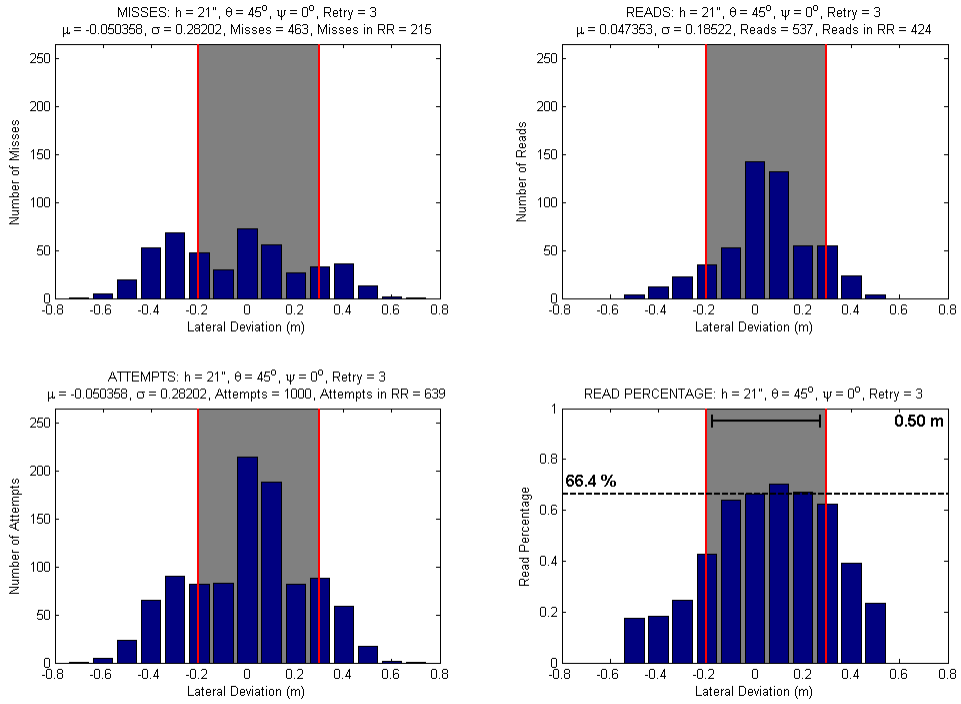

Figure 3.13: Height = Medium, Pitch = 45°, Yaw = 0°

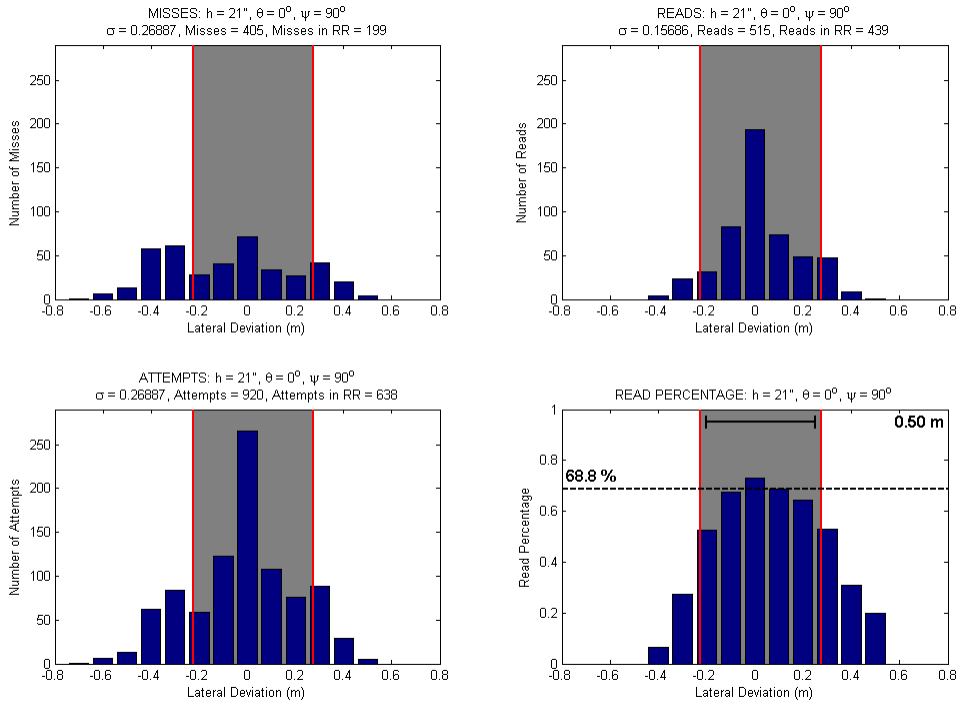

Figure 3.14: Height = Medium, Pitch = 0°, Yaw = 90°

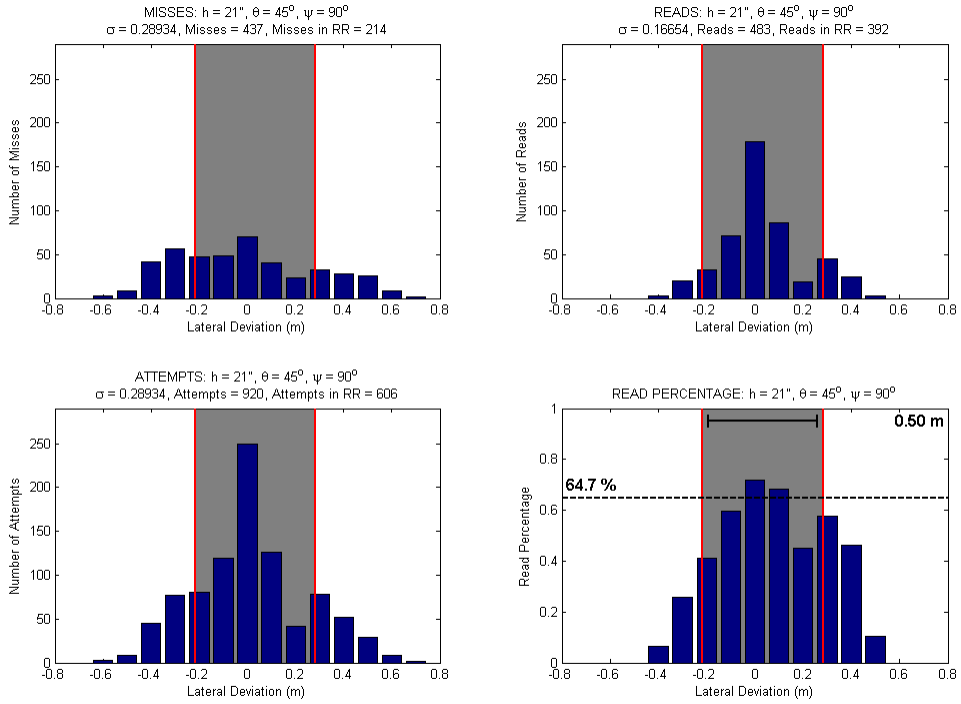

Figure 3.15: Height = Medium, Pitch = 45°, Yaw = 90°

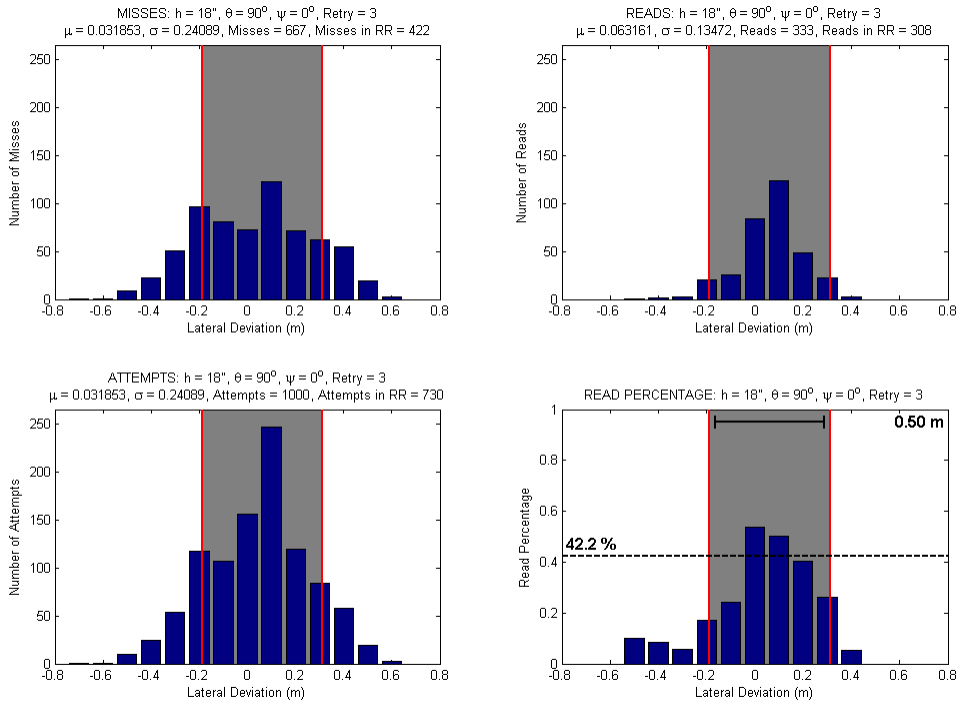

Figure 3.16: Height = Medium, Pitch = 90°, Yaw = 0°

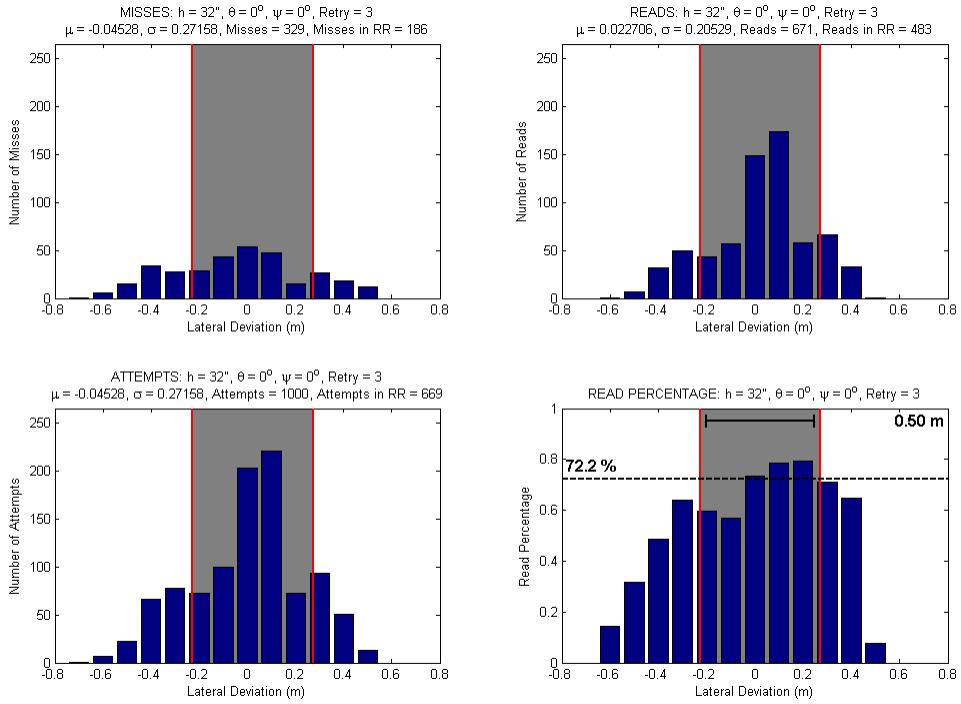

Figure 3.17: Height = High, Pitch = 0°, Yaw = 0°

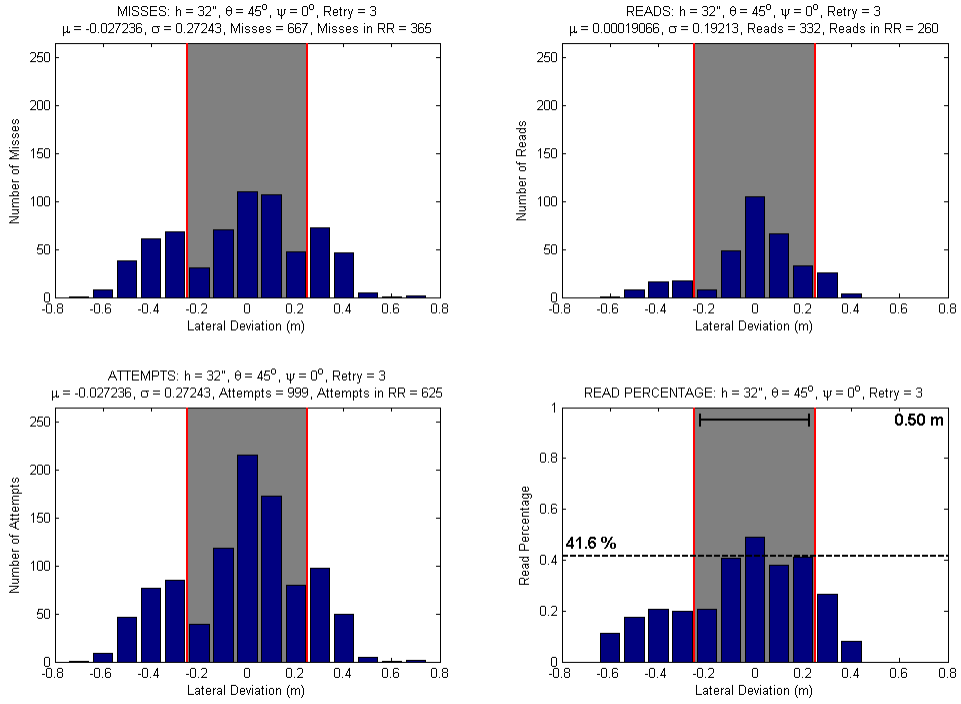

Figure 3.18: Height = High, Pitch = 45°, Yaw = 0°

The above analysis showed that the RFID equipment was not able to provide a read percentage of 100% for the desired read range of half a lane width (~6 ft). Moreover, a read percentage of 100% was not even achieved for read attempts in which the RFID transmit antenna passed directly over the center of the tag. Also, both read range and read percentage were independent of the speeds over which the RFID equipment was tested (30 -70 mph). Finally, when the RFID antennas were at their highest setting, and parallel to the ground, the best performance, in terms of overall read percentage, was achieved. These results, as well as a few other less significant trends which were discovered, are summarized below.

Read Range

- Read range is quite difficult to quantify, as it is a function of distribution of read attempts
- Read range is fairly independent of speed, in the range 30 – 70 mph
- Read range increases as the RFID antennas' height increases
- Read range is independent of yaw angle, indicating an omnidirectional antenna

Read Percentage

- Read percentage is fairly independent of speed, in the range 30 – 70 mph
- For the low setting, the read percentage is independent of pitch angle
- For the medium and high settings, as the pitch angle of the RFID antennas increases, the read percentage decreases
- Read percentage is independent of yaw angle, indicating an omnidirectional antenna

3.5.2.2 Latency as a Function of RFID Antenna Orientation

Latency is also an important characteristic of the RFID equipment used in the VPS system because it affects the system's ability to accurately position vehicles passing RFID tags. As an example, assume that the RFID system's mean latency is 1 s. At 70 mph, the vehicle would be roughly 31 m past the tag when the RFID reader finally finished processing the tag read. While this may seem like an unacceptable amount of error, it is in fact, not. The positioning error due to the mean latency would be common among all vehicles, and thus, would cancel out in applications[15] where only the relative positions of vehicles was required. Also, mean latency could be corrected for in applications where absolute positioning was required. The variability in latency, however, will not cancel out and cannot be corrected for, and thus, is of primary concern in the latency analysis.

Table 3.8 shows the results of the second group of experiments, which were conducted to determine the relationship between RFID antenna orientation, speed, mean latency and the standard deviation of latency. Notice that the mean latency and standard deviation of latency are independent of RFID antenna orientation and that there is no discernable pattern in relationship to speed.

[15] One such application which requires only relative positioning of vehicles is the electronic brake light, which will be discussed in much greater detail in chapter 5.

Table 3.8: Data analysis results for latency as a function of RFID antenna orientation.

Height (h)	Pitch (θ)	Yaw (ψ)	Tries	Speed (mph)	Latency (μ)	Latency (σ)	Latency (μ)	Latency (σ)
Low (10")	0°	0°	3	30	0.64	0.31	0.56	0.28
				40	0.52	0.24		
				50	0.64	0.32		
				60	0.48	0.25		
				70	0.48	0.22		
Low (10")	45°	0°	3	30	0.65	0.33	0.56	0.28
				40	0.49	0.20		
				50	0.62	0.34		
				60	0.53	0.22		
				70	0.53	0.30		
Low (12")	90°	0°	3	30	0.59	0.34	0.55	0.29
				40	0.53	0.22		
				50	0.64	0.36		
				60	0.51	0.28		
				70	0.44	0.22		
Medium (21")	0°	0°	3	30	0.64	0.31	0.54	0.27
				40	0.53	0.22		
				50	0.58	0.34		
				60	0.50	0.19		
				70	0.46	0.20		
Medium (21")	0°	90°	3	30	0.60	0.29	0.55	0.29
				40	0.50	0.20		
				50	0.63	0.36		
				60	0.53	0.26		
				70	0.45	0.21		
High (32")	0°	0°	3	30	0.65	0.31	0.57	0.27
				40	0.53	0.17		
				50	0.64	0.36		
				60	0.52	0.23		
				70	0.52	0.25		

Because latency was independent of RFID antenna orientation and speed, all of the above data was compiled and used to generate the histogram of Figure 3.19. Notice the great degree of variability in the latency. Also notice that three of the histogram's bins contain many more samples than the other bins. Given that the number of "tries" was set to three for this data set, it was possible that these spikes in the histogram corresponded to the RFID reader attempting to read the tag once, twice and three times. In order to determine if this hypothesis was true, data was collected to determine the effect of the "tries" setting on latency.

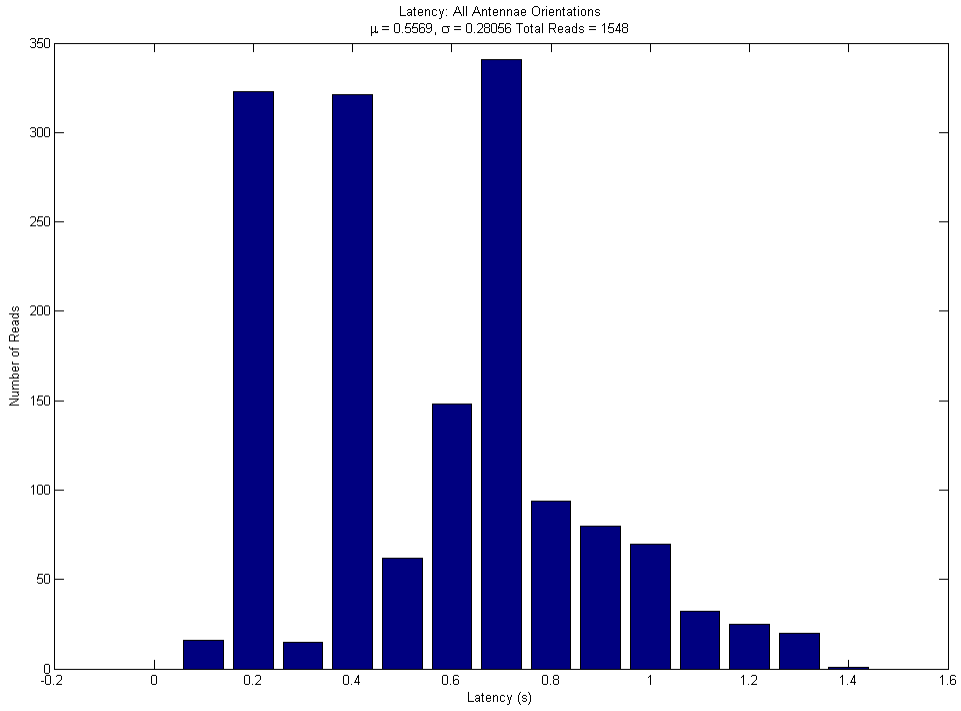

Figure 3.19: Latency histogram including data from all latency vs. RFID antenna orientation experiments.

3.5.2.3 Latency and Read Percentage as a Function of "Tries"

"Tries", as described by the RFID reader's user manual, "tells the reader how many times it should repeat the read command each time a scan is to be performed" [14]. This description leads one to believe that latency and read percentage would be directly proportional to the number of "tries". Because of this, and the three spikes that were present in the latency histogram for the previous data set, it was decided that the "tries" setting's relationship to latency and read percentage should be further investigated.

Given that the previous experiments showed that latency was independent of speed and RFID antenna orientation, the "tries" analysis was performed for only one RFID antenna orientation and two speed settings: low speed (30 mph) and high speed (70 mph). Table 3.9 summarizes the results.

Table 3.9: Data analysis results for latency and read percentage as a function of "tries".

Height (h)	Pitch (θ)	Yaw (ψ)	Tries	Speed (mph)	Latency (μ)	Latency (σ)	Read Percentage (%)	Total Read Percentage (%)
Medium (21")	0°	0°	1	30	0.18	0.04	41.8	46.7
				70			58.5	
Medium (21")	0°	0°	3	30	0.59	0.32	66.3	69.3
				70			70.0	

Medium (21")	0°	0°	5	30	0.90	0.45	88.6	84.8
				70			79.6	
Medium (21")	0°	0°	7	30	1.01	0.55	91.8	87.0
				70			81.5	
Medium (21")	0°	0°	9	30	1.4	0.74	83.1	81.1
				70			77.7	

Notice that mean latency and the standard deviation of latency both increased, as expected, as the "tries" setting was increased. Read percentage also increased as "tries" increased, however, it reached a maximum at a "tries" setting of 7, after which, read percentage began to fall. This was likely due to the fact that the length of time required to perform more than 7 "tries" began to exceed the length of time for which the RFID tags were in the read field of the RFID antennas.

Figures 32 and 33 more clearly show these results. Notice, in Figure 3.20, that a maximum read percentage was achieved for a "tries" setting of 7. Figure 3.21 shows that mean latency (solid line) and the standard deviation of latency (dotted lines) both increased as "tries" increased. These results are significant, because they could be used to help tailor the RFID equipment for a specific application. As Figures 32 and 33 show, one could sacrifice a bit of latency to improve read percentage, so, depending on the application, one would need to choose a "tries" setting so that a suitable read percentage is achieved. As an example, consider the HOT lane application, where accurate vehicle positioning is not important. For this application one would want to set "tries" to 7, to maximize read percentage, so that vehicles are accurately tolled.

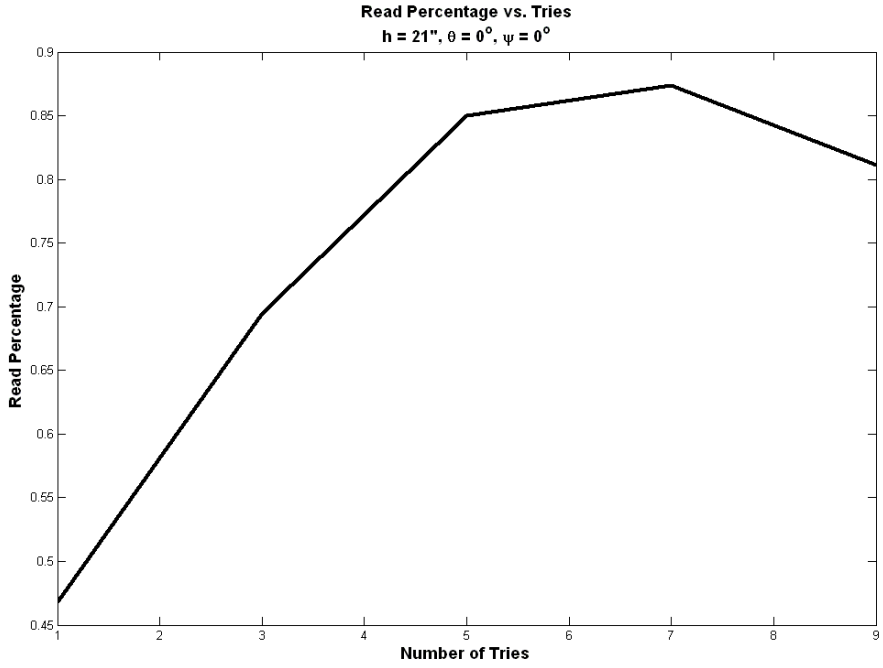

Figure 3.20: Read percentage vs. "Tries" for Height = Medium, Pitch = 0°, Yaw = 0°

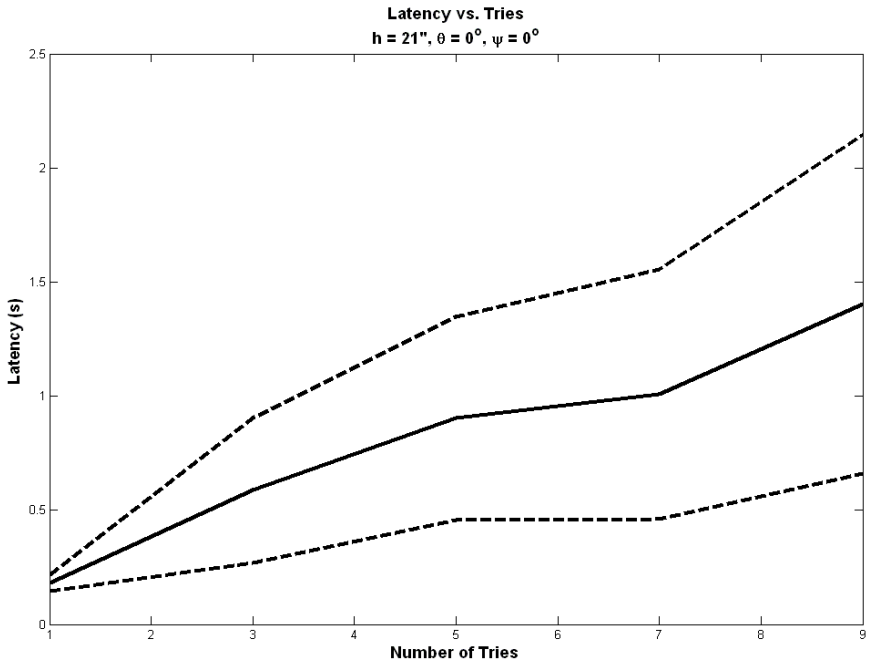

Figure 3.21: Latency vs. "Tries" for Height = Medium, Pitch = 0°, Yaw = 0°

3.5.2.4 New Tag Reliability

After analyzing individual tag data after the first set of experiments, it was found that certain tags performed considerably worse than others in terms of overall read percentage. To determine if tags performed poorly due to some spatial condition, such as greater interference at its location, reflections off surrounding metal, etc., the entire set of 50 tags was replaced. The next two sets of experiments were then performed using the second set of tags, and individual tag read percentage was analyzed.

Figure 3.22 shows the performance for each individual tag in the first tag set. Notice that the performance of tags 19 and 39 was significantly worse than that of the other tags. To determine if this poor performance was associated with the tags themselves, or the locations of the tags, a similar analysis was performed on the second tag set.

Figure 3.23 shows the performance for the second set of tags. Notice that the performance of tags 19 and 39 in the second tag set was comparable to that of the other tags in the set, and was considerably better than the performance of the corresponding tags in the first tag set. Also notice that in the second tag set, the performance of tags 2, 31 and 47 was significantly worse than that of the other tags, and was considerably worse than the performance of the corresponding tags in the first tag set. Thus, one can conclude that the poor performance of these 5 tags (19 and 39 from tag set one, and 2, 31 and 47 from tag set two) was due to the tags themselves, and not some other factor associated with the locations of the tags.

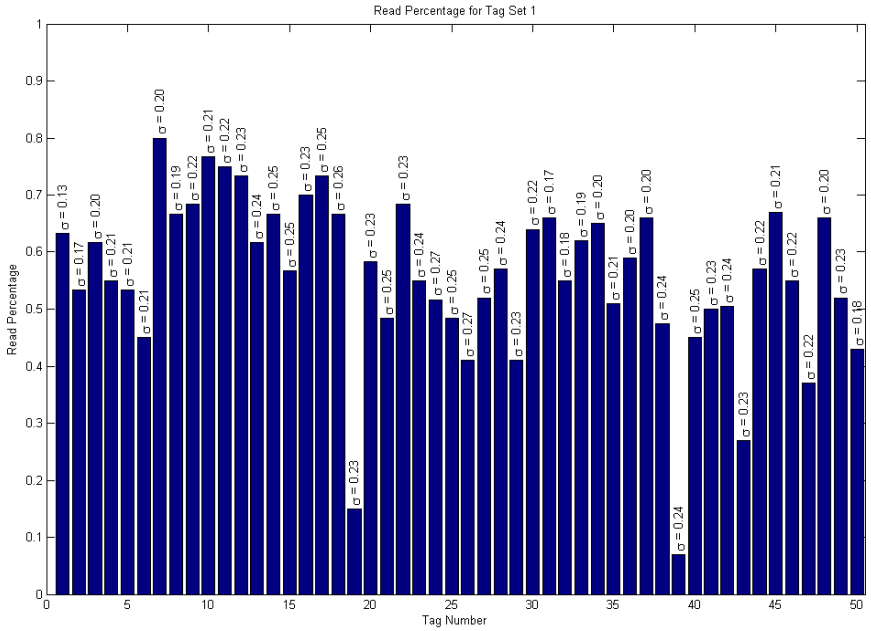

Figure 3.22: Individual tag read percentages for tag set one.

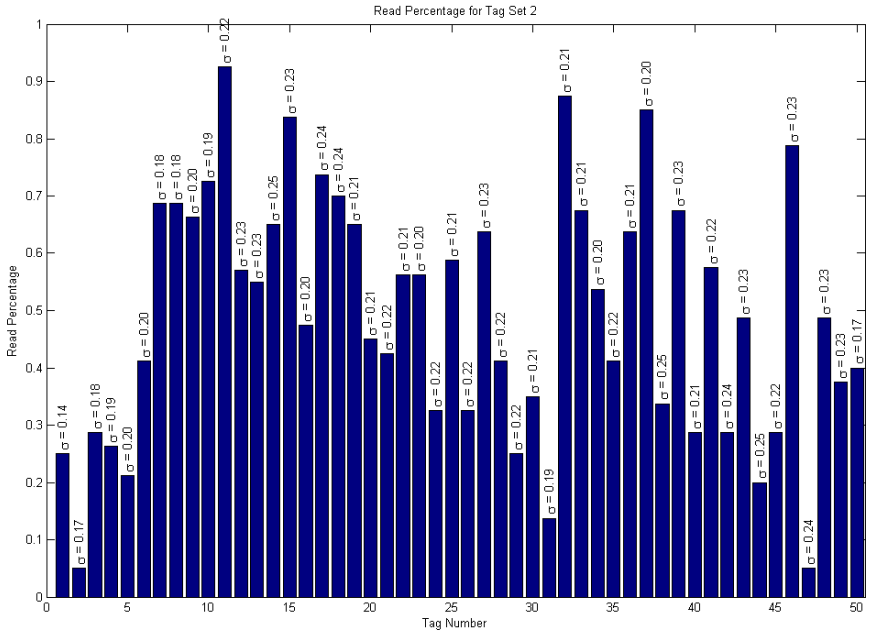

Figure 3.23: Individual tag read percentages for tag set two.

3.5.3 Discussion of Results

Based on the above experimentation, it was possible to suggest an optimum configuration for the Matrics RFID equipment. The best performance, in terms of read percentage, was achieved when the RFID antennas were at their highest height, and parallel to the pavement. Also, a "tries" setting of 7 achieved maximum read percentage. Thus, the overall read percentage would be maximized by placing the RFID antennas at their highest setting, parallel to the pavement, with "tries" set to 7.

This particular "tries" configuration (7), however, provides both a larger mean latency, and greater variability in the latency. Furthermore, placing the RFID antennas at a height of 32" and parallel to the pavement was not conducive to the suggested e-plate installation method. It is worth noting, however, that each of the RFID antenna orientations at the low setting provided a good read percentage (~ 62 %) for a "tries" setting of 3. This is important since the low setting (12" above the pavement), is much closer to the location of many vehicles' front license plate holder, and is thus, a much more likely height for the installation of e-plates. With the low setting, as with all other settings, the "tries" would have to be optimized for each application because of the tradeoff between read percentage and latency.

3.6 Problems Encountered During Sensor Characterization

During the above experimentation, two major problems were encountered which eliminated the possibility of building a field operational VPS system using the Matrics RFID equipment.

3.6.1 Interference

In performing the experiments at Mn/ROAD, it was found that data could not be written to the read/write tags. Also, when traveling in a westbound direction, read percentage during the day was dramatically lower than at night. After consulting with the Mn/ROAD staff, it seemed that the only logical explanation for these two problems was that there was some type of interference present in the 902 – 928 MHz range, which was frequency band on which the RFID reader operated. This hypothesis explained the problem with writing to tags, since writing is much more sensitive to interference. It also explained why read percentage was considerably higher during the day, when the test vehicle traveled eastbound. Consider that if the interference originated west of the test track, then when the vehicle traveled in an eastbound direction, the back end of the vehicle would shield the reading of the tags from the interference. This shielding would allow for improved tag reading when traveling eastbound. Thus, the most likely explanation for these two problems, and the fact that they occurred only during the day, was that there was some type of interference in the 902 – 928 MHz range which was only present during the day, and which originated somewhere west of the test track. Because of these two problems during daylight hours, all of the above experiments were conducted between the hours of 8 PM and 4 AM in order to maximize performance.

3.6.2 New Tag Reliability

Based on the new tag reliability analysis (see section 3.5.2.4), it was determined that 5 out of the 100 tags performed much more poorly than the other tags (10% read percentage versus 80% read

percentage). Also, during the course of preparing the above experiments, it was found that roughly 5 tags out of 100 did not work at all. Thus, approximately 10% of the tags which were received provided insufficient performance for use in a VPS system, which is an unacceptable failure rate. For a field operational test, the manufacturer would have to guarantee that each tag placed on the road conformed to some predetermined minimum performance threshold.

3.7 Suggestions for a Next Generation Reader

The above analysis identified a number of problems with the Matrics hardware, which would make it unacceptable for use in a deployable VPS system. In order for VPS to work, existing RFID technology must improve, or a custom reader that is optimized for ITS applications should be designed. The following problems, which were discovered when characterizing the Matrics equipment, must be addressed when choosing or designing the new reader.

1. The tag read performance must be near 100% for speeds in the range 0 – 100 mph. To achieve this, the system must have greater immunity to interference.
2. The percentage of new RFID tags which are faulty must be reduced to ensure that each tag placed on the pavement is guaranteed to work.
3. The read range must extend to the lane boundaries. This could be achieved by considering alternative tag installations to overcome a short read range, or by designing a new RFID system which provides a greater read range (ie. redesign antennas, increase read power, etc.).
4. In order to allow for the system to be installed within a front-mounted electronic license plate, the system must be miniaturized.
5. In order to improve the position estimate, an RFID system must be designed such that the latency is more deterministic to allow for correction.
6. A method to easily affix the tags to the road, so that they are protected from moisture, traffic, etc., must be determined.

4 A Basic Electronic Brake Light Implementation using VPS

In order to demonstrate the use of the VPS system, and how one would implement an ITS application using it, a demonstration of a prototype electronic brake light was implemented and demonstrated to be functional.

4.1 Concept

The electronic brake light concept is one that has been identified by the Crash Avoidance Metrics Partnership (CAMP) as being a high priority safety application which will be enabled by vehicle-vehicle and/or vehicle-infrastructure communication [6]. Currently, drivers determine when to decelerate by monitoring the brake lights of a single downstream vehicle: its lead vehicle. The electronic brake light system is intended to extend the driver's look-ahead range by monitoring the activity of multiple downstream vehicles. In its most simple form, it would alert the driver if any of the vehicles in front of him are decelerating harshly. Such a system would be capable of warning drivers about impending severe deceleration much earlier than in the case when only the lead vehicle is monitored. The system would also prove useful when visibility is limited, such as during poor weather conditions, or when the driver is distracted.

This concept proposes to use inter-vehicle communication to broadcast the application of a vehicle's brakes to nearby vehicles. However, auto manufacturers have not addressed what should be contained in the brake apply message nor how to route the messages. If vehicle position is not included in the brake apply message, it is likely to have adverse affects on the adjacent lane of traffic and vehicles ahead of the vehicle applying its brakes. The lane position information provided by VPS is precisely that needed to enable deployment of electronic brake

lights. Only vehicles in the same lane of traffic and behind the vehicle in question should be warned that brakes ahead have been applied.

4.2 Test Track Installation

The first step in performing the demonstration of the electronic brake light was to outfit the test track. The test track was outfitted with 40 RFID tags. Tags 1 – 20 were placed in the right lane with a spacing of 76.2 m, and tags 21 – 40 were placed in the left lane, with the same longitudinal position as that of tags 1 – 20. Figure 4.1 shows the installation location of the first two tags in each lane (1, 2, 21, and 22).

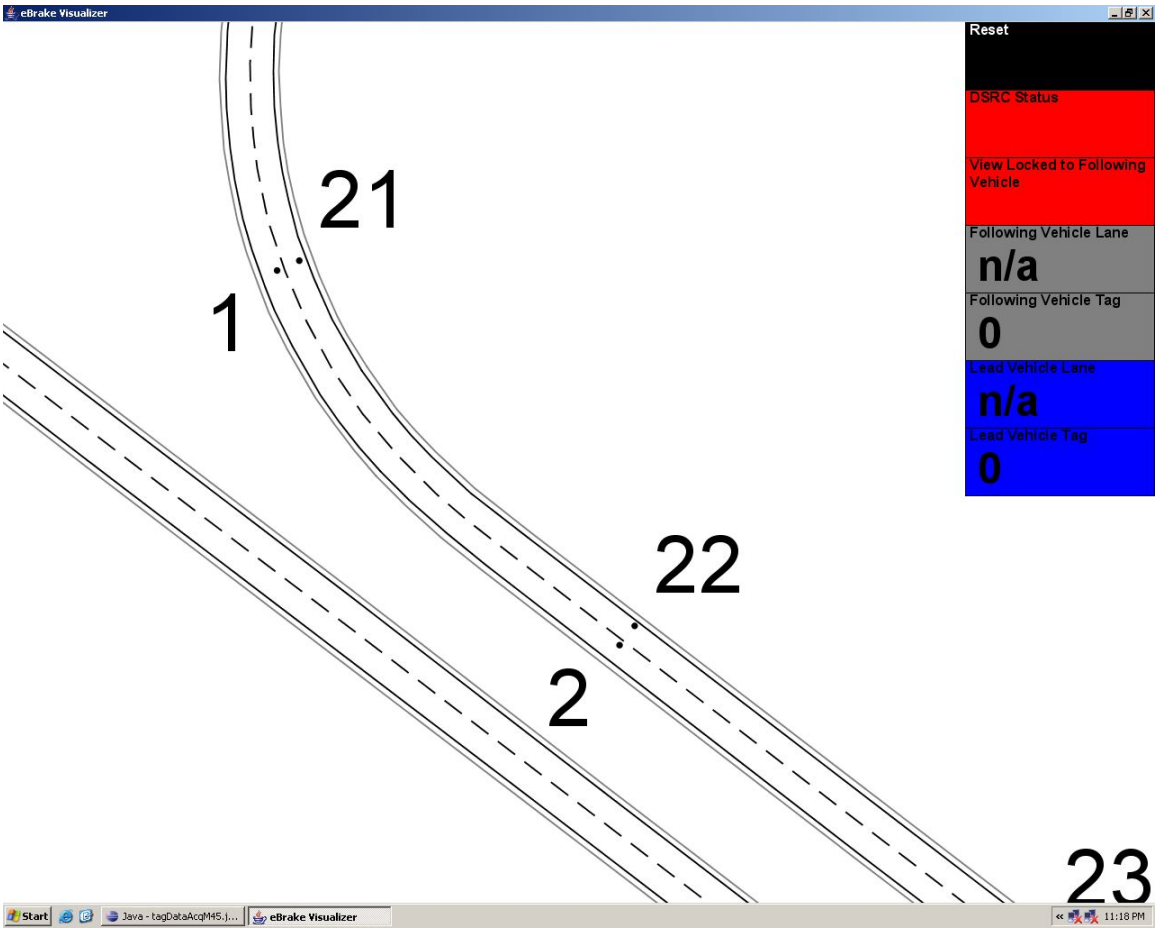

Figure 4.1: RFID tag placement on test track.

In order to simplify the placement and removal of each of the tags, they were first bonded to a piece of white Plexiglas. Figure 4.2 shows a tag (# 37) attached to the Plexiglas.

Figure 4.2: RFID tag bonded to Plexiglas.

To further simplify the electronic brake light demonstration, each tag was placed so that when the left wheels of the test vehicle were directly on top of the test track's centerline (for right lane driving) or the fog line (for left lane driving) the phase center of the RFID transmit antenna passed directly over the center of the RFID tag. This was done to help the driver pass over the tags with the antennas centered over the tags. Because the read range of the tags was so small, any slight deviation to the left or right of the tags would result in the tag not being read, which would have been problematic for demonstrating the usefulness of the electronic brake light. Figure 4.3 shows the test vehicle, with its left wheels directly on top of the centerline. Notice that the RFID transmit antenna, which is located on the vehicle's driver side, is directly above the RFID tag.

Figure 4.3: Picture showing RFID transmit antenna centered directly over RFID tag.

4.3 Host Vehicle Installation

The host vehicle's installation was identical to that of the sensor characterization installation, with the exception of the DSRC unit and buzzer. The DSRC unit was added so that the lead vehicle's harsh deceleration messages could be received, in order to warn the driver by sounding the buzzer. Figure 4.4 shows a block diagram for the equipment installed in the host vehicle. Also, notice the GPS unit. The vehicle's position was determined using VPS[16], and the GPS unit was used solely for the purposes of post-experimental data analysis. The RFID reader antennas were installed in the same position as shown in Figure 3.3.

[16] VPS position was acquired/updated only when an RFID tag was read. For this demonstration, dead reckoning using vehicle speed data from the OBDII connector was not used, as suggested in section 2.4.3.

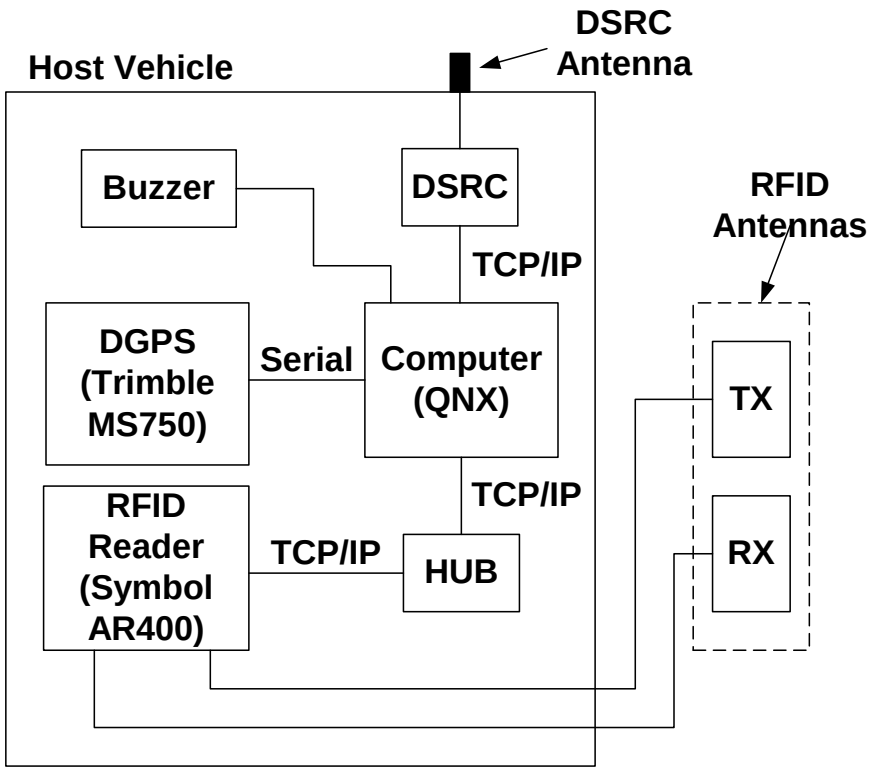

Figure 4.4: Host vehicle installation block diagram.

4.4 Lead Vehicle Installation

The lead vehicle installation is shown in Figure 4.5. Notice the lack of RFID equipment. We were unable to procure an additional set of RFID hardware, and thus, VPS position was simulated. Figure 4.6 shows how VPS position was computed through the use of the vehicle's GPS position and a digital map of the test track. By correlating the GPS position with the digital map, the lane of travel was first determined. Then, only at instants when the vehicle crossed the dotted lines was the position updated to the most recently passed RFID tag. For example, assume the vehicle in Figure 4.6 continues in its current lane. At the instant it crosses the dotted line running through RFID tags 2 and 22, the vehicle's position would be updated to the right lane of travel at longitudinal position 2. One subtle difference between the VPS position of the lead vehicle and host vehicle was that the lead vehicle never missed reading tags, because the tag reading was simulated via GPS. The host vehicle, on the other hand, did miss reading tags, because the read percentage for the RFID equipment was not 100%.

Also notice the IMU, which was not present in the host vehicle installation. The IMU was used to sense harsh deceleration activity, which triggered the broadcast of the braking message via the DSRC radio.

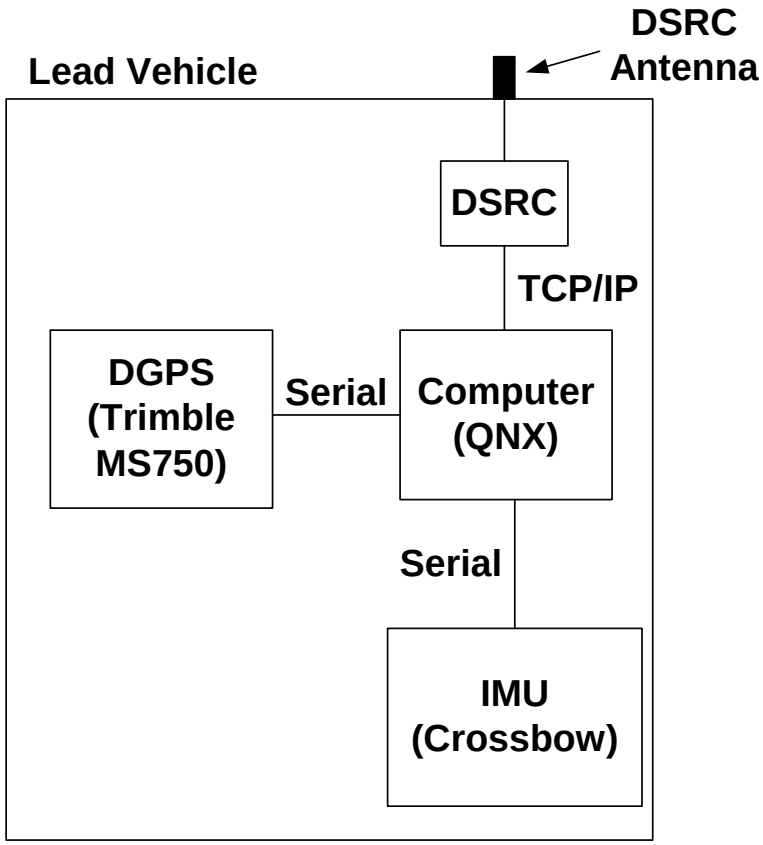

Figure 4.5: Lead vehicle installation block diagram.

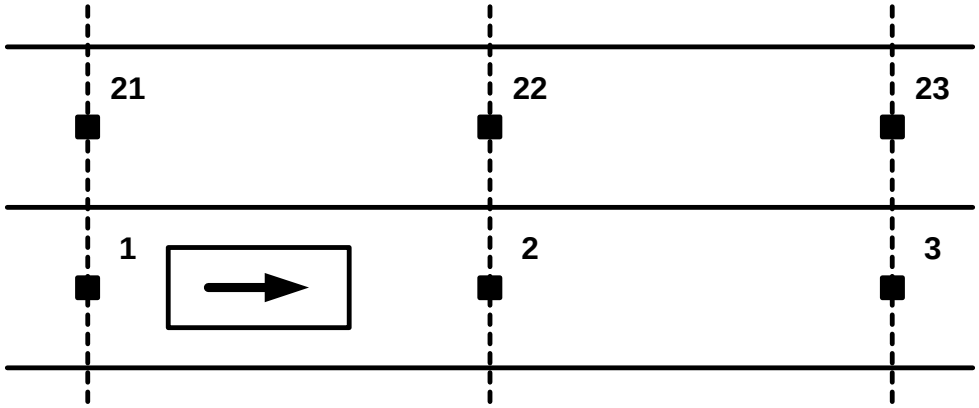

Figure 4.6: GPS simulation of VPS position.

4.5 Description of the System's Operation

The system's operation, as previously described, was quite simple. The vehicles would acquire VPS position (host vehicle), or a simulated VPS position (lead vehicle) each time a tag was passed. If the lead vehicle braked harshly (greater than ¼g), a braking message was broadcast.

The host vehicle received the broadcast message and if it was located in the same lane, and behind the lead vehicle, the buzzer was sounded for 1 second. Figure 4.7 shows the two vehicles at their start position.

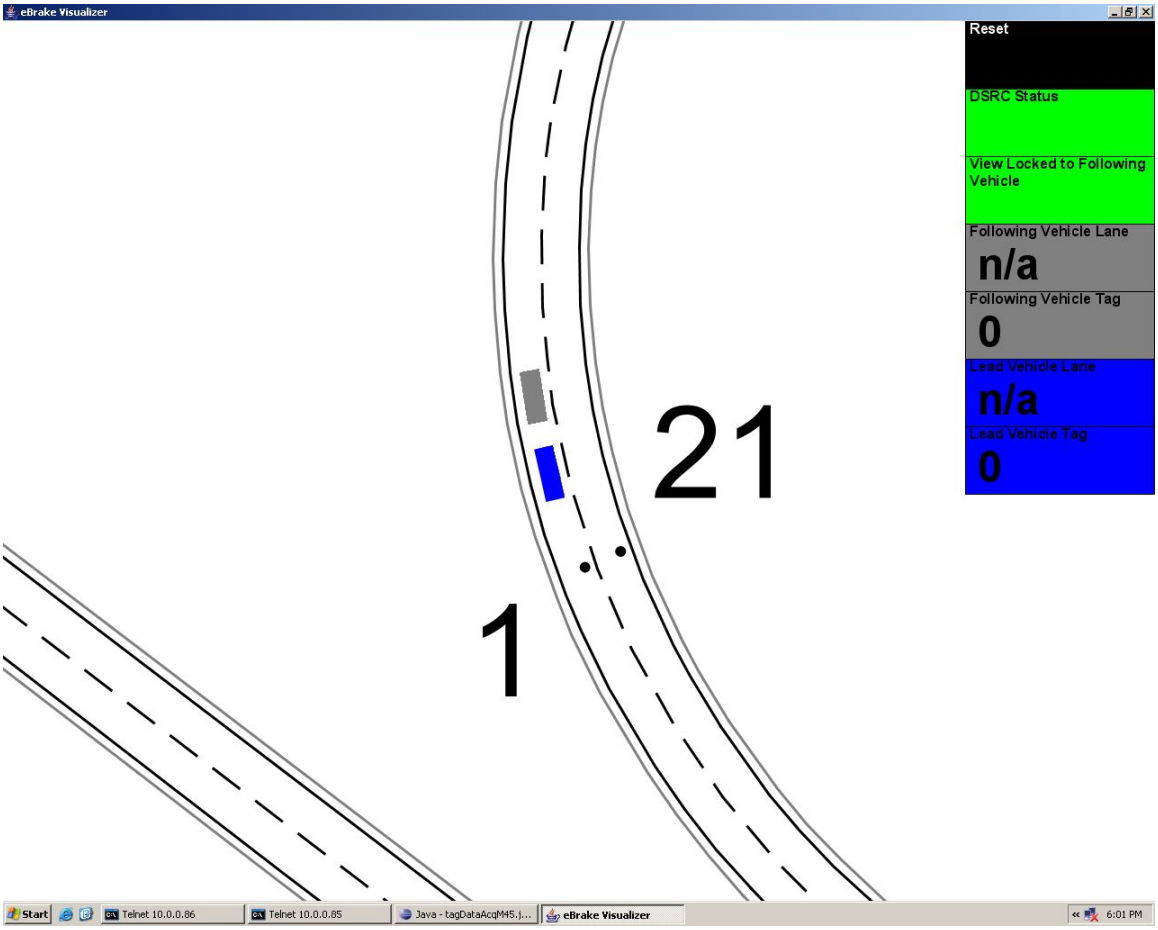

Figure 4.7: Electronic brake light demonstration start position.

Figure 4.8 shows the vehicles traveling along test track. Notice that as the RFID reader installed in the host vehicle (gray) reads the RFID tags, they are highlighted in green on the display, whereas unread tags remained white[17]. It is important to note that the lead vehicle (blue) used a simulated VPS position which was computed by correlating its GPS coordinates with a digital map of the test track. As such, the lead vehicle never missed tags, as would the host vehicle.

[17] Because the read percentage for the RFID equipment was not 100%, it was possible that tags could be missed.

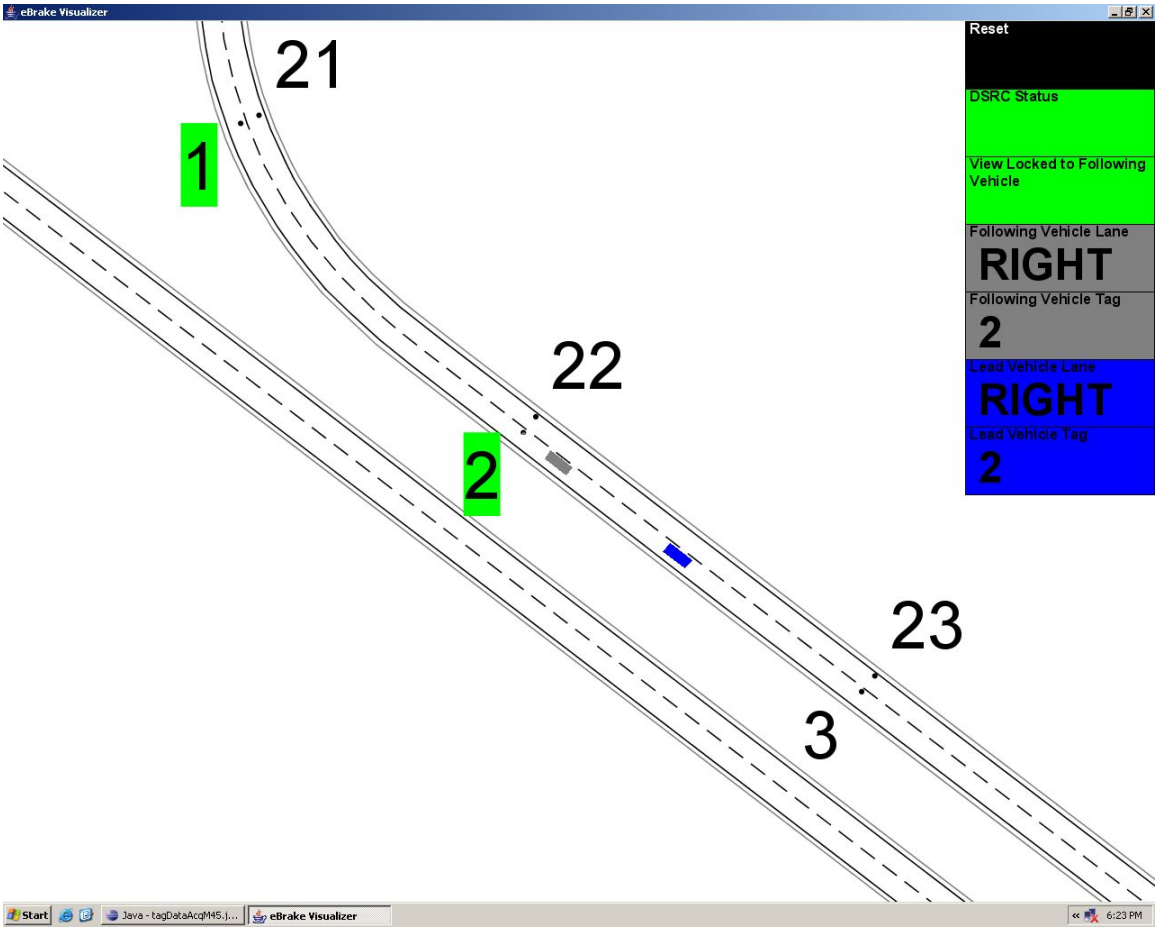

Figure 4.8: Normal driving during electronic brake light demonstration.

Figure 4.9 shows a situation where the lead vehicle brakes harshly. To indicate this harsh braking, the lead vehicle turned red on the display. Also note that because the host vehicle was behind the lead vehicle, and in the same lane, the buzzer in the host vehicle sounded. Also notice that tag 3 was not read, and remained white, whereas the read tags turned green.

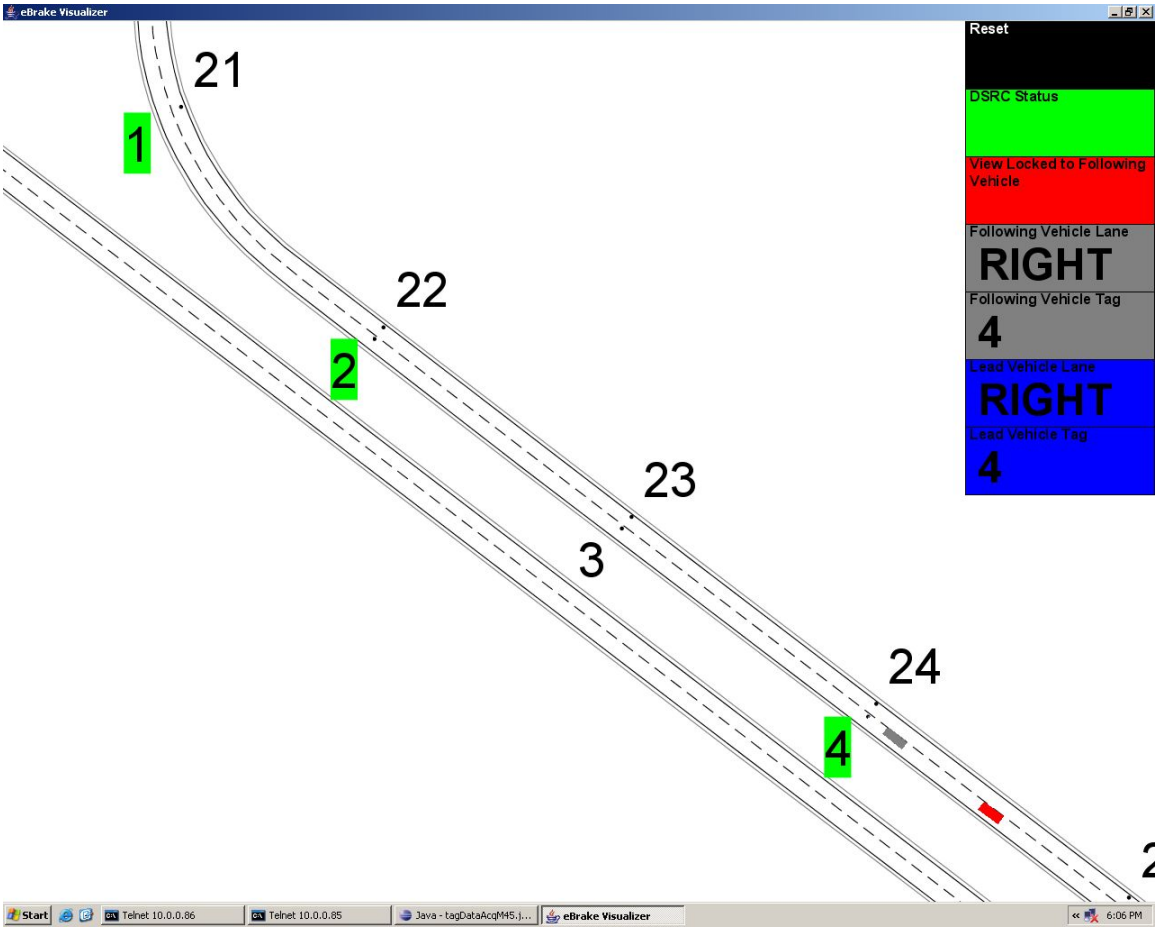

Figure 4.9: Gray vehicle is warned.

Figure 4.10, on the other hand, shows a situation where the buzzer did not sound. Notice that the host vehicle was behind the lead vehicle but was in the opposite lane. Because it was not in the same lane, the buzzer did not have sound.

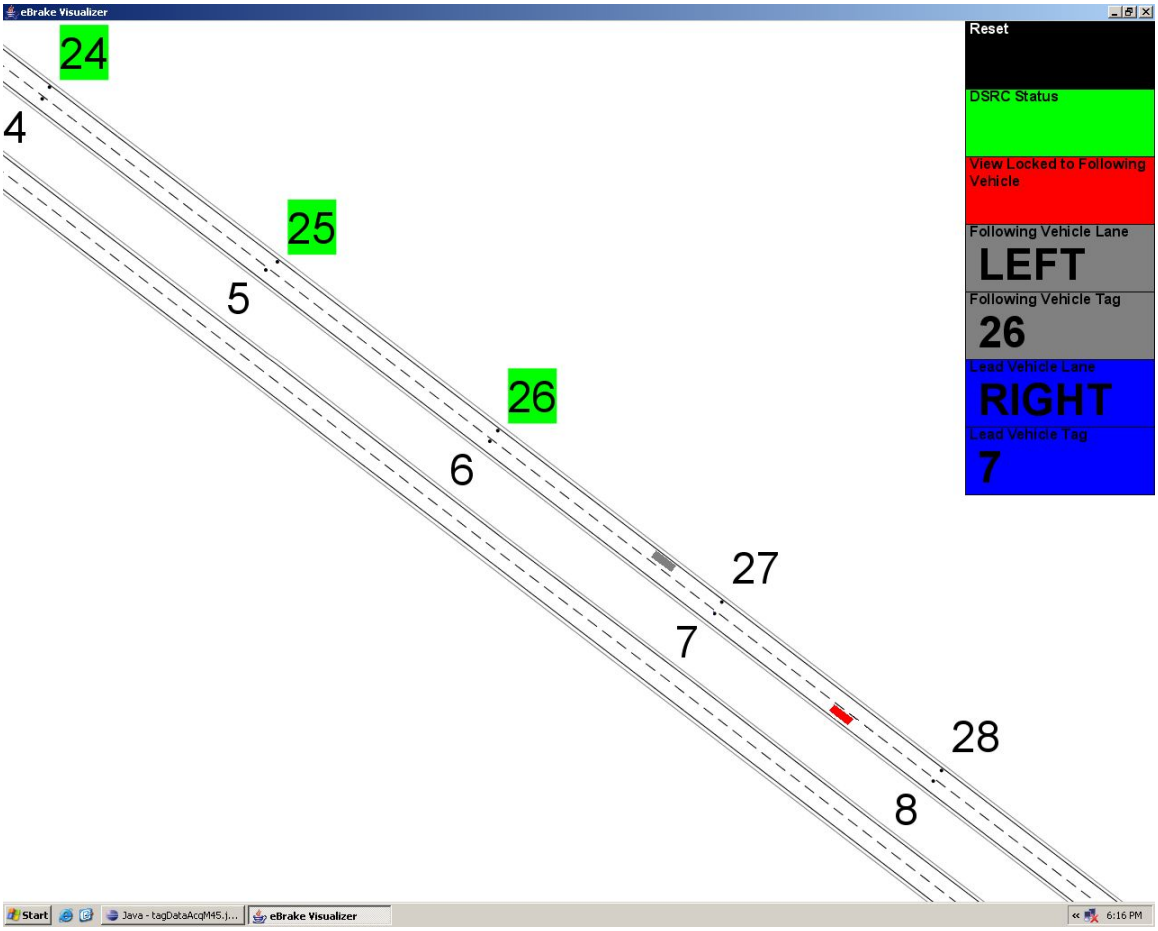

Figure 4.10: Gray vehicle is not warned.

While only two cases are presented here, all possible relative positions between the two vehicles were tested, and the system was found to work properly. Figure 4.11 shows the relative positions that were tested. Relative positions 1 – 4 are the scenarios where the host vehicle was behind the braking vehicle, whereas relative positions 5 – 8 are the scenarios where the host vehicle was in front of the braking vehicle. Notice that only when the host vehicle was in the same lane and behind the braking vehicle, was the driver warned.

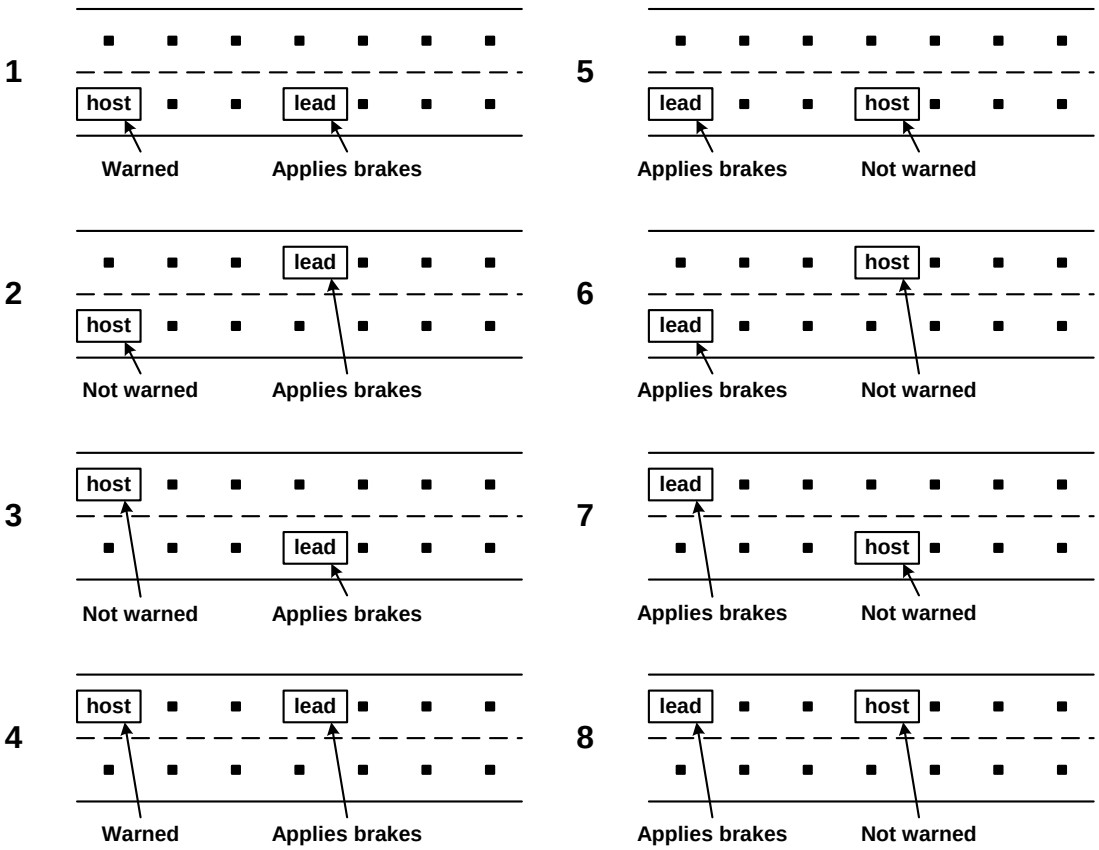

Figure 4.11: Relative positions between the lead and host vehicles that were tested.

5 A More Robust Approach to the Electronic Brake Light and its Implications on VPS

This chapter discusses the design of a risk metric for use in driver support systems which aim to reduce the likelihood of rear-end collisions. The risk metric will indicate a level of rear-end crash risk associated with a platoon of vehicles located immediately in front of the host, and could be displayed to the driver to provide him with a measure of the risk associated with the unseen events ahead. It is important to note that throughout this chapter, it is assumed that only the host vehicle is performing the risk metric computation.

There have been several attempts at designing systems to help drivers avoid rear-end crashes using radar; the systems range from adaptive cruise control (ACC) to rear-end collision warning systems. Past designs for rear-end collision warning systems [3, 4, 26 – 31] used radar to acquire range, range rate and deceleration data. A more novel approach proposed the use of radar to detect the range and range rate for a platoon of three vehicles, which included the host, and the two vehicles immediately downstream of the host [5]. It is likely that these systems could be improved upon if the host was able to acquire range, range rate, deceleration, vehicle length and brake light status data from all vehicles in the lead platoon. With the emergence of dedicated short range communication (DSRC) as a means to support the necessary vehicle-vehicle and vehicle-infrastructure communication [6], the ability to have access to this data becomes increasingly more viable.

The new approach presented herein assumes that via DSRC and VPS[18], position, velocity, acceleration, vehicle length and brake light status data for a platoon of vehicles located in front of the host vehicle will be available. This data will be used to compute the risk metric associated with the downstream platoon, which could be used to provide feedback to the driver by way of a driver support system. Such an implementation is unique from prior rear-end collision avoidance algorithm designs in its use of data from the entire lead platoon, as well as its use of VPS as the enabling position sensing medium.

5.1 Chapter Outline

This chapter will first introduce the problem of determining the rear-end crash risk metric as well as the stability definitions which will be used during its derivation. The implications of the stability definitions on the risk metric's computation will also be considered. After reviewing this background material, the method for computing the risk metric will be presented.

The method for computing the risk metric is presented below by first computing the risk metric for a single pair of vehicles, one following the other. In this case, the risk metric can be physically interpreted as the minimum deceleration required by the host vehicle to avoid a crash with the lead vehicle (also sometimes called the principal other vehicle or POV). Following the derivation of the minimum deceleration to avoid a crash for the two vehicle case, the computation is extended to compute the risk metric for a platoon of vehicles. After discussing the computation for a platoon of vehicles, a method for tightening the lower bound estimate of the risk metric by using brake light information, which is applicable only when vehicle trajectory histories[19] are known, is presented. This lower bound (the minimum level of braking required to avoid a crash) will reduce the likelihood of false positives.

Sample risk metric computations are then performed on platoons for two cases:

1. When vehicle trajectory histories are not known (no tightening of lower bound using brake light information).
2. When vehicle trajectory histories are known (tightening of lower bound using brake light information).

While the sample calculations for platoons without vehicle trajectory histories would not be performed in practice, they are useful for demonstrating the computation of the risk metric, and for helping the reader relate the risk metric's computed value to the physical state of the platoon (ranges, range rates, and accelerations).

As a final step, the risk metric's sensitivity to positioning error will be determined. Using this information, the longitudinal positioning accuracy that must be provided by VPS, to guarantee that the risk metric falls within some predetermined error tolerance, will be calculated.

[18] It is proposed that this position information be provided by VPS, rather than GPS, because of the problems associated with GPS which were discussed in section 1.1.

[19] Vehicle trajectory history refers to knowledge of past acceleration, speed, position and brake light status data for each vehicle in the platoon, which would have to be stored in a memory buffer.

5.2 Problem Introduction and Stability Definitions

Assume we have a platoon of vehicles, as shown in Figure 5.1. Vehicle 0 is the host vehicle, and vehicles 1 to n comprise the platoon of vehicles located immediately downstream of the host. In our case, the host is most concerned with avoiding a collision with vehicle 1.

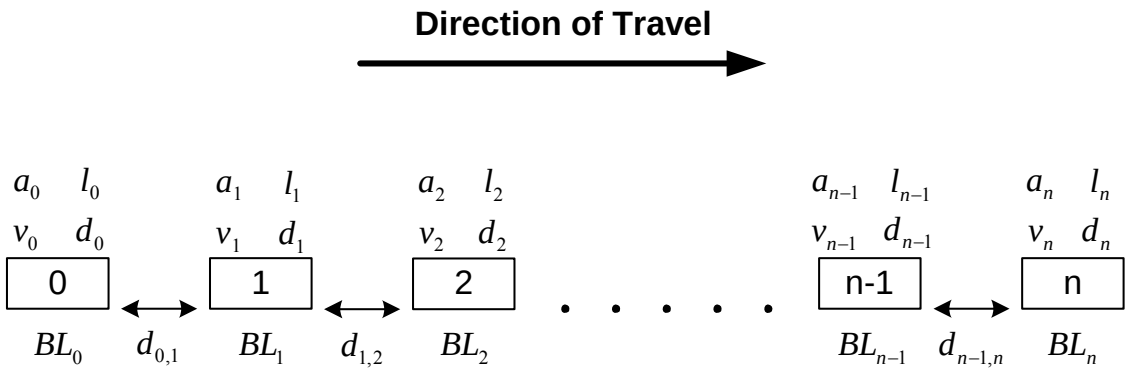

Figure 5.1: A platoon of vehicles showing the data that will be available for risk metric computation.

Notice that for each vehicle i, we are given the following data:

$a_i = i^{th}$ vehicle's acceleration
$v_i = i^{th}$ vehicle's speed
$d_i = i^{th}$ vehicle's longitudinal position
$l_i = i^{th}$ vehicle's length
$BL_i = i^{th}$ vehicle's brake light status (on/off)

From this data, we can also directly calculate:

Range = $d_{i,i+1} = (d_{i+1} - l_{i+1}) - d_i$
Range rate = $v_{i,i+1} = v_{i+1} - v_i$
Relative acceleration = $a_{i,i+1} = a_{i+1} - a_i$

Figure 5.2 helps to illustrate how we arrived at the above equations.

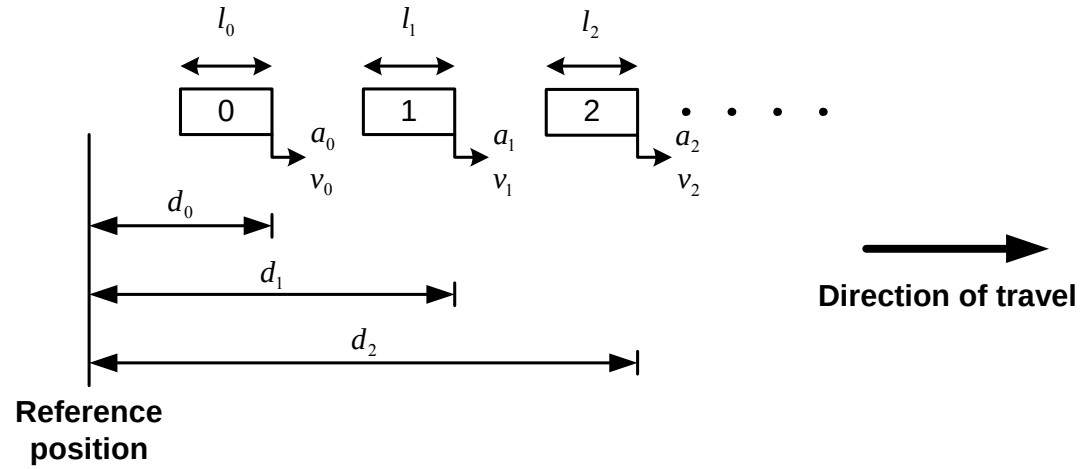

Figure 5.2: Data used to compute range.

We will now define some mathematical relationships that define various levels of stability which lead to a measure of risk. The disturbance that we will be concerned with is braking occurring downstream of the host.

Definition:
The platoon of vehicles shown in Figure 5.1 is stable if:

$$\begin{matrix} v_{i,i+1}(t) > 0 \quad \forall t \geq 0 \\ d_{i,i+1}(0) \geq 0 \end{matrix} \qquad \text{for } i = 0,1,...,n$$

This definition implies that the range rate for each pair of vehicles in the platoon is positive $\forall t \geq 0$ and that the initial range for each pair of vehicles is such that the vehicles are not in a crashed state. It guarantees that no two vehicles in the platoon will crash $\forall t \geq 0$. Moreover, the headways, $d_{i,i+1}(t)$, will strictly increase. Thus, stable platoons present no immediate risk to the host vehicle.

Definition:
The platoon of vehicles shown in Figure 5.1 is instantaneously stable at time t if:

$$\begin{matrix} v_{i,i+1}(t) > 0 \\ d_{i,i+1}(t) \geq 0 \end{matrix} \qquad \text{for } i = 0,1,...,n$$

This implies that the range is greater than or equal to zero, and the range rate is positive at time t.

Definition:
The platoon of vehicles shown in Figure 5.1 is marginally stable if:

$$\begin{matrix} v_{i,i+1}(t) = 0 \quad \forall t \geq 0 \\ d_{i,i+1}(0) \geq 0 \end{matrix} \qquad \text{for } i = 0,1,...,n$$

Although marginally stable platoons present no immediate risk to the host vehicle, it is important that they are accounted for in the risk metric's computation since any small braking disturbance injected into a marginally stable platoon, will cause it to become unstable .

Definition:
The platoon of vehicles shown in Figure 5.1 is instantaneously marginally stable at time t if:

$$\begin{matrix} v_{i,i+1}(t) = 0 \\ d_{i,i+1}(t) \geq 0 \end{matrix} \qquad \text{for } i = 0,1,...,n$$

This implies that the range is greater than or equal to zero, and the range rate is equal to zero at time t.

Definition:
The platoon of vehicles shown in Figure 5.1 is unstable if:

$$\begin{matrix} v_{i,i+1}(t) < 0 \quad \forall t \geq 0 \\ d_{i,i+1}(0) \geq 0 \end{matrix} \qquad \text{for } i = 0,1,...,n$$

This implies that the range is greater than or equal to zero, and the range rate is negative. If a platoon is unstable, it presents an immediate risk to the host vehicle.

Definition:
The platoon of vehicles shown in Figure 5.1 is instantaneously unstable at time t if:

$$\begin{matrix} v_{i,i+1}(t) < 0 \\ d_{i,i+1}(t) \geq 0 \end{matrix} \qquad \text{for } i = 0,1,...,n$$

This implies that the range is greater than or equal to zero, and the range rate is negative at time t.

NOTE: All future references to stability, marginal stability or instability will refer to their instantaneous counterparts.

5.3 Considering the Stability Classifications when Computing the Risk Metric

When determining an algorithm to calculate the risk metric associated with the lead platoon, one must ensure that it will account for all cases by considering the implications of the stability definitions. Below we discuss how a platoon's stability classification will affect the risk metric.

5.3.1 Stable Platoon

If a platoon is stable, it presents no risk. These platoons are not considered when computing the risk metric (ie. the risk is not calculated and is simply set to zero).

5.3.2 Marginally Stable Platoon

If a platoon is marginally stable, it presents no immediate risk. However, because a small disturbance will cause the platoon to become unstable, one must consider marginally stable platoons in the risk metric calculations. It is important to keep in mind that two platoons that are marginally stable will have different levels of associated risk if a disturbance occurred. For example, assume platoon 1 is marginally stable at time t, and $d_{i,i+1}(t) = 100 \ \ m$, and $v_i(t) = 10 \ \ m/s$. Platoon 2 is also marginally stable at time t, but $d_{i,i+1}(t) = 10 \ \ m$, and $v_i(t) = 10 \ \ m/s$. If a braking disturbance occurs at vehicle n, platoon 2 would be at a greater risk of producing a collision because the small ranges between vehicles would require the drivers to be much more vigilant than those of platoon 1. Thus, the risk metric must return a higher value for platoon 2 than for platoon 1.

5.3.3 Unstable Platoon

If a platoon is unstable, it presents an immediate risk, and the risk metric must be computed.

5.4 Computation of the Risk Metric

The approach chosen to compute the risk metric involves the computation of the minimum deceleration to avoid a crash between longitudinally adjacent vehicles. This computation is then propagated along the entire platoon, to arrive at a lower bound on the deceleration required by the host vehicle (vehicle 0) to avoid a collision with the lead vehicle (vehicle 1). In this section, the derivation of the minimum deceleration to avoid a crash between adjacent vehicles is first presented. After presenting this derivation, the method for computing the final risk metric by propagating the minimum deceleration computation along the entire platoon is shown.

5.4.1 Calculating the Minimum Deceleration to Avoid a Crash for a Pair of Adjacent Vehicles

Using the vehicle data shown in Figure 5.1, and assuming a driver reaction time, t_r, one can compute a minimum bound on the deceleration required to safely prevent a collision between a pair of adjacent vehicles in a platoon. For example, assume that vehicle n begins braking at time $t = 0$. Vehicle $n-1$ will continue in its current state until the driver reacts at time $t = t_r$, at which point it will begin braking in response to the braking of vehicle n. The minimum rate at which vehicle $n-1$ must brake in order to avoid a collision with vehicle n is defined as $a_{\min,n-1}$. We will first calculate $a_{\min,n-1}$ for a pair of vehicles and then, in a later section, use the result to compute the risk metric for a platoon of vehicles.

Definition:
The "contact state", which applies to two vehicles following one another, is said to occur at time t_c if the range and range rate become zero at time t_c, and if the range rate is non-negative $\forall t > t_c$. This can be expressed mathematically as:

$$\begin{matrix} v_{i,i+1}(t_c) = 0 \\ d_{i,i+1}(t_c) = 0 \end{matrix} \text{ and } v_{i,i+1}(t) \geq 0 \quad \forall t > t_c$$

Figures 48 and 49 show the acceleration activity for vehicle $i+1$ and vehicle i. Vehicle $i+1$ is driving with an acceleration of a_{i+1}, and at $t = 0$, begins to decelerate at a rate of $a_{brake,i+1}$. Vehicle i is driving with an acceleration of a_i, and at $t = t_r$ it responds to the braking of vehicle $i+1$ by braking at a rate of $a_{\min,i}$, the minimum deceleration required to avoid a collision with vehicle $i+1$. We will now calculate this $a_{\min,i}$.

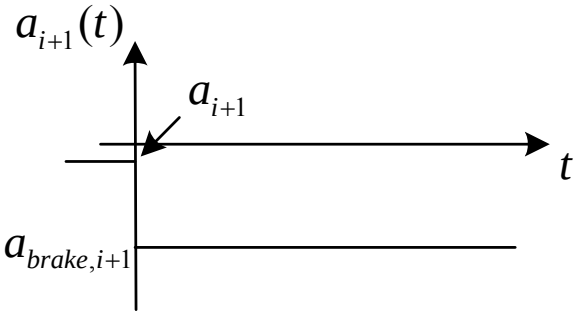

Figure 5.3: Acceleration of lead vehicle (vehicle i+1).

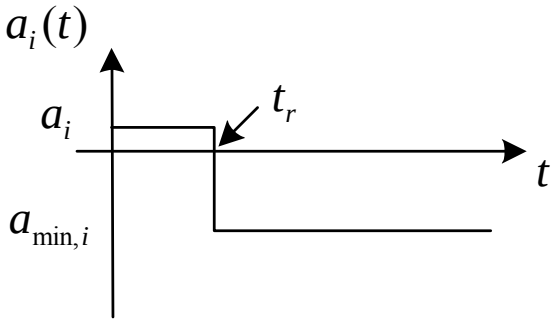

Figure 5.4: Acceleration of following vehicle (vehicle i).

By taking the acceleration functions from the above graphs, and integrating them once to acquire speed, and twice to acquire position, we arrive at the following formulae for acceleration, speed and position for each vehicle.

$$a_{i+1}(t) = a_{brake,i+1} \quad t \geq 0 \tag{1}$$

$$v_{i+1}(t) = v_{i+1}(0) + \int_0^t a_{i+1}(\tau) d\tau = a_{brake,i+1} t + v_{i+1}(0) \quad t \geq 0 \tag{2}$$

$$d_{i+1}(t) = d_{i+1}(0) + \int_0^t v_{i+1}(\tau)d\tau = \tfrac{1}{2} a_{brake,i+1} t^2 + v_{i+1}(0)t + d_{i+1}(0) \quad t \geq 0 \tag{3}$$

$$a_i(t) = \begin{cases} a_i & 0 \leq t < t_r \\ a_{\min,i} & t \geq t_r \end{cases} \tag{4}$$

$$v_i(t) = v_i(0) + \int_0^t a_i(\tau)d\tau = \begin{cases} a_i t + v_i(0) & 0 \leq t < t_r \\ a_{\min,i}(t - t_r) + a_i t_r + v_i(0) & t \geq t_r \end{cases} \tag{5}$$

$$\begin{aligned} d_i(t) &= d_i(0) + \int_0^t v_i(\tau)d\tau \\ &= \begin{cases} \tfrac{1}{2} a_i t^2 + v_i(0)t + d_i(0) & 0 \leq t < t_r \\ \tfrac{1}{2} a_{\min,i}(t - t_r)^2 + \left[a_i t_r + v_i(0)\right] \cdot (t - t_r) + \tfrac{1}{2} a_i t_r^{\,2} + v_i(0)t_r + d_i(0) & t \geq t_r \end{cases} \end{aligned} \tag{6}$$

Using the definitions for range, range rate, and relative acceleration as given in section 5.2, as well as equations (1) through (6), we arrive at the following relationships for the range, range rate, and relative acceleration.

$$a_{i,i+1}(t) = \begin{cases} a_{brake,i+1} - a_i & 0 \leq t < t_r \\ a_{brake,i+1} - a_{\min,i} & t \geq t_r \end{cases} \tag{7}$$

$$\begin{aligned} v_{i,i+1}(t) &= v_{i,i+1}(0) + \int_0^t a_{i,i+1}(\tau)d\tau \\ &= \begin{cases} (a_{brake,i+1} - a_i)t + v_{i,i+1}(0) & 0 \leq t < t_r \\ (a_{brake,i+1} - a_{\min,i})(t - t_r) + (a_{brake,i+1} - a_i)t_r + v_{i,i+1}(0) & t \geq t_r \end{cases} \end{aligned} \tag{8}$$

$$\begin{aligned} d_{i,i+1}(t) &= d_{i,i+1}(0) + \int_0^t v_{i,i+1}(\tau)d\tau \\ &= \begin{cases} \tfrac{1}{2}(a_{brake,i+1} - a_i)t^2 + v_{i,i+1}(0)t + d_{i,i+1}(0) & 0 \leq t < t_r \\ \tfrac{1}{2}(a_{brake,i+1} - a_{\min,i})(t - t_r)^2 + \left[(a_{brake,i+1} - a_i)t_r + v_{i,i+1}(0)\right] \cdot (t - t_r) & \\ \quad + \tfrac{1}{2}(a_{brake,i+1} - a_i)t_r^{\,2} + v_{i,i+1}(0)t_r + d_{i,i+1}(0) & t \geq t_r \end{cases} \end{aligned} \tag{9}$$

When solving the above equations for $a_{\min,i}$, the minimum deceleration to avoid a crash, three possible cases arise.

1. The following vehicle and lead vehicle reach the contact state and the lead vehicle is moving.

2. The following vehicle and lead vehicle reach the contact state and the lead vehicle is stopped.
3. The following vehicle's velocity is less than the lead vehicle's velocity (ie. $v_{i+1}(t) > v_i(t)$)

Each of these cases yields a different solution for the minimum deceleration to avoid a crash, and thus, they must be examined independently. When considering each case in more detail, the differences between each of them will become clear.

5.4.1.1 Case 1: Reaching the Contact State with the Lead Vehicle Moving

First we impose the $v_{i,i+1}(t_c) = 0$ condition on (8) when $t \geq t_r$ and find that:

$$t_c = t_r - \frac{(a_{brake,i+1} - a_i)t_r + v_{i,i+1}(0)}{a_{brake,i+1} - a_{\min,i}} \tag{10}$$

Now, imposing the $d_{i,i+1}(t_c) = 0$ condition on (9) when $t \geq t_r$, and substituting in for t_c as given by (10), we find that:

$$a_{\min,i} = a_{brake,i+1} - \frac{\frac{1}{2}\left[(a_{brake,i+1} - a_i)t_r + v_{i,i+1}(0)\right]^2}{\frac{1}{2}(a_{brake,i+1} - a_i)t_r{}^2 + v_{i,i+1}(0)t_r + d_{i,i+1}(0)} \tag{11}$$

Equation (11) represents the minimum deceleration required to avoid a crash with the lead vehicle, given that the two vehicles reach the contact state with the lead vehicle moving.

5.4.1.2 Case 2: Reaching the Contact State with the Lead Vehicle Stopped

The above value for $a_{\min,i}$ will be invalid if the lead vehicle comes to rest at some time $t < t_c$. In order to handle this case, we must compute the time at which the lead vehicle comes to rest, t_{lead}, and check it against t_c. If $t_{lead} < t_c$, then we have case 2 in which the contact state is reached with the lead vehicle stopped. Otherwise, we have case 1, and the prior calculation for $a_{\min,i}$ is valid.

From (2) it is straightforward to show that:

$$t_{lead} = \frac{-v_{i+1}(0)}{a_{brake,i+1}} \tag{12}$$

As previously stated, if $t_{lead} < t_c$, then the following vehicle reaches the contact state with the lead vehicle stopped. In this case, the distance traveled by the following vehicle during the reaction time delay, plus the braking distance must equal the braking distance of the lead vehicle, plus the initial range between the two vehicles. This can be expressed as:

$$d_{delay,i} + d_{braking,i} = d_{i,i+1}(0) + d_{braking,i+1}$$

Equivalently, if we decompose $d_{i,i+1}(0)$ using the definition given in the problem introduction we have:

$$d_{delay,i} + d_{braking,i} + d_i(0) = d_{i,i+1}(0) + d_{braking,i+1} + d_{i+1}(0) - l_{i+1} \quad (13)$$

From equations (3) and (12) it is straightforward to show that:

$$d_{braking,i+1} = -\frac{v_{i+1}(0)^2}{2a_{brake,i+1}} \quad (14)$$

Also, the left hand side of (13) is simply (6) for $t \geq t_r$

$$d_{delay,i} + d_{braking,i} + d_i(0) = \quad (15)$$
$$\tfrac{1}{2}a_{\min,i}(t-t_r)^2 + [a_i t_r + v_i(0)]\cdot(t-t_r) + \tfrac{1}{2}a_i {t_r}^2 + v_i(0)t_r + d_i(0)$$

Substituting (14) and (15) into (13), we get:

$$\tfrac{1}{2}a_{\min,i}(t-t_r)^2 + [a_i t_r + v_i(0)]\cdot(t-t_r) + \tfrac{1}{2}a_i {t_r}^2 + v_i(0)t_r = d_{i,i+1}(0) - \frac{v_{i+1}(0)^2}{2a_{brake,i+1}} \quad (16)$$

Also, at the contact state, the velocity of the following vehicle must be zero. So, from equations (5) and (6), we find that:

$$t_c = t_r + \frac{-[a_i t_r + v_i(0)]}{a_{\min,i}} \quad (17)$$

Solving (15) when $t = t_c$, as given in (16), we get:

$$a_{\min,i} = \frac{-\tfrac{1}{2}[a_i t_r + v_i(0)]^2}{d_{i,i+1}(0) - \frac{v_{i+1}(0)^2}{2a_{brake,i+1}} - \tfrac{1}{2}a_i {t_r}^2 - v_i(0)t_r} \quad (18)$$

Equation (18) represents the minimum deceleration required to avoid a crash with the lead vehicle, given that the two vehicles reach the contact state with the lead vehicle stopped.

5.4.1.3 Case 3: The Two Vehicles are in a Stable State

If $v_{i+1}(t) > v_i(t)$ then the two vehicles are in a stable state and $a_{\min,i} = 0$, since two vehicle in this state present no risk to the host vehicle's driver.

5.4.2 Using the Minimum Deceleration to Avoid a Crash to Compute the Risk Metric for a Platoon of Vehicles

The risk metric is computed by propagating the minimum deceleration to avoid a crash computation along the entire platoon. The resulting risk metric will, thus, be a minimum bound on the deceleration required by the host vehicle (vehicle 0) to avoid a crash with the lead vehicle (vehicle 1).

5.4.2.1 Finding the Largest Non-Stable Platoon

The first step in computing the risk metric is finding the largest non-stable platoon of which the host vehicle is a member. To find the largest non-stable platoon, one simply must find the largest consecutive string of vehicles, starting with the host vehicle, for which the relative velocities are non-increasing. For example, the largest non-stable platoon for the platoon shown at an instant in time in Figure 5.5, comprises vehicles 0 – 3 since $v_4 > v_3$.

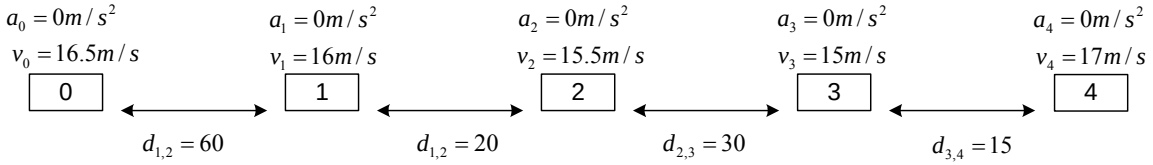

Figure 5.5: Choosing the largest non-stable platoon.

5.4.2.2 Prediction of Future Vehicle States

The previously derived formulae for $a_{\min,i}$ are only applicable when the braking of vehicle $i+1$ begins at $t = 0$. Thus, the state for each vehicle upstream of vehicle i must be determined at the time its predecessor begins braking. For example, assume that $t_r = 1.5s$ and that vehicle n begins braking at $t = 0$. One can directly apply the above formulae to find $a_{\min,n-1}$. Vehicle n-2's leader, vehicle n-1, however, does not begin braking at $t = 0$ due to the reaction time of vehicle n-1's driver. Thus, one must first predict the state of vehicle n-2 at $t = 1.5s$, the time at which vehicle n-1 begins braking. Then, using the new predicted state at time $t = 1.5s$, one can apply the above formulae to determine $a_{\min,n-2}$. This method can be used to determine $a_{\min,i}$ for each vehicle in the platoon. The following generalizes the state prediction algorithm which must be used to calculate $a_{\min,i}$ when $i < n-1$.

First, we assume that the initial vehicle accelerations will remain constant throughout the prediction window, and thus:

$$a_{i,predicted} = a_i$$

$$a_{i+1,predicted} = a_{i+1}$$

Calculating the velocity and position estimates for each vehicle, we get:

$$v_{i,predicted}(t) = v_i(0) + \int_0^{(n-1-i)t_r} a_{i,predicted}\,dt = v_i(0) + a_{i,predicted}(n-1-i)t_r$$

$$v_{i+1,predicted}(t) = v_{i+1}(0) + \int_0^{(n-1-i)t_r} a_{i+1,predicted}\,dt = v_{i+1}(0) + a_{i+1,predicted}(n-1-i)t_r$$

$$d_{i,predicted}(t) = d_i(0) + \int_0^{(n-1-i)t_r}\int_0^{t} a_{i,predicted}\,d\tau dt = d_i(0) + v_i(0)(n-1-i)t_r + \tfrac{1}{2}a_{i,predicted}[(n-1-i)t_2]^2$$

$$d_{i+1,predicted}(t) = d_{i+1}(0) + \int_0^{(i-2)t_r}\int_0^{t} a_{i+1,predicted}\,d\tau dt = d_{i+1}(0) + v_{i+1}(0)(i-2)t_r + \tfrac{1}{2}a_{i+1,predicted}[(i-2)t_2]^2$$

Using the above to determine the predictions for relative acceleration, range rate, and range predictions, we get:

$$a_{i,i+1,predicted} = a_{i+1,predicted} - a_{i,predicted}$$

$$v_{i,i+1,predicted}(t) = v_{i,i+1}(0) + \int_0^{(n-1-i)t_r} a_{i,i+1,predicted}\,dt = v_{i,i+1}(0) + a_{i,i+1,predicted}(n-1-i)t_r$$

$$d_{i,i+1,predicted}(t) = d_{i,i+1}(0) + \int_0^{(n-1-i)t_r}\int_0^{t} a_{i,i+1,predicted}\,d\tau dt$$
$$= d_{i,i+1}(0) + v_{i,i+1}(0)(n-1-i)t_r + \tfrac{1}{2}a_{i,i+1,predicted}[(n-1-i)t_2]^2$$

These new predicted states can now be substituted into the previously derived formulae for computing $a_{\min,i}$.

5.4.2.3 Propagation of Braking Activity along the Platoon and Final Computation of Risk Metric

After predicting the state of the next vehicle in the platoon (vehicle n-2) at the time when its leader (vehicle n-1) begins braking, one simply applies the formulae for calculating $a_{\min,n-2}$ using the new predicted state and assuming that the lead vehicle (vehicle n-1) is braking at $a_{\min,n-1}$. This method can be applied along the entire platoon and will give a lower bound on the braking, or in other terms, the minimum deceleration required by the host vehicle to avoid a crash with the lead vehicle.

The final choice for the risk metric is $a_{\min,0}$, the minimum lower bound acceleration required for the host vehicle to avoid a crash with its leader. This method for propagating the minimum deceleration computation works well for most cases, however, consider the case when a vehicle

in the platoon is braking at a rate greater than the minimum level required to avoid a collision with its leader (ie. $a_{\min,i} > a_i \quad \forall i > 0$, remembering that a is less than zero when a vehicle is braking). Should this situation arise, one must assume that the lead vehicle is braking at a_i, the lead vehicle's actual deceleration, rather than $a_{\min,i}$, when propagating the minimum deceleration computation. This can be generalized as follows:

$$a_{\min,\,final,i} = \begin{cases} a_{\min,i} & i = 0 \\ \min\left\{a_{\min,i}, a_i\right\} & \forall i > 0 \end{cases} \tag{19}$$

Thus, when propagating minimum deceleration computation along the platoon, one must compute $a_{\min,i}$ for vehicle i, and assume that vehicle i brakes at a rate of $a_{\min,\,final,i}$. Thus, the final risk metric for the host vehicle is $a_{\min,\,final,0}$.

5.4.3 Tightening the Risk Metric's Lower Bound by Refining the Reaction Time Estimate using Brake Light Information

By using brake light information, it is possible to refine the reaction time estimate each time a new data sample is received. Keep in mind that, in practice, brake light status cannot be determined simply by measuring deceleration, since a vehicle may be traveling up hill, or be driving into a strong wind.

To illustrate how brake light information for this purpose, consider the three vehicle platoon shown in Figure 5.6.

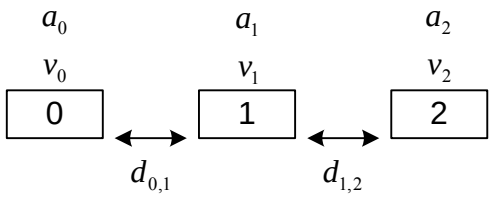

Figure 5.6: Vehicle platoon used to demonstrate reaction time refinement.

First, assume that each driver has a reaction time of $t_{r,i} = 1.5s$, and that the data sample rate is 10 Hz. Also assume that the vehicles in the platoon are reporting their brake light status (on/off) at each data sample. At $t = 0$ vehicle 2 begins braking. So, we calculate $a_{\min\,final,1}$ using the method described previously, where $t_{r,1} = 1.5s$. We then predict the future states of vehicles 0 and 1 at time $t = 1.5s$ because of the reaction time of vehicle 1's driver, and finally, we calculate $a_{\min,0}$ using $t_{r,0} = 1.5s$. At the next sample, $t = 0.1$ s, we repeat the calculation, except this time our estimate of the reaction time for vehicle 1 and vehicle 2 are $t_{r,1} = 1.4s$ and $t_{r,0} = 1.5s$. The benefit of modifying the reaction time estimate for vehicle 1 is twofold:

1. The computation of $a_{\min,final,1}$ will use the new reaction time estimate for vehicle 1 ($t_{r,1} = 1.4s$), which will improve the estimate of the minimum deceleration to avoid a crash.
2. The prediction window for vehicle 0 will be reduced to 1.4 s, the new estimate of the reaction time of vehicle 1. Reducing the length of the prediction window will reduce the likelihood that radical changes in driver behavior can occur during this time. Radical changes in driver behavior, such as sudden braking or lane change maneuvers, would likely lead to false positives in a rear-end collision warning system which uses the risk metric.

At each subsequent time step, we continue to decrement $t_{r,1}$ until vehicle 1's brake lights turn on, at which time the driver has reacted, and $t_{r,1} = 0s$. Once vehicle 1 has reacted to vehicle 2's braking, one begins to refine the estimate of vehicle 0's reaction time in a similar manner.

Keep in mind that it may take longer than 1.5 s for the driver to react, in which case, the above algorithm would begin to give negative reaction times. Thus, if the reaction time estimate reaches 0.1 s, and at the next sample, the vehicle's brake lights are still not on, a reaction time of 0.1 s should be used. The reaction time should be held at 0.1 s for all future calculations, until the its brake lights turn on, at which time the reaction time becomes $t_{r,i} = 0s$.

Using this method, as brake lights propagate backwards, the reaction times become 0, and the estimate of the risk metric (i.e. of the lower bound deceleration $a_{\min,0}$) improves.

5.5 Risk Metric Calculation on Platoons for which Vehicle Trajectory History is Not Known

This section is used to demonstrate the general use of the risk metric. Examples will be presented that will show that platoons which intuitively present greater risk to the host vehicle, do in fact yield a greater level of risk. For these examples, because we do not have vehicle trajectory histories, it is not possible to refine the reaction time estimate using brake light information.

5.5.1 Handling the Lack of Vehicle Trajectory History

Because of the lack of vehicle trajectory history, $t_r = 0$ is chosen to simplify the equations used to calculate $a_{\min,0}$. Although vehicle trajectory histories are not known, and we have chosen $t_r = 0$, the following examples will demonstrate the general use of the risk metric. In fact, the computations performed in this chapter identically mimic those that would occur at each time step if vehicle trajectory histories were known, with the exception that the reaction time estimates cannot be refined due to the lack of brake light information.
Setting $t_r = 0$ in equations (10), (11), (12), (18) we get:

5.5.1.1 Case 1: Collision with a Moving Vehicle

$$t_c = -\frac{v_{i,i+1}(0)}{a_{brake,i+1} - a_{\min,i}} \tag{20}$$

$$a_{\min,i} = a_{brake,i+1} - \frac{\frac{1}{2} v_{i,i+1}(0)^2}{d_{i,i+1}(0)} \tag{21}$$

5.5.1.2 Case 2: Collision with a Stopped Vehicle

$$t_{lead} = \frac{-v_{i+1}(0)}{a_{brake,i+1}} \tag{22}$$

$$a_{\min,i} = \frac{-\frac{1}{2} v_i(0)^2}{d_{i,i+1}(0) - \frac{v_{i+1}(0)^2}{2 a_{brake,i+1}}} \tag{23}$$

Also, since $a_{\min,final,0}$ is independent of reaction time, equation (19) does not change.

The following procedure was used to calculate the final risk metric for the sample calculations, in which vehicle trajectory histories were not known.

Step 1: Set $i = n$, $a_{brake,n} = a_n(0) - 1$, (-1 is the disturbance injected at lead vehicle)

Step 2: Assume Case 1 and calculate $a_{\min,i-1}$ and t_c

Step 3: Calculate t_{lead}

Step 4: If $t_{lead} > t_c$, $a_{\min,final,i-1} = \min\{a_{\min,i-1}, a_{i-1}\}$, $\rightarrow$ GOTO 6

Step 5: If $t_{lead} \le t_c$, Case 2, calculate $a_{\min,i-1}$,
$a_{\min,final,i-1} = \min\{a_{\min,i-1}, a_{i-1}\}$, $\rightarrow$ GOTO 6

Step 6: Set $a_{brake} = a_{\min,final,i-1}$

Step 7: Predict future states of vehicles $i-2$ and $i-1$

Step 8: Decrement i

Step 9: If $i > 0$ $\rightarrow$ GOTO 2

Step 10: Final risk metric = $a_{\min,0}$

5.5.2 Sample Calculations

In order to illustrate how the risk metric is calculated, the following sample calculations are provided. The sample calculations also show that platoons which intuitively should yield greater risk, in fact do. Keep in mind that the risk metric can be physically interpreted as the minimum acceleration required to avoid a crash, and thus, its value is negative, when risk is present. Large

negative values are associated with greater risk, while small negative values (close to 0) are associated with less risk.

In the following examples, the range, range rate, and acceleration data is given. For each example, the risk metric will be computed using the algorithm presented in the previous section. The actual results of the risk metric calculation will follow the descriptions of the seven examples.

Example 1:

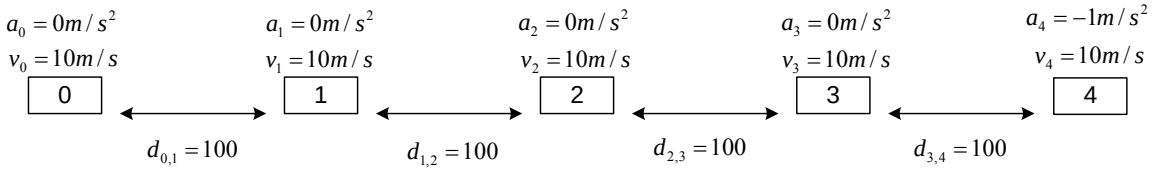

Example 2:

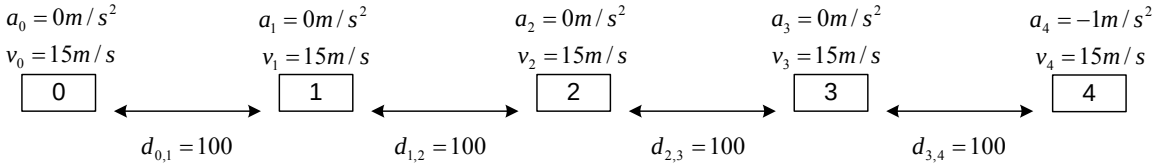

The risk metric for example 2 should indicate greater risk than that of example 1 because of the increase in vehicle speeds.

Example 3:

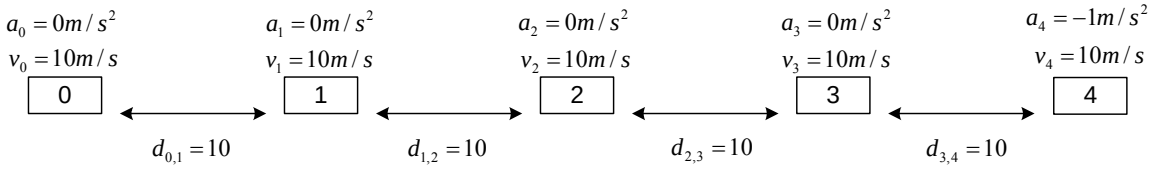

The risk metric for example 3 should indicate greater risk than that of example 1 because of the decrease in vehicle headways.

Example 4:

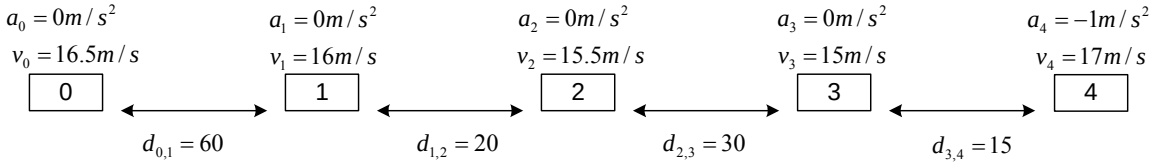

Notice in example 4 that vehicles 3 and 4 are stable. This means that vehicle 4 presents no risk to vehicle 3, and can be eliminated from the risk metric's computation. Thus, the beginning of the computation will begin at vehicle 3, since vehicles 0 – 3 form an unstable platoon.

Example 5:

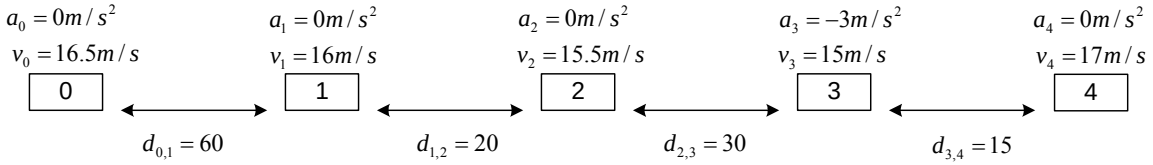

The risk metric for example 5 should indicate greater risk than that of example 4 because of the braking activity of vehicle 3.

Example 6:

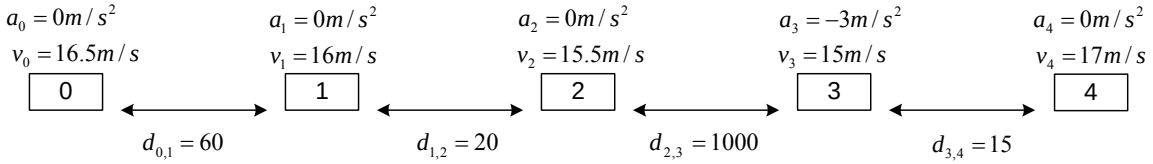

The risk metric for example 6 should indicate less risk than that of examples 4 and 5 because of the large headway between vehicles 2 and 3.

Example 7:

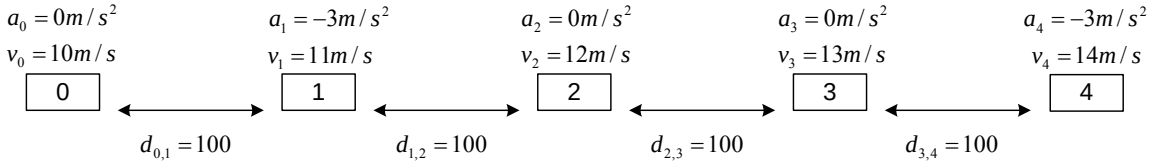

Example 7 shows a stable platoon. Thus, the metric should be zero.

5.5.3 Sample Calculation Results

Table 5.1 summarizes the results of the sample calculations. Notice that the hypothesized relationships between the risk metrics were found to be true.

Table 5.1: Risk metric results for the seven examples shown above.

Example	Risk Metric
1	-0.1163
2	-0.2332
3	-0.7143
4	-0.6858
5	-1.1928
6	-0.1272
7	0

$metric_1 > metric_2$

$metric_1 > metric_3$

$metric_4 > metric_5$

$metric_6 > metric_4$

$metric_6 > metric_5$

$metric_7 = 0$

5.6 Risk Metric Calculation on Platoons for which Vehicle Trajectory History is Known

In order to test that the risk metric functions as expected, one would need a complete history of data for a platoon of vehicles, which includes all of the information shown in Figure 5.1. Without this data, it is not possible to refine the reaction time estimate by using brake light information, which is crucial to implementing a working system in which false positives are minimized. Because no such naturalistic data exists, the creation of a simulated traffic flow in MATLAB was required. The simulation created a moving platoon of vehicles which exhibited realistic characteristics of a traffic flow, after which a shockwave was initiated by braking activity of the platoon's lead vehicle. Then, at each time step (f = 10 Hz, T = 0.1 s) the risk metric's value was calculated.

This section will show how the simulated traffic flow was created, as well as how the risk metric was computed at each time step of the simulation. Also, to show the benefit of computing the risk metric using data from a lead platoon, the risk metric will be computed when only the lead vehicle is considered, as well as when the entire lead platoon was considered.

5.6.1 Simulation of a Traffic Flow

The first step, as stated above, was to create a simulated traffic flow. To do this, the lead vehicle's acceleration profile was chosen, and the speed and position trajectories were computed through integration of the acceleration profile. The acceleration profile of each subsequent vehicle in the platoon was governed by a car following model, and again, speed and position trajectories were computed through integration. Several microscopic follow-the-leader[20] models were considered, including models developed by Pipes [15], Chandler et al. [16], Gazis et al. [17], and Gipps [18]. The Gipps model, which is used by the UK Transport Research Laboratory highway simulation package, SISTM, attempts to model different behavioral features of drivers [19]. A modified version of the Gipps model was shown to fit the highest number of maneuvers which are characteristic of human-controlled vehicles (aggressiveness, target speed, etc.) [21]. In addition, the model was used to accurately fit 90% of car-following test data from the SAVME database [20], and consequently, is the model recommended for the design and evaluation of collision warning and avoidance systems [21]. Thus, we chose to use the modified Gipps model when evaluating the risk metric's performance through simulation. The model is represented by the following difference equation:

[20] A follow-the-leader car following model is one in which vehicle i 's acceleration is a function of its own kinematics data, and vehicle $i+1$'s kinematics data.

$$v_i(t+\tau) = \min\begin{cases} v_i(t) + 2.5a_i\tau\left(1 - \dfrac{v_i(t)}{V_i}\right)\sqrt{0.025 + \dfrac{v_i(t)}{V_i}} \\ b_i\tau + \sqrt{(b_i\tau)^2 - b_i\left[2\left[x_{i+1}(t) - s_{i+1} - x_i(t) - v_i(t)\tau\right] - \dfrac{v_{i+1}(t)^2}{\hat{b}}\right]} \end{cases}$$

where $i = 0,...n-1$ (n = lead vehicle)

The model parameters are defined as follows:

a_i = maximum acceleration of vehicle i
b_i = maximum deceleration of vehicle i
$\hat{b}$ = estimated value for b_{i+1}
s_i = length of vehicle i plus a margin, if desired
V_i = desired speed of vehicle i
$x_i(t)$ = the location of the front of vehicle i at time t
$v_i(t)$ = the actual speed of vehicle i at time t
τ = $\frac{1}{2}$ the reaction time

For the simulation, we chose:

$\tau = \frac{2}{3}$ s
$a_i = 2$ m/s^2
$b_i = -6$ m/s^2
$\hat{b} = -8$ m/s^2
$s_i = 5$ m
$V_i = 31$ m/s = 70 mph

These values were chosen because they are fairly realistic. Note that the value for τ is multiplied by 2 in the model formula, and thus, 2τ = 1.33 s is in fact the estimate of the driver's reaction time, which is quite similar to the risk metric's assumed value of 1.5 s.

5.6.2 Creating Shockwaves in the Traffic Flow

After choosing the car following model, and choosing the realistic parameters shown above, a lead vehicle acceleration profile was created which ensured that the following vehicles were subjected to a shockwave. Figures 52 and 53 show the two sample trajectories for the lead vehicle of the platoon. Each trajectory was used to create a simulated shockwave in the platoon which followed the lead vehicle.

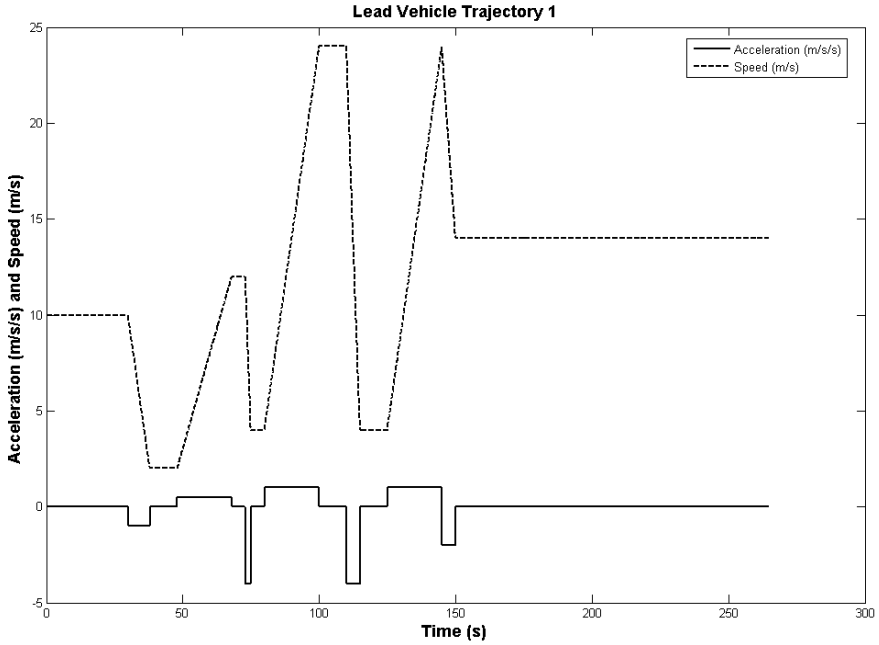

Figure 5.7: First sample trajectory for the lead vehicle which causes three shockwaves.

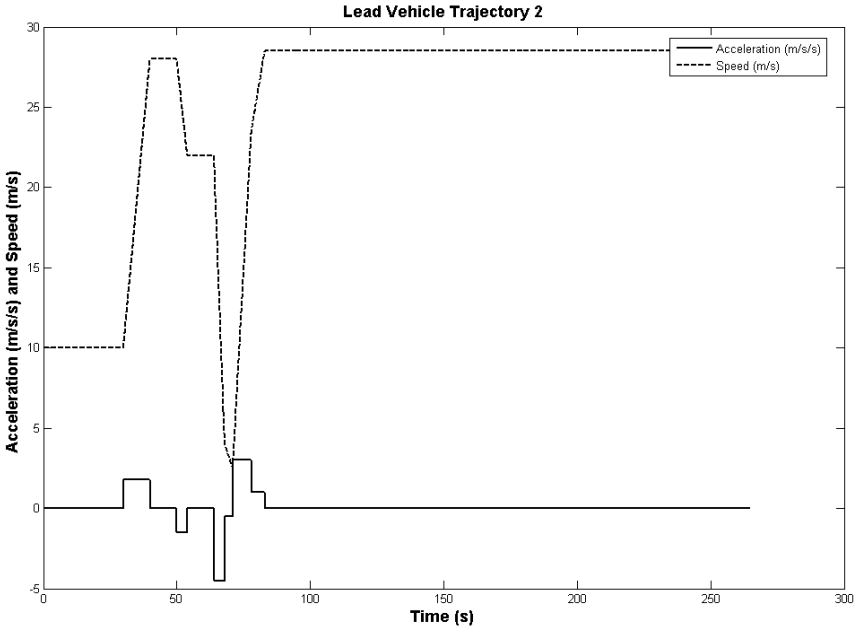

Figure 5.8: Second sample trajectory for the lead vehicle which causes two shock waves.

A platoon with a total of ten vehicles, the leader plus nine followers, was created and was shown to yield the desired shockwave effect. Figures 54 and 55 show the positions of the ten vehicles

as a function of time. Notice that shockwaves are present in both plots. In the two plots, the shockwaves have been highlighted with red (gray if printed in black and white) ovals.

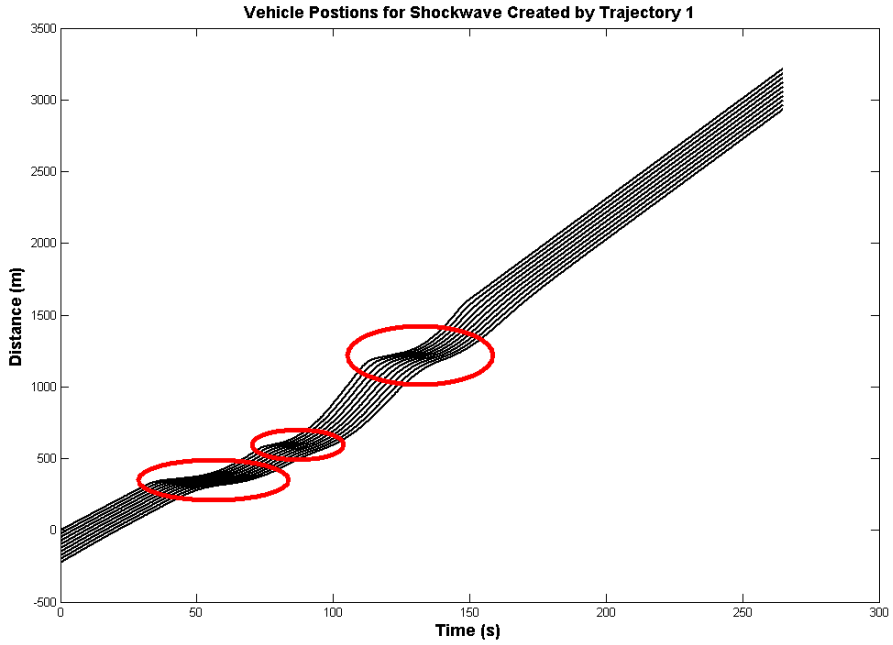

Figure 5.9: Shockwave due to first sample trajectory for the lead vehicle.

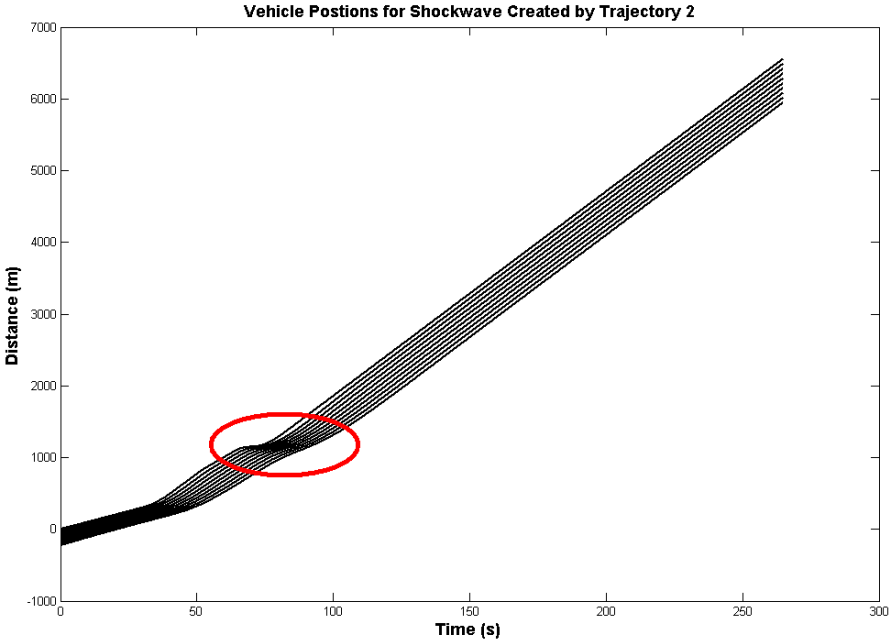

Figure 5.10: Shockwave due to second sample trajectory for the lead vehicle.

5.6.3 Risk Metric Computation on the Simulated Traffic Flow

After ensuring that both lead vehicle acceleration profiles caused a shockwave to propagate along the platoon, the risk metric was calculated for the host vehicle, which was chosen to be the seventh upstream vehicle. The risk metric was calculated using the method presented earlier, which refines the driver reaction time estimate by using brake light information. A nominal value of $t_r = 1.5 \ \ s$, the generally accepted mean driver perception-reaction time [22], was assumed, and brake lights for vehicle i were considered to be in the ON state when $a_i < -\frac{1}{20} g$, and OFF otherwise. Also, rather than using a static number of look-ahead vehicles to calculate the risk metric, only vehicles within a ten-second headway of the host vehicle were used to perform the calculation. This ensured that only vehicles of immediate consequence to the host were accounted for in the risk metric's computation. The following pseudocode was used to calculate the risk metric for the simulated traffic flow.

Step 1: Set $i = n$, $a_{brake,n} = a_n(0)$

Step 2: Assume Case 1 and determine reaction time to be used in calculation, as per algorithm outlined in section 5.4.3

Step 3: Calculate $a_{\min,i-1}$ and t_f

Step 4: Calculate t_{lead}

Step 5: If $t_{lead} > t_f$, $a_{\min,\, final,i-1} = \min\{a_{\min,i-1}, a_{i-1}\}$, $\rightarrow$ GOTO 6

Step 6: If $t_{lead} \le t_f$, Case 2, calculate $a_{\min,i-1}$,
$a_{\min,\, final,i-1} = \min\{a_{\min,i-1}, a_{i-1}\}$, $\rightarrow$ GOTO 6

Step 7: Set $a_{brake} = a_{\min,\, final,i-1}$

Step 8: Predict future states of vehicles $i-2$ and $i-1$

Step 9: Decrement i

Step 10: If $i > 0 \rightarrow$ GOTO 2

Step 11: Final risk metric = $a_{\min,0}$

Figures 56 and 57 show screen captures of the simulated platoon. The host vehicle is colored green (gray if printed in black and white), and the vehicles within the ten-second look-ahead headway, which were used in the risk metric's computation, are colored black. Figure 5.11 shows the platoon when they just begin moving. Figure 5.12 shows the platoon at the onset of the shockwave, when the lead vehicle begins to decelerate. Notice that at the onset of the shockwave, the number of look-ahead vehicles increased from four to six due the smaller headways between the vehicles.

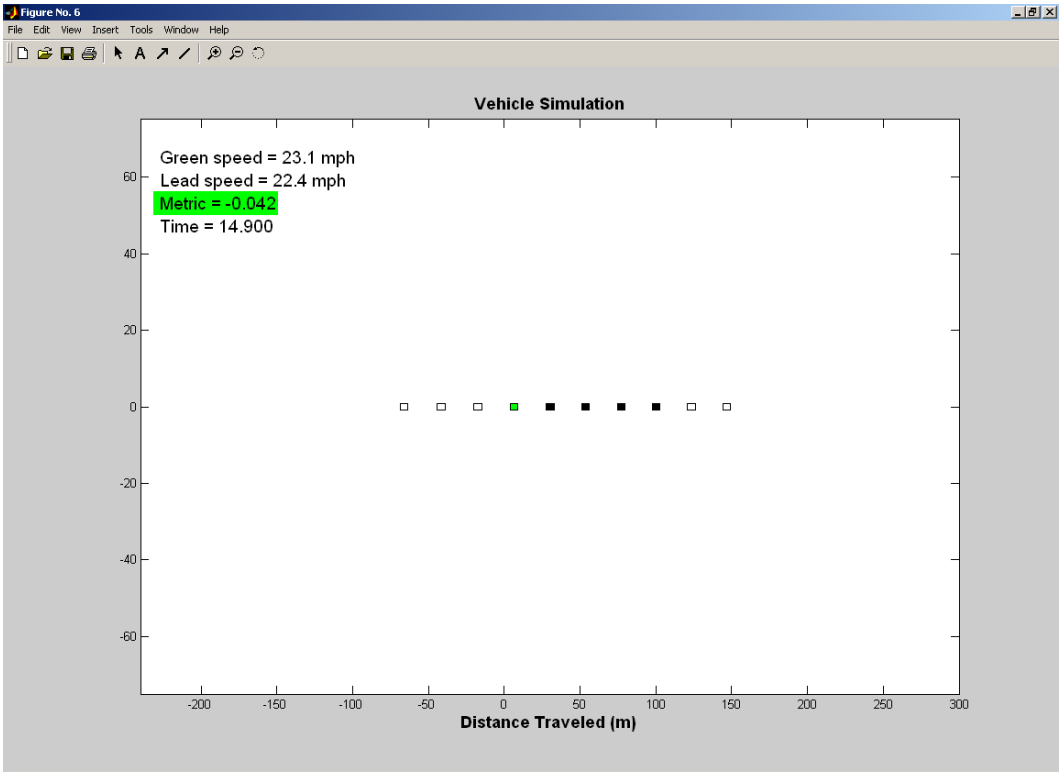

Figure 5.11: Initial state of simulated vehicle platoon.

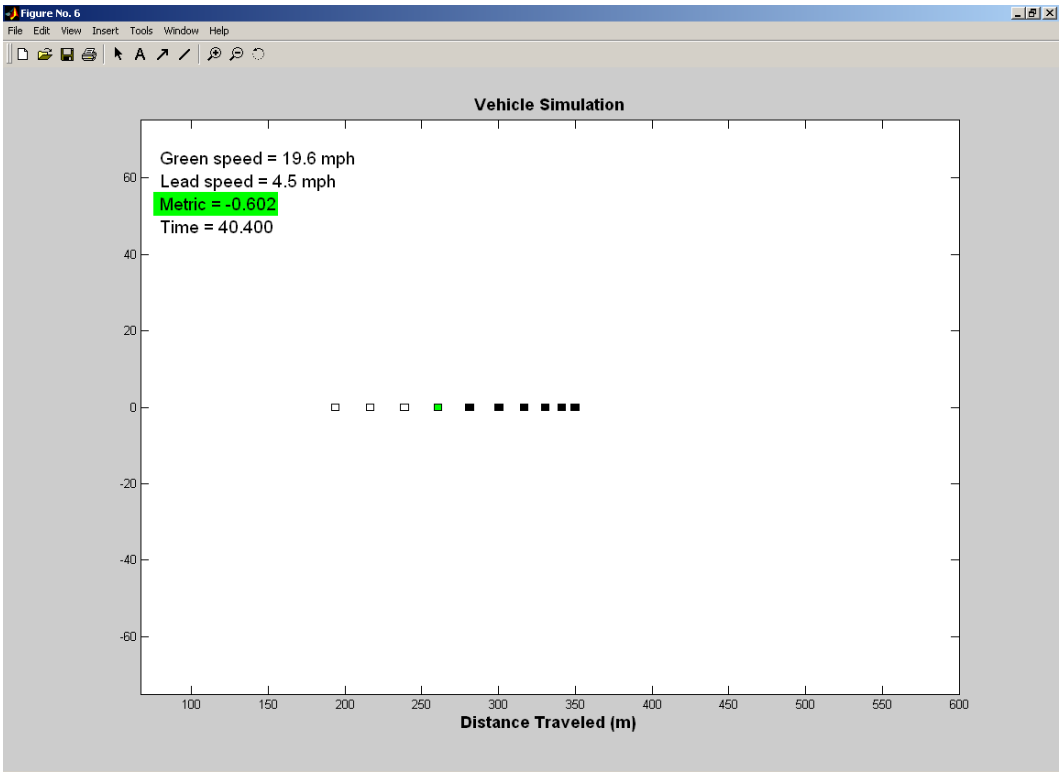

Figure 5.12: Platoon at the onset of a shockwave.

5.6.4 Simulation Results

To show the results of the simulation, the host vehicle's actual acceleration, the risk metric's value, and the number of look-ahead vehicles used in the risk metric's computation were all plotted on the same axes. Figure 5.13 shows the results for the first sample lead vehicle trajectory in which three shockwaves were induced, and Figure 5.14 shows the results for second sample lead vehicle trajectory, in which one shockwave was induced. In both of these simulations the number of look-ahead vehicles was chosen dynamically (all vehicles within a ten-second headway of the host). Notice that the risk metric quite accurately predicted the future deceleration activity of the host vehicle. Also notice that during critical periods, where the driver was decelerating, the number of look-ahead vehicles increased to yield a better preview as to what was happening downstream. It is also worth noting that in both of these simulations, there were no false positives, where the driver would be incorrectly warned of impending deceleration activity. Graphically, a false positive would be present if the risk metric's value dropped to a low value, and within a short period of time the host vehicle did not begin to decelerate at a rate similar to that indicated by the risk metric.

To compare the above results with existing rear-end collision avoidance systems, the above simulations were repeated with the number of look-ahead vehicles set to one: the number of look-ahead vehicles used by existing systems when only radar sensing is used. Figure 5.15 shows the results for the first sample lead vehicle trajectory, and Figure 5.16 shows the results for second sample lead vehicle trajectory. Notice that the number of look-ahead vehicles is a constant one, and that in comparison to the results when the look-ahead was dynamic, less preview of impending braking activity was provided to the host vehicle's driver.

Also notice that Figures 60, 61, 62, and 63 label each of the four host vehicle deceleration events as Event 1 – 4. Figures 63 and 64 show zoomed views of each of the four events with the 10-second look-ahead simulation results plotted beside the 1-vehicle look-ahead simulation results for easy comparison. Based on this analysis, we concluded that the risk metric, in simulation, performed as desired. It accurately predicted the future braking of the host vehicle, and provided the host vehicle's driver with more preview than that of the 1-vehicle look-ahead case. Although for events 1 – 3 quantifying the amount of additional preview by using a 10-second look-ahead was difficult, it was straightforward for event 4. Looking at the bottom two plots of Figure 5.18, which correspond to event 4, one can see that in the 10-second look-ahead case, the risk metric rapidly drops to a value of $-1.5\ m/s^2$ at 66 s, which gives the driver roughly 4 s of preview, since he actually began to decelerate at 70 s. In the 1-vehicle look-ahead case the risk metric only begins to drop at 69 s, which provides the driver with only 1 s of preview.

The zoomed in figures also show areas in which the risk metric takes on positive values. To explain this, consider a two-vehicle platoon where vehicle 0 is the host, and is following vehicle 1. If vehicle 1's speed is greater than that of vehicle 0, the risk metric is 0, since the distance between the two vehicles is increasing; otherwise, the risk metric is computed using the method described in this chapter. So, if vehicle 1's speed is slightly less than that of vehicle 0, and is accelerating, the acceleration that vehicle 0 must apply to reach the contact state with vehicle 1 is likely to be positive. At the instant that vehicle 1's speed becomes greater than that of vehicle 0, because of its acceleration, the metric will instantaneously switch to a value of 0. This scenario is the cause of the positive risk metric values shown in the simulation results.

These results make it clear that, in simulation, the new proposed method of computing a rear-end collision risk metric by using data from a lead platoon, rather than data from only the lead vehicle, allows one to provide earlier warnings to the host vehicle's driver. The next step in the risk metric's development would be to test it using real data, but unfortunately none exists, and as one can imagine it would be very difficult to acquire such data until a time when wireless communication between vehicles is fully deployed (DSRC). Following the testing of the risk metric in the field, it would be the job of a cognitive psychologist to investigate how the risk metric could be used to derive a suitable warning system, or continuous feedback driver support system to provide information to the driver, and to model the response of the driver to the warnings. Once these steps are complete, one must reevaluate the effectiveness of the system when each vehicle in the platoon is outfitted with the driver warning system to ensure that unintended consequences are minimized. These steps, however, are beyond the scope of this report, but should be the focus of future research.

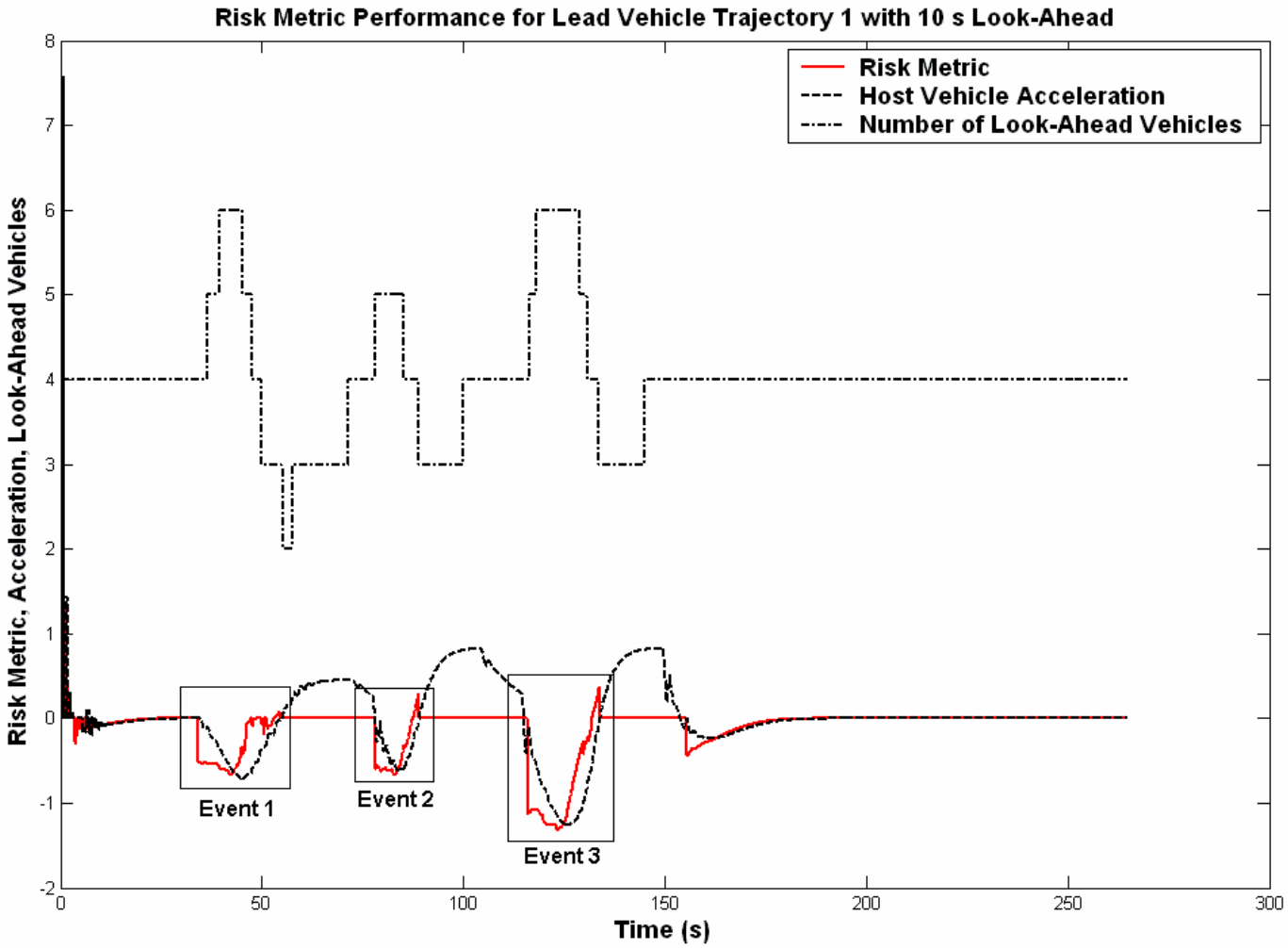

Figure 5.13: Results of risk metric computation for host vehicle in response to first sample trajectory for lead vehicle. (10 s vehicle look-ahead)

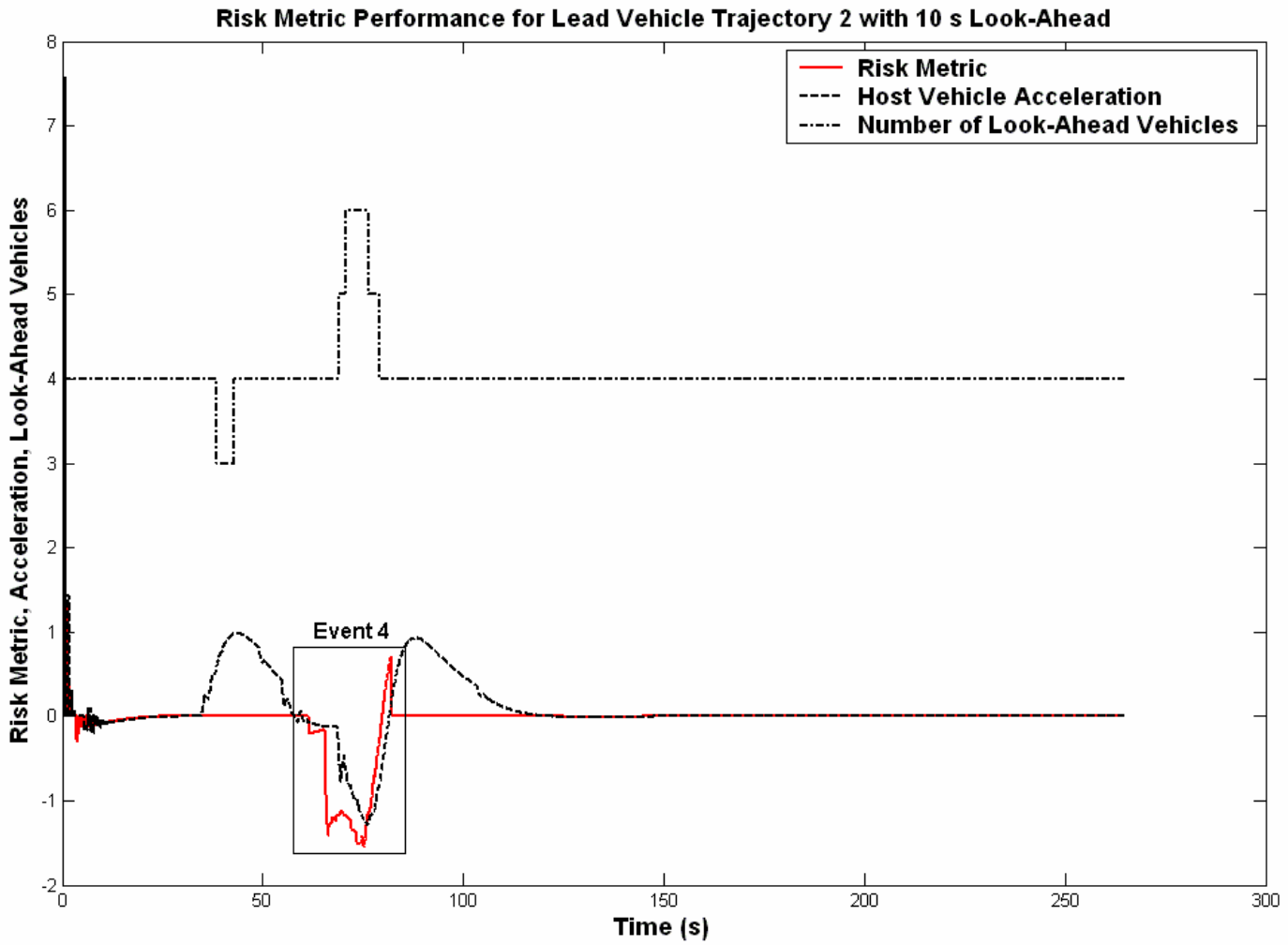

Figure 5.14: Results of risk metric computation for host vehicle in response to second sample trajectory for lead vehicle. (10 s vehicle look-ahead)

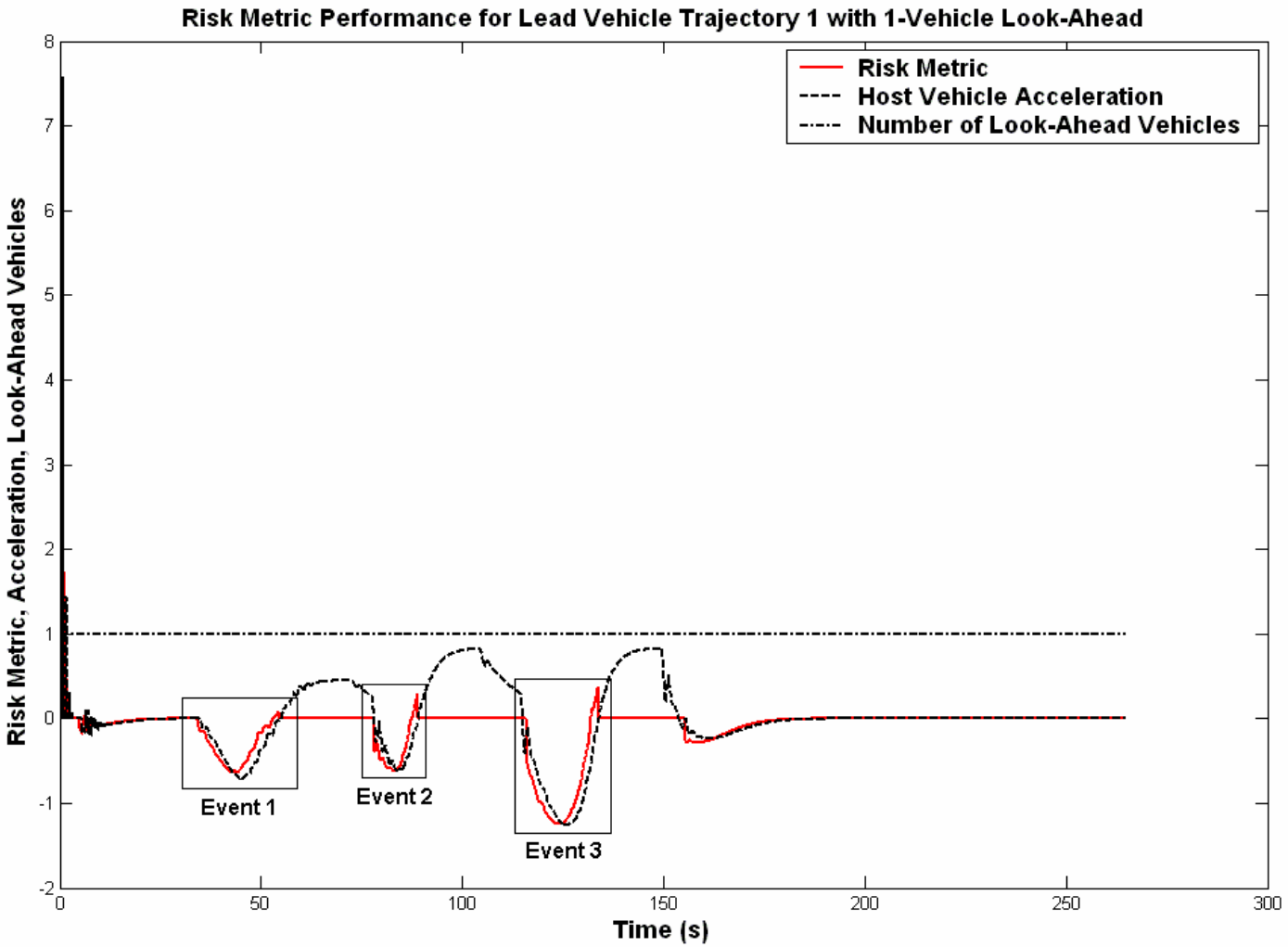

Figure 5.15: Results of risk metric computation for host vehicle in response to first sample trajectory for lead vehicle. (1-vehicle look-ahead)

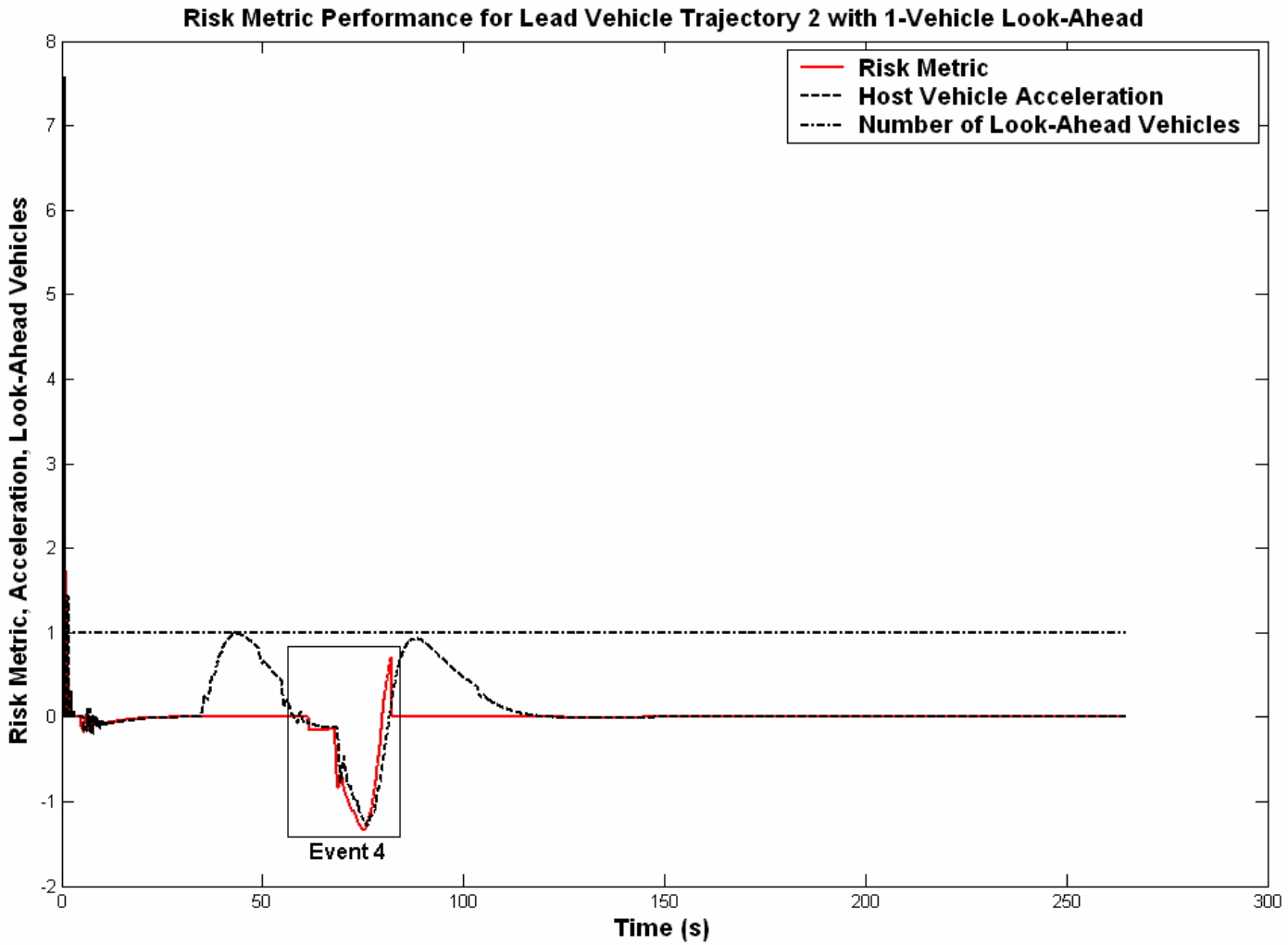

Figure 5.16: Results of risk metric computation for host vehicle in response to second sample trajectory for lead vehicle. (1-vehicle look-ahead)

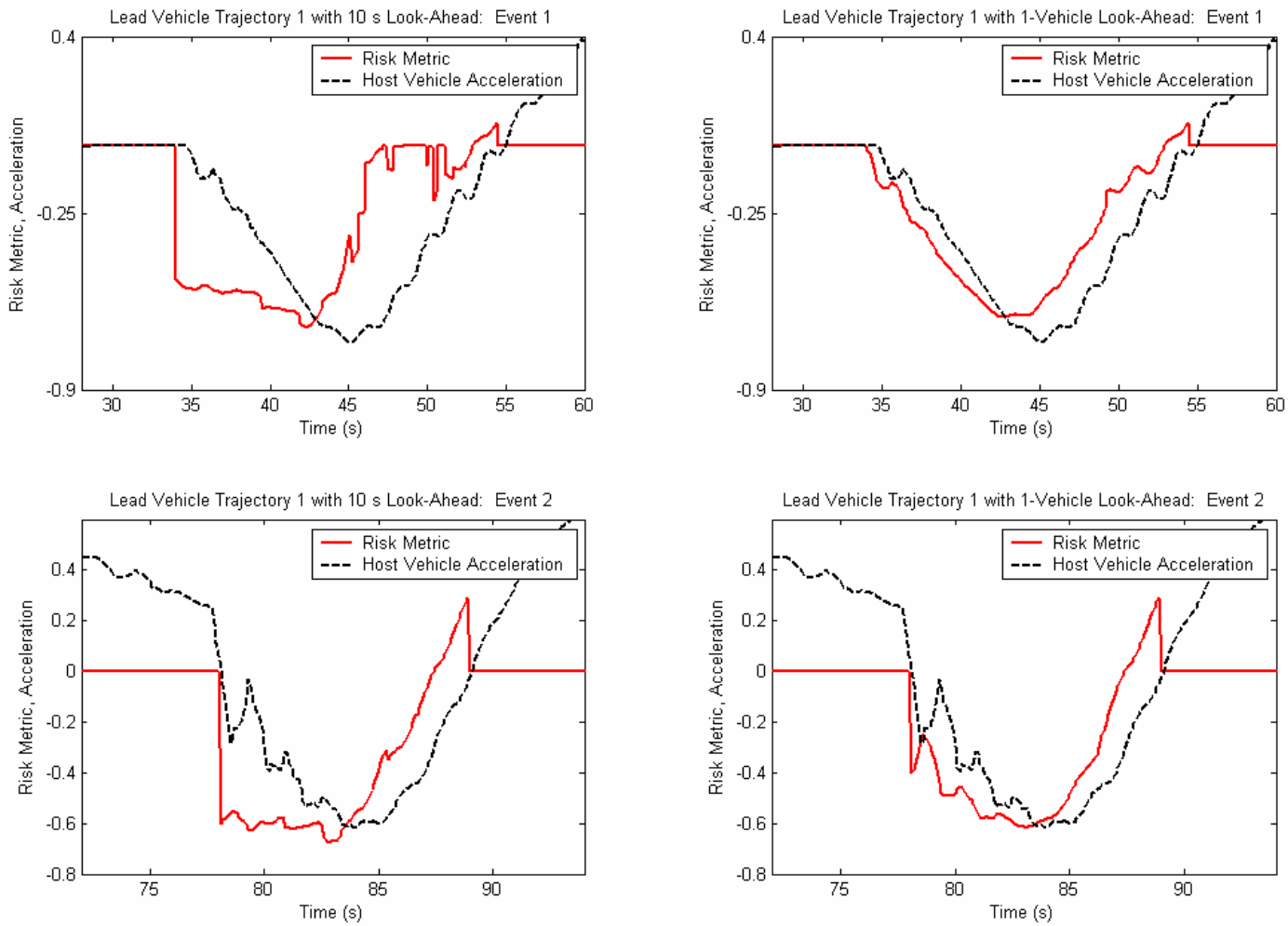

Figure 5.17: Performance comparison for events 1 and 2.

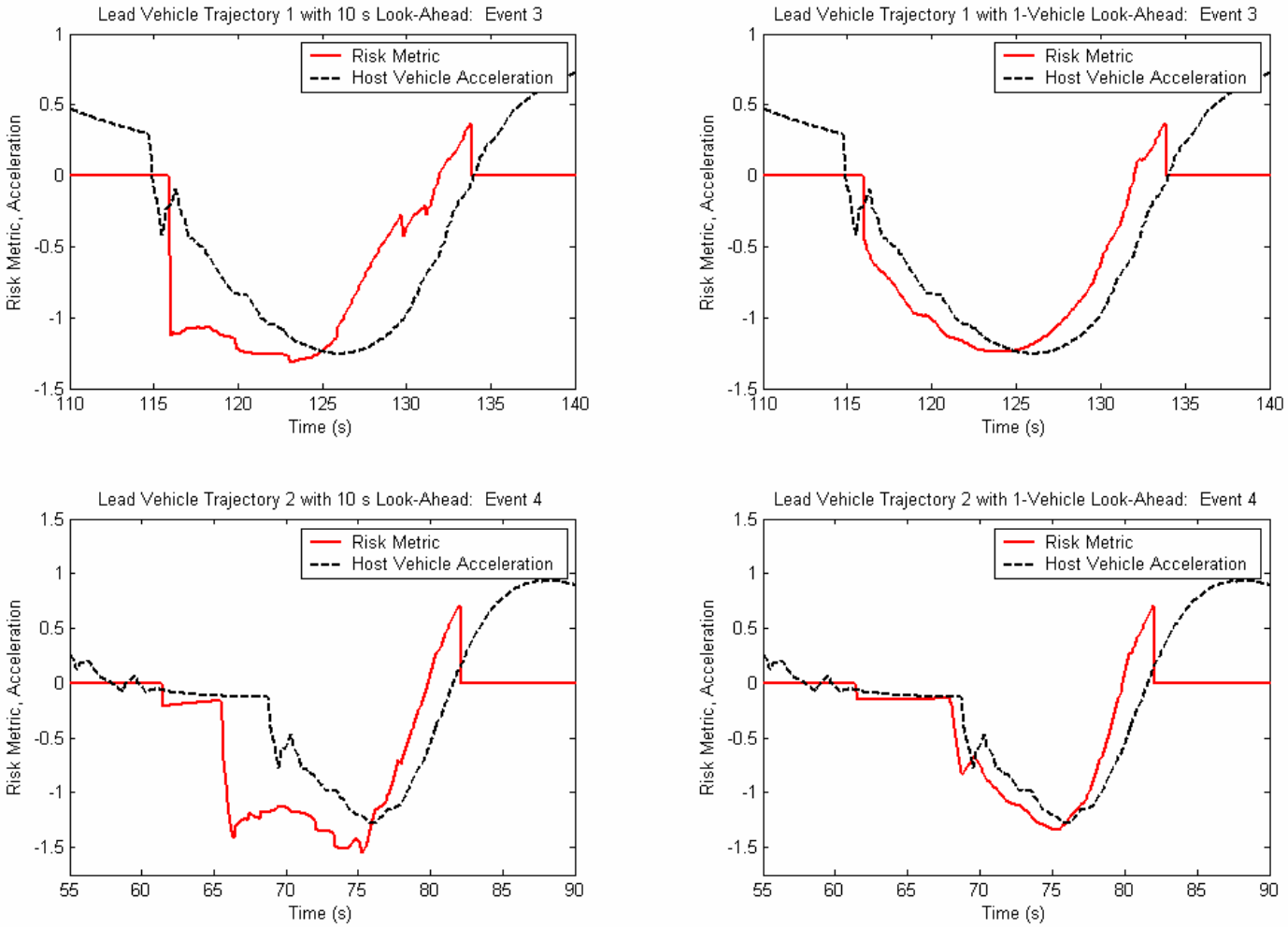

Figure 5.18: Performance comparison for events 3 and 4.

5.7 Risk Metric Sensitivity to Positioning Error

In order to determine the implications of the risk metric on the VPS system or for any positioning sensor, one must investigate how vehicle positioning error affects the accuracy of the calculated risk metric. After the risk metric's sensitivity to vehicle positioning error is understood, the positioning accuracy of the VPS system can be more clearly defined, after which a suggested system specification can be derived.

To determine the risk metric's sensitivity to positioning error, MATLAB was used to create random platoons of vehicles. Random platoons of n vehicles were created in the following manner.

1. Set $i = 1$, choose $-3 < a_i < 0 \ \ m/s^2$, $10 < v_i < 30 \ \ m/s$ (both uniformly distributed), and $d_i = 0 \ \ m$.
2. Increment i
3. Choose $-3 < a_i < 0 \ \ m/s^2$.
4. Choose $v_i = v_{i-1} - (\frac{1}{4} randn - \frac{1}{4}) \ \ m/s$, where $randn$ is a normal random variable with $\sigma = 1$, $\mu = 1$.
5. Choose $0.5 < headway < 3.0 \ \ s$, $d_i = d_{i-1} - headway \cdot v_i \ \ m$.
6. If $i < n \rightarrow$ GOTO 2

NOTE: The above algorithm assumes that the length of each vehicle is zero.

For random platoons, ranging in length from 2 to 20 vehicles, the risk metric was calculated ($metric$). Then, a normally distributed position error with σ ranging from 0 – 10 m was added to the positions of each of the vehicles, and the risk metric was again calculated ($metric_{err}$). The risk metric error was then calculated as follows:

$$metric_{\%err} = \frac{\left\| metric - metric_{err} \right\|_2}{\left\| metric \right\|_2} \times 100 \qquad (24)$$

Using this method, Figure 5.19 was created. For each platoon length, position error pair in Figure 5.19, 1000 random platoons were created.

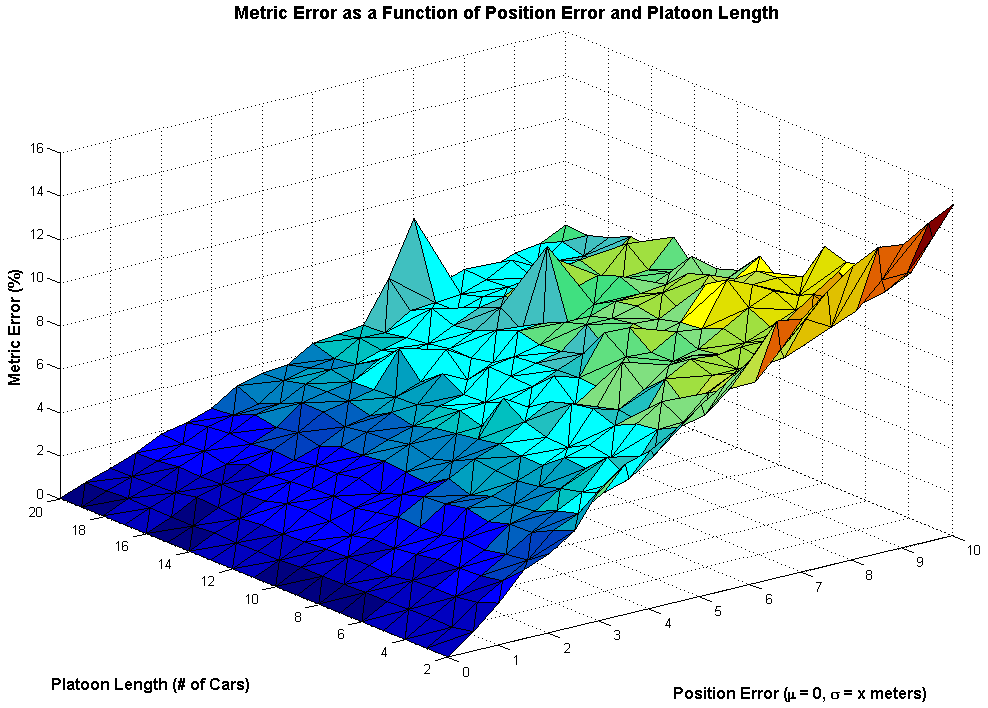

Figure 5.19: Risk metric error as a function of position error and platoon length for randomly created vehicle platoons.

In the above analysis, notice that we only consider the effect of variability of the position. Since only the relative positions of each of the vehicles are important for this application, rather than their absolute positions, the mean errors in position will cancel out, because they are common among all vehicles. Thus, we only concern ourselves with the variability of position. Also note that because we do not have complete vehicle trajectory histories, the above plot does not refine the reaction time estimate using brake light information, and thus, simply assumes a reaction time of zero as in the sample calculations of section 5.5.

A least squares fit to the above data was performed and is shown below, in Figure 5.20.

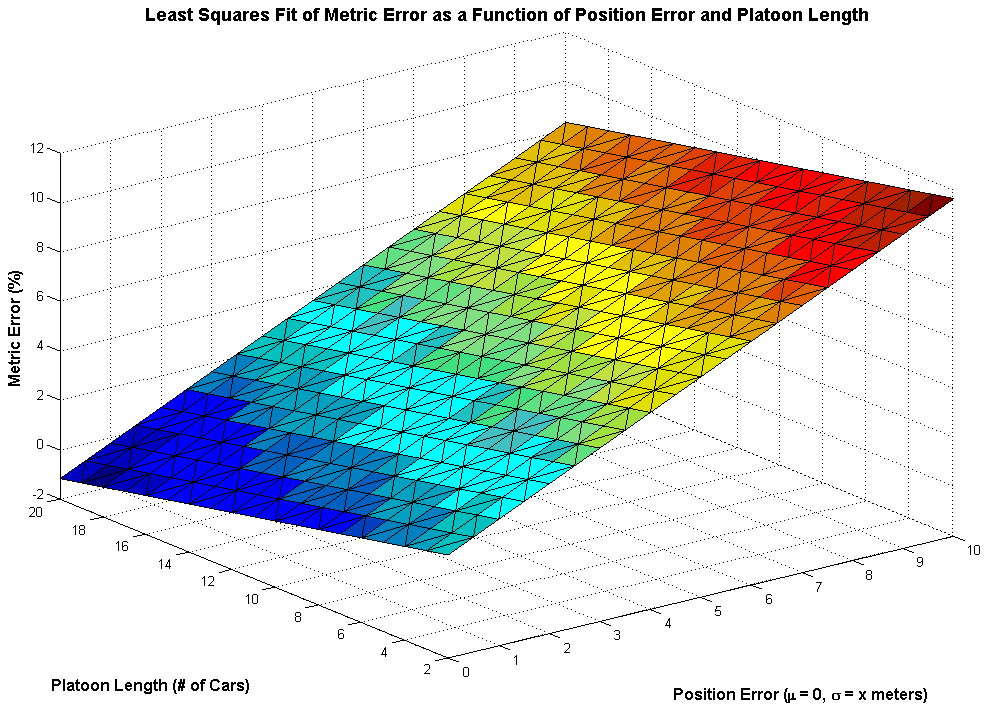

Figure 5.20: Least squares fit to data of Figure 5.19.

In general,

- As the position error increases, the risk metric error increases
- As the platoon length increases, the risk metric error decreases (this is likely due to positioning errors canceling out one another as the platoon length increases)
- Large spikes in the risk metric occur when the positioning error associated with two vehicles causes the range between them to become very small

5.8 VPS Specification

Given that the above risk metric was computed based on VPS position, two logical questions arise:

1 How accurate must VPS be?
2 What are the specifications for such a VPS system?

In short, that question cannot be answered. One must first determine the amount of error that can be tolerated in the final computed value of the risk metric. One must then choose the maximum platoon length for which the risk metric will be computed. Finally, one must choose the speeds over which system performance must be guaranteed. After each of these parameters is chosen, it would be possible to precisely specify the performance of VPS. What follows is a sample calculation, where the above parameters are chosen, and a VPS specification is computed.

5.8.1 VPS Positioning Error

Figure 5.21 shows the computation of VPS position when there is no sensor error. It also assumes that the vehicle's speed between the tags is constant, and that dead reckoning is used to compute position when the vehicle is between tags.

Let,

x = tag spacing
v = vehicle's actual speed
t = time since tag was read/passed
d_{tag} = longitudinal position of tag

It follows that the position of the vehicle is:

$d = d_{tag} + vt$ = vehicle position

given that there are no sensor errors.

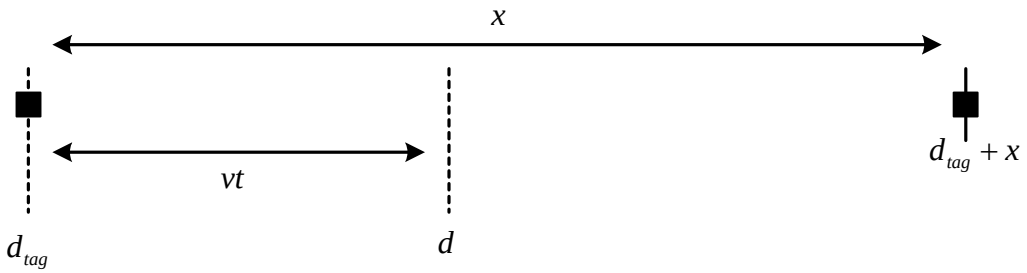

Figure 5.21: VPS position calculation without sensor error.

Figure 5.22 shows the computation of VPS position, where it is assumed that there is tag read latency, and vehicle speed error. It is again assumed that the vehicle's speed between the tags is constant.

Let,

x = tag spacing
v = vehicle's actual speed
t = time since tag was read
δv = vehicle speed error (2σ)
t_l = mean tag read latency
δt_l = tag read latency error (2σ)
$\hat{v} = v + \delta v$ = estimate of vehicle speed
$\hat{t}_l = t_l + \delta t_l$ = estimate of tag read latency
$\hat{t} = t + \hat{t}_l = t + t_l + \delta t_l$ = estimate of time since tag was passed

d_{tag} = longitudinal position of tag

It follows that the estimate of the vehicle's position is:

$\hat{d} = d_{tag} + \hat{v}\hat{t} = d_{tag} + (v + \delta v)(t + t_l + \delta t_l)$ = estimate of vehicle position

given that there are sensor errors, including tag read latency, and speed measurement error.

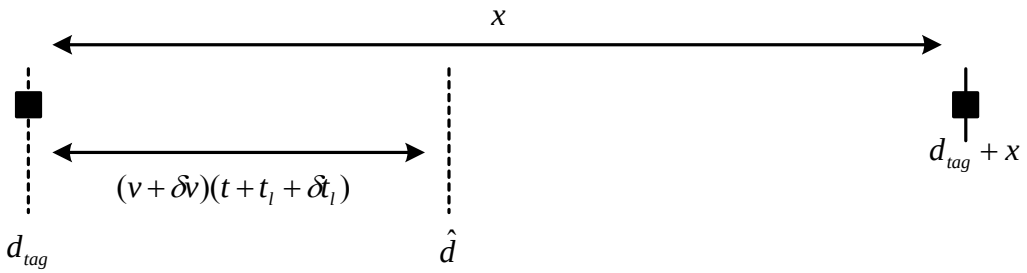

Figure 5.22: VPS position calculation with RFID tag read latency and vehicle speed error.

Thus, the error between the actual vehicle position and the estimated vehicle position is:

$$d_{error} = \hat{d} - d = [d_{tag} + (v + \delta v)(t + t_l + \delta t_l)] - [d_{tag} + vt] = (v + \delta v)(t_l + \delta t_l) + \delta vt \qquad (25)$$

Let t_{tag1} be the time at which tag 1 was passed.
Let t_{tag2} be the time at which tag 2 was passed.

Thus, the length of time since the last tag was read, t, satisfies the following inequality:

$$t \le t_{tag2} - t_{tag1} \qquad (26)$$

Also, because v is assumed to be constant between tags we have the following relationship:

$$\frac{x}{v} = t_{tag2} - t_{tag1} \qquad (27)$$

Using equation (25), which represents the vehicle's positioning error, and making substitutions using equations (26) and (27), we obtain the following:

$$d_{error} = (v + \delta v)(t_l + \delta t_l) + \delta vt$$
$$d_{error} \le (v + \delta v)(t_l + \delta t_l) + \delta v(t_{tag2} - t_{tag1}), \text{ since } t \le t_{tag2} - t_{tag1}$$
$$d_{error} \le (v + \delta v)(t_l + \delta t_l) + \frac{\delta v}{v}x, \text{ since } \frac{x}{v} = t_{tag2} - t_{tag1} \qquad (28)$$

This final equation, (28), relates VPS's positioning error to the OBDII speed error, the tag read latency, tag read latency variability, and tag spacing. This is important since it allows one to determine the minimum tag spacing required to provide the positioning accuracy necessary to guarantee that the risk metric error is within some tolerance. A sample calculation which uses (28) will be provided in the next section.

5.8.2 Final VPS Specification Based on Platoon Risk Metric

Using Figure 5.20 and equation (28), one can compute the latency, OBDII speed accuracy, and tag spacing required such that the percentage error of the computed risk metric satisfies some predetermined error tolerance. As an example, assume we require a maximum of 5% error in the risk metric, where the risk metric error is as defined in (24). Also assume that we will look ahead a maximum of 10 vehicles. From Figure 5.20, we find that a positioning error with $\sigma = 5$ m will satisfy the 5% risk metric error for platoon lengths of 10 or less vehicles. Thus, assuming the positioning error is normally distributed, we can be confident that 95% of the time a positioning error with $2\sigma = 10$ m will yield a risk metric within the 5% tolerance. Applying this to equation (28) we find that,

for the $+2\sigma$ values for t_l and δv,

$$(v + \delta v)(t_l + \delta t_l) + \frac{\delta v}{v} x \le 10 \ \ m \tag{29}$$

and for the -2σ values for t_l and δv,

$$(v - \delta v)(t_l - \delta t_l) - \frac{\delta v}{v} x \ge -10 \ \ m \tag{30}$$

Using equations (29) and (30), we will be able to compute the minimum tag spacing to achieve a desired level of position accuracy.

Assume that $t_l = 0.05$ s and $\delta t_l = 0.01$ s and that the OBDII speed output of each vehicle has a 2σ error of 1%. Substituting these values into equations (29) and (30), we get equations (31) and (32), respectively.

$$(v + 0.01v)0.06 + \frac{0.01v}{v} x \le 10 \tag{31}$$
$$0.0606v + 0.01x \le 10$$

$$(v - 0.01v)0.04 - \frac{0.01v}{v} x \ge -10 \tag{32}$$
$$-0.0396v + 0.01x \le 10$$

Now, we need to choose the speeds over which we guarantee the system's performance, so that we can make a substitution for v in equations (31) and (32). Choose an operating range of $0 - 40 \ \ m/s$.

For $v = 0 \ \ m/s$ both (31) and (32) show that $x \leq 1000 \ \ m$.

For $v = 40 \ \ m/s$ we get:

$$0.0606(40) + 0.01x \leq 10$$
$$0.01x \leq 7.576$$
$$x \leq 757.6 \ \ m$$

from (31), and

$$-0.0396(40) + 0.01x \leq 10$$
$$0.01x \geq 11.584$$
$$x \leq 1158.4 \ \ m$$

from (32).

Thus, for $t_l = 0.05 \ \ s$ and $\delta t_l = 0.01 \ \ s$, a 2σ speed error of 1%, platoon lengths up to 10 vehicles, 5% error in the risk metric, we require the VPS position to provide a 2σ error of 10 m. Combining these requirements, we find that a tag spacing of less than 757.6 m is required, if the system is to operate in the $0 - 40 \ \ m/s$ range.

This distance of 757.6 m is very large, and would present a problem for detecting lane changes. In order to detect lane changes correctly, which is necessary to ensure the correct operation of a rear-end collision avoidance system which uses the risk metric, one must space the tags with a spacing of half the minimum distance required to make a lane change. [23] showed, through the analysis of naturalistic data, that the mean length of a lane change in the speed range of 45 – 55 mph was 6.28 s, or 140.4 m. This mean, however, was substantially higher than the absolute minimum time required to make a lane change. Experimental data showed that the minimum time required to make a lane change took 2 s at 60 mph, and 4 s at 30 mph, or 53.6 m. Thus, the minimum tag spacing should be ~ 25 m to ensure proper lane change detection, as discussed in section 2.4.1. This spacing will also yield very good positioning accuracy, since the accumulation of error when dead reckoning will be eliminated every 25 m of travel.

6 Conclusions

The goal of the work presented in this report was not to build a fully functional, deployable VPS system, because, from the onset, it was understood that this was not possible within the limited time frame of this project. What we did achieve, however, is listed below.

1. A better understanding of passive RFID technology, including a thorough investigation of the performance limitations which hinder it from being immediately useful in an ITS setting.
2. A simplistic implementation of one of the high-priority DSRC-enabled applications outlined by CAMP which requires lane level position, to demonstrate that VPS can overcome the existing limitations of GPS and digital maps.
3. A rear-end collision avoidance risk metric which is computed using VPS position from a platoon of vehicles located immediately in front of the host vehicle.
4. An analysis of the positioning accuracy needed to ensure that the risk metric's value fell within a tolerable range of its actual value, and the implications of the required positioning accuracy on the VPS system.

These four objectives were examined, and the results were presented in chapters 1 through 5 of this document. This chapter will briefly summarize the results of the previous chapters, and make suggestions for future research in the area of vehicle positioning using RFID technology.

6.1 Introduction

Based on an investigation of existing vehicle positioning systems, it was determined that none would be capable of satisfying all of the requirements for the high-priority applications outlined by the US DOT Vehicle-Infrastructure Integration initiative, which aims to enable vehicle-

vehicle and vehicle-infrastructure communication through the use of a new wireless communication protocol (DSRC). As one can imagine, communication with surrounding vehicles and infrastructure makes possible a wide gamut of ITS applications. Many of those applications, however, require reliable, lane-level, accurate vehicle positions, which cannot be ubiquitously provided by existing positioning technologies. Thus, the RFID positioning system, called VPS, was proposed.

6.2 The VPS System

The concept of VPS is a simple one: install RFID tags in the road, and RFID readers on vehicles. As vehicles pass over the tags, they acquire the data stored in the RFID tags. This simple concept, as we see it, will inexpensively and reliably enable a number of ITS applications.

Each RFID tag stores four important fields: road identifier, lane identifier, direction of travel identifier and longitudinal position, as measured from a standard reference (ie. mile marker). In addition to these core fields, additional fields can be stored in the tags to support other ITS applications.

The RFID reader can be most logically installed through the use of a front-mounted electronic license plate (e-plate). The e-plate would contain not only an RFID reader, but also a DSRC unit to facilitate communication with surrounding vehicles, as well as the infrastructure. It may also include a short range communication mechanism, such as Bluetooth or hard-wires, to allow for communication with in-vehicle systems.

Technically, there are two major requirements imposed on the VPS system: RFID tag read range and data transfer capability. It was shown that the maximum amount of data that could be stored in the tags, after making some reasonable assumptions about the response time, transfer rate, read range, and maximum vehicle speed, was roughly 600 bits, which compared favorably to the required storage space. Also, optimal read ranges were described for each of the possible installation methods.

Given these system operation requirements, we proceeded by attempting to build a working VPS system using existing third party RFID hardware.

6.3 Characterizing an RFID Sensing System

In order to determine if third party RFID hardware could provide the performance required by VPS, hardware was purchased, and extensive characterization experimentation was completed. These experiments were designed to determine read percentage, new tag reliability, and latency as a function of RFID antenna orientation, vehicle speed, tag set number, and “tries”.

In order to perform the experiments, a development version of an e-plate, the suggested final installation mechanism, was built and installed in a vehicle. A test track was outfitted with RFID tags every 250 feet, and laps were driven, using different settings for each of the independent variables (RFID antenna orientation, vehicle speed, “tries”, and tag set number). Data was

collected to ensure that latency, read percentage and new tag reliability could be determined during the post-experimental analysis.

After analyzing the data, it was determined that existing RFID hardware could not provide the performance required of a VPS system. Some of the more significant problems, which would prevent the tested prototype from being suitable for a VPS system, included:

1. The read range was too small.
2. The read percentage was not high enough.
3. The variability of latency was too great.
4. The read percentage, in the wake of interference, was dramatically reduced.
5. The variability in tag reliability was too great.

Although these problems prevented the hardware from being used to build a field operational VPS system, a simple implementation of an ITS application could still be built to demonstrate the usefulness of VPS.

6.4 A Basic Implementation of the Electronic Brake Light

The electronic brake light, as outlined by CAMP, was chosen as the application to demonstrate the VPS system. Not only was this application listed by CAMP as being one of high-priority, it was also thought to be the application which required the highest degree of positioning accuracy. Thus, if VPS could support this application, it would also be able to support all other applications.

For this application, a vehicle which brakes "harshly" broadcasts its position, using DSRC, so that vehicles located in the same lane and behind the braking vehicle can be warned of the impending deceleration. In essence, the system extends the field of view of the host vehicle's driver from one vehicle (the lead vehicle), to several vehicles.

To demonstrate the system, the e-plate development system used to characterize the RFID hardware was installed in the host vehicle, with the addition of the DSRC communication block as a means to receive the 'harsh braking' message from the lead vehicle, and a buzzer to be used as a simple driver warning system. The lead vehicle was outfitted with a similar system, but without RFID hardware, since procuring an additional set of RFID hardware was not possible. For this vehicle, however, a simulated VPS position was calculated using GPS coordinates to overcome the lack of RFID hardware. As a final step, the test track was outfitted with RFID tags in both lanes, with a spacing of 250 feet.

The demonstration of the system involved both vehicles proceeding along the test track in a typical car-following scenario, where their only position reference was that gathered from the VPS system. At various times, the lead vehicle would decelerate harshly and broadcast a "severe braking" message. The host vehicle would intercept the message, and determine if warning the driver was required. Only if the host vehicle was located in the same lane, and behind the lead vehicle was the driver warned by sounding the buzzer. This simple demonstration worked remarkably well, given the RFID hardware's limitations discovered during its characterization.

6.5 A More Robust Approach to the Electronic Brake Light and its Implications on VPS

Although the simple electronic brake light implementation worked reasonably well when using a VPS system built from existing RFID hardware, a field operational electronic brake light could not be implemented, because of the limitations discussed earlier. In order to better understand what type of performance VPS must provide, a more sophisticated brake light implementation was proposed and simulated in MATLAB. This more sophisticated system, we believe, requires the highest degree of positioning accuracy when compared to other potential VPS enabled applications. As such, a potential system was designed, and its implications on the VPS positioning accuracy required were investigated.

First, a risk metric was designed which would intuitively indicate a level of risk associated with a platoon of vehicles traveling along a road. It was assumed that the host vehicle would acquire all of the data necessary for the risk metric's computation via DSRC communication. The data set required included the position, speed, acceleration, vehicle length and brake light status for each vehicle in the lead platoon. Since no such "real" data existed, simulated data was created through the use of a microscopic car-following model.

For the simulation, a platoon of vehicles was created and a host vehicle was added at the queue's tail. The simulation was performed and the risk metric was computed at each time increment. It was then shown that the risk metric was able to give the host vehicle's more preview of future braking activity. Finally, given that the risk metric was able to accurately provide the driver of the host vehicle with a preview of the needed future braking activity, the implications on VPS specifications were determined.

When investigating the risk metric's implications on VPS, it was shown that if given an acceptable error tolerance for the risk metric, the variability in the OBDII speed[21], the variability in the tag read latency, the maximum platoon length, and the range of speeds over which performance must be guaranteed, one can compute the minimum tag spacing to provide the necessary positioning accuracy.

6.6 Recommendations for Future Research

The most important outcome of the above research is that, for various reasons, the current state of commercially available RFID technology will not support the design of a vehicle positioning system, although the concept showed great promise. If one were to design custom RFID hardware which was optimized for use in ITS applications, a workable solution can be developed. That is one option that seems reasonable, if rapid deployment is desired.

Another option is to wait for generation-two RFID equipment to become available. The promises of generation two RFID technology seem to deal with many of the problems which we

[21] As suggested in section 2.4.3, the vehicle's speed would be acquired from the OBDII connector to refine the position estimate when the vehicle is in between tags by using dead reckoning.

found within this investigation. Most notably, generation two RFID is said to provide greater immunity to interference, higher read percentages, and greater read ranges. One may want to perform the sensor characterization experiments of Chapter 3 using generation two hardware, which was first released in late 2005.

Also, the electronic brake light application which was discussed in detail in Chapter 5 must be more thoroughly explored. Chapter 5 presented only the design and simulation of a rear-end crash risk metric which used data from several vehicles situated in front of the host vehicle. In simulation the risk metric worked well, however, one would want to verify its effectiveness when using naturalistic data. Also, Chapter 5 did not discuss the design of a driver warning system based on the metric, or the response of the driver to such a system's warnings. Note that drivers often switch lanes during an imminent rear-end crash, so it is important to also provide lane change warning to the driver as well, another application facilitated by VPS. Given successful outcomes in the above, one would also want to investigate the possibility of unintended consequences if each vehicle in the platoon was instrumented with the electronic brake light system.

As a final note, it is important to remember that RFID technology is still in its infancy and that as it progresses, it is very likely that a robust VPS system can be built.

References

[1] P. Cheng, M. Donath, X. Ma, S. Shekar, and K. Buckeye, "Evaluation of Nationwide Differential Global Positioning System for Assessing Road User Charges", *Transportation Research Board: Journal of the Transportation Research Board*, No. 1864, TRB, National Research Council, Washington, D.C., 2004, pp.38 – 44.

[2] "Traffic Safety Facts 2003: A Compilation of Motor Vehicle Crash Data from the Fatality Analysis Reporting System and the General Estimates System", *National Highway Traffic Safety Administration*, Washington, DC, 2003.

[3] D. J. LeBlanc, R. J. Kiefer, R. K. Deering, M. A. Shulman, M. D. Palmer, J. Salinger, "Forward Collision Warning: Preliminary Requirements for Crash Alert Timing", *Intelligent Vehicle Initiative (IVI): Technology and Navigation Systems*, Warrendale, PA, SAE report number 2001-01-0462, 2001.

[4] A. L. Burgett, A. Carter, R. J. Miller, W. G. Najm, D. L. Smith, "A Collision Warning Algorithm for Rear-end Collisions", *National Highway Traffic Safety Administration*, Washington, DC, Paper number 98-S2-P-31, 1998.

[5] R. Ervin, S. Bogard, P. S. Fancher, "Radar Detection of Vehicles in a String: Gaining Situation Awareness of a Propagating Conflict", *Transportation Research Board,* Washington, DC, Paper number 01-0531, 2001.

[6] "Vehicle Safety Communications Consortium, Task 3 Final Report: Identify Intelligent Vehicle Safety Applications Enabled by DSRC", Crash Avoidance Metrics Partnership, Farmington Hills, MI, March 2005.

[7] *United States Patent and Trademark Office*, [online], Available: http://www.uspto.gov/, 2005, (Accessed December 15, 2005).

[8] *European Patent Office*, [online], Available: http://www.european-patent-office.org, 2005, (Accessed December 15, 2005).

[9] J. R. Tuttle, "RFID System in Communication with Vehicle On-board Computer", U. S. Patent 6,112,152, August 29, 2000.

[10] P. A. Nysen, "Environmental Location System", U. S. Patent 6,259,991 B1, July 10, 2001.

[11] D. S. Breed, W. E. DuVall, W. C. Johnson, "Wireless Sensing and Communication of Roadways", U. S. Patent 6,758,089 B2, July 6, 2004.

[12] C. Carrender, "System and Method for Acquisition Management of Subject Position Information", U. S. Patent Application Publication US 2004/0027243 A1, February 12, 2004.

[13] M. M. Nielsen, "New cost-effective concept for automatic vehicle location (AVL) offers more features and benefits for bus passengers, operators, and authorities", *Bus 2000: The Heart of City Transportation*, 2000, pp. 39-46.

[14] *AR400 User Manual*, Matrics, Inc., Rockville, MD, 2004, p. 56.

[15] L. A. Pipes, "An Operational Analysis of Traffic Dynamics", *Journal of Applied Physics*, Vol. 24, No. 3, pp. 274 – 281, 1953.

[16] R. E. Chandler, R. Herman, E. W. Montroll, "Traffic dynamics; studies in car following", *Operations Research*, Vol. 6, 165 – 184, 1958.

[17] D. C. Gazis, R. Herman, and R. Rothery, "Non-linear follow-the-leader models of traffic flow", *Operations Research*, Vol. 9, pp. 545 – 567, 1961.

[18] P. G. Gipps, "A behavioural car-following model for computer simulation", *Tranportation Research Board*, Vol. 15-B, pp. 403 – 414, 1981.

[19] R. Eddie Wilson, "An analysis of Gipps's car-following model of highway traffic", *IMA Journal of Applied Mathematics*, Vol. 66, pp. 509-537, 2001.

[20] R. Ervin, et al., *System for Assessment of the Vehicle Motion Environment (SAVME)*: Univ. Michigan Transportation Research Institute, UMTRI-2000–21–1, 2000.

[21] K. Lee, H. Peng, "Identification and verification of a longitudinal human driving model for collision warning and avoidance systems", *Int. J. Vehicle Autonomous Systems*, Vol. 2, Nos. 1/2, pp. 3 – 17, 2004.

[22] N. D. Lerner, "Brake Reaction Times of Older and Younger Drivers", *Proceedings of the Human Factors and Ergonomics Society 37th Annual Meeting*, 1993.

[23] S. E. Lee, E. C. B. Olsen, and W. W. Wierwille, "A Comprehensive Examination of Naturalistic Lane-Changes", *National Highway Traffic Safety Administration*, Washington, DC, Report number DOT HS 809 702, March 2004.

[24] H. Oh, C. Yae. D. Ahn, and H. Cho, "5.8 GHz DSRC Packet Communication System for ITS Services", *IEEE Vehicular Technology Conference*, pp. 2223 – 2227, Fall 1999.

[25] K. Finkenzeller, *RFID Handbook : Fundamentals and Applications in Contactless Smart Cards and Identification*, 2nd edition, West Sussex, England: John Wiley & Sons, 2004.

[26] G. Widmann, W. Bauson, and S. Alland, "Development of Collision Avoidance Systems at Delphi Automotive Systems", *1998 IEEE International Conference on Intelligent Vehicles*, October 28 – 30, 1998.

[27] J. Woll, "VORAD Collision Warning Radar", *Proceedings of the IEEE International Radar Conference*, pp. 369 – 372, May, 1995, Alexandria, Virginia.

[28] R. Tribe, K. Prynne, and I. Westwood, "Intelligent Driver Support", *Proceedings of the 2nd World Congress on Intelligent Transportation Systems*, Vol. III, pp. 1187 – 1192, November 9 – 11, Yokohama, Japan, 1995.

[29] H. Araki, K. Yamada, Y. Hiroshima, and T. Ito, "Development of Rear-end Collision Avoidance System", *Proceedings of the 1996 IEEE Intelligent Vehicles Symposium*, pp. 224 – 229, September 19 – 20, Tokyo, Japan, 1996.

[30] T. Butsuen, A. Doi, H. Sasaki, "Development of a Collision Avoidance System with Automatic Brake Control", *Proceedings of the 1st World Congress of Transportation Telematics and Intelligent Vehicle Highway Systems*, pp. 2079 – 2086, 1994.

[31] A. Gorjestani, "Radar Based Longitudinal Virtual Bumper Collision Avoidance System Implemented on a Truck", M. S. Thesis, University of Minnesota – Twin Cities, Minneapolis, MN, 1999.

[32] "Minnesota Motor Vehicle Crash Facts, 2004", Minnesota Department of Public Safety, Office of Traffic Safety, St. Paul, MN, August 2005.

[33] "Freeway Volume-Crash Summary, Twin Cities Metropolitan Area, Continuation Report, 2002 Data", Minnesota Department of Transportation, Office of Traffic – Security and Operations, Freeway Operations Section, Regional Transportation Management Center, March 2004.

Appendix A

Appendix A

A.1 Patent US 6,112,152 [9]

Title: RFID system in communication with vehicle on-board computer

Abstract:

A system comprising a vehicle on-board computer; and a wireless transponder device coupled to the vehicle on-board computer. The system performs a variety of functions because of its ability to transmit and receive data from other transponders which may be remote from the vehicle or located in the vehicle at a location spaced apart from the system. Remote transponders are spaced apart from the vehicle. The remote transponders can be positioned, for example, at a gas station, toll boot, service center, dealership, parking lot, or along a roadside.

A.2 Patent US 6,259,991 [10]

Title: Environmental location system

Abstract:

A system and method for determining a location. The system employs encoded information devices dispersed through the environment, each having a non-unique code associated therewith. The codes from the encoded information devices are acquired as a reading device passes nearby, and stored. The codes from a proximate set of information devices are correlated with a map or mapping relation to determine one or more consistent positions within the environment. The information devices are preferably passive acoustic wave transponders, and the mapping relation may be a pseudorandom sequence or a defined map.

A.3 Patent US 6,758,089 [11]

Title: Wireless sensing and communication system of roadways

Abstract:

Wireless sensing and communication system including sensors located on the vehicle, in the roadway or in the vicinity of the vehicle or roadway and which provide information which is transmitted to one or more interrogators in the vehicle by a wireless radio frequency mechanism. Power to operate a particular sensor is supplied by the interrogator or the sensor is independently

connected to either a battery, generator, vehicle power source or some source of power external to the vehicle. The sensors can provide information about the vehicle and its interior or exterior environment, about individual subsystems, or about the roadway, ambient atmosphere, travel conditions and external objects. The sensors arranged on the roadway or ancillary structures would include pressure sensors, temperature sensors, moisture content or humidity sensors, and friction sensors.

A.4 Patent Application Publication US 2004/0027243 A1 [12]

Title: System and method for acquisition management of subject position information

Abstract:

A system and method for acquisition management of subject position information that utilizes radio frequency identification (RFID) to store position information in the position tags. Tag programmers receive position information from external positioning systems, such as Global Positioning System (GPS), from manual inputs, such as keypads, or other tag programmers. The tag programmers program each position tag with the received position information. Both the tag programmers and the position tags can be portable or fixed. Implementations include portable tag programmers and fixed position tags for subject position guidance, and portable tag programmers for collection sample labeling. Other implementations include fixed tag programmers and portable position tags for subject route recordation. Position tags can contain other associated information such as destination address of an affixed subject for subject routing.

A.5 New cost-effective concept for automatic vehicle location (AVL) offers more features and benefits for bus passengers, operators, and authorities [13]

Summary of Article:

- AVL concept based on passive RFID tags embedded in the roadway with tag readers on vehicles
- Tags are embedded in the roadway at strategic positions, e.g. at traffic intersections, bus stops, limited access areas and entry and exit to terminals, depots, etc.
- RFID reader mounted underneath the vehicle reads the tags
- Tags store unique codes which refer to position and direction of travel information in a central database
- In between tags, vehicle position data is derived from odometer readings
- In cities where buildings, bridges, tunnels, etc. obstruct GPS signals, tags are used for positioning
- The vehicle transmits vehicle ID code, RFID tag code, odometer readings, optional GPS signals and other data with a time stamp to the infrastructure
- The infrastructure processes the incoming data and uses it for various applications
- Applications include traffic light priority, and passenger information
- Traffic light priority based on this system has been implemented in Kolding, Denmark

- Emergency vehicles are given traffic light priority so they can minimize their response time
- The arrival time of an emergency vehicle at an intersection can be calculated by the infrastructure since the vehicle's position and speed are known through the use of RFID tags and odometer readings
- Passenger information for railways has been implemented using this system at Naerumbanen, Denmark
- It is used to give accurate, real-time passenger information about arrival and departure times
- The arrival times can be dynamically updated since the train's position is known by the infrastructure through the use of RFID tags